ESTROGEN DEPENDENT PREMATURE LETHALITY DUE TO GUT DYSFUNCTION IN A TRANSGENIC TDP-43 MOUSE MODEL

Dissertation

zur

Erlangung der naturwissenschaftlichen Doktorwürde

(Dr. sc. nat.)

vorgelegt der

Mathematisch-naturwissenschaftlichen Fakultät

der

Universität Zürich

von

Thorsten Ewald Bernhard Läufer

aus

Deutschland

Promotionskomitee

Prof. Dr. Adriano Aguzzi (Vorsitz)

Prof. Dr. Manuela Neumann (Leitung)

Prof. Dr. Peter Sonderegger

Zürich, Juli 2014

Meiner Mutter gewidmet

(1949 – 2010)

1. Table of Contents

2. Abbreviations

ALS ..... *amyotrophic lateral sclerosis*

APOA2 ..... *apolipoprotein A-II*

BSA..... *bovine serum albumin*

C. Elegans ..... *Caenorhabditis elegans*

C9ORF72 ..... *chromosome 9 open reading frame 72*

$CaCl_2$..... *calcium chloride*

CDK6 ..... *cyclin-dependent kinase 6*

cDNA..... *complementary DNA*

CFTR ..... *cystic fibrosis transmembrane conductance regulator*

CHMP2B ..... *charged multivesicular body protein 2b*

CTF ..... *C terminal fragment*

DAB..... *3,3'-Diaminobenzidine*

DLB ..... *dementia with Lewy bodies*

DNA ..... *deoxyribonucleic acid*

EDNRB ..... *endothelin receptor, type B*

EDTA ..... *ethylenediaminetetraacetic acid*

ENS..... *enteric nervous system*

fALS ..... *familial amyotrophic lateral sclerosis*

FBS ..... *fetal bovine serum*

FTD ..... *frontotemporal degeneration*

FTLD ..... *frontotemporal lobe dementia*

FTLD-U ..... *FTLD with ubiquitin-positive inclusions*

FUS ..... *fused in sarcoma/translocated in sarcoma*

GDNF ..... *glial cell-derived neurotrophic factor*

GRN ..... *granulin*

H&E ..... *hematoxylin and eosin*

HCL ..... *hydrochloric acid*

HDAC6 ..... *histone deacetylase 6*

Hepes ..... *4-(2-hydroxyethyl)-1-piperazineethanesulfonic acid*

HITS-CLIP ..... *high-throughput sequencing of RNA isolated by crosslinking immunoprecipitation*

hnRNP ..... *heterogeneous nuclear ribonucleoprotein*

HRP ..... *horseradish peroxidase*

hTDP-43 ..... *human TDP-43*

ICC ..... *interstitial cells of Cajal*

IF ..... *immunofluorescence*

IHC ..... *immunohistochemistry*

KCl ..... *potassium chloride*

kDa ..... *kilodalton*

KH_2PO_4 ..... *monopotassium phosphate / potassium dihydrogen phosphate*

M ..... *molar mass*

MAP1B ..... *microtubule-associated protein 1B*

MAPT ..... *microtubule-associated protein tau*

$MgCl_2$ ..... *magnesium chloride*

miRNA ..... *microRNA*

mRNA ..... *messenger RNA*, *messenger RNA*

NaCl ..... *sodium chloride*

NES ..... *nuclear export signal*, *nuclear export signal*

NLS ..... *nuclear localization signal*, *nuclear localization signal*

Nonidet P-40 ..... *octylphenoxypolyethoxyethanol*

OMPA ..... *tetraisopropylpyrophosphoramide*

OPTN ..... *optineurin*

p ..... *p-value*

PaGE ..... *Paw grip endurance*

PBS ..... phosphate buffered saline

PCR ..... *polymerase chain reaction*

PFN1 ..... *profilin-1*

PGC-1α ..... *peroxisome proliferator-activated receptor gamma coactivator 1-alpha*

PMSF ..... *phenylmethanesulfonylfluoride*

PrP ..... prion protein promotor

PVDF ..... *polyvinylidene fluoride*

RET ..... *rearranged during transfection*

RIPA ..... radio immunoprecipitation assay

RNA ..... *ribonucleic acid*

RRM ..... *RNA recognition motif*

sALS ..... *sporadic amyotrophic lateral sclerosis*

SC35 ..... *serine/arginine-rich splicing factor 2*

SD ..... *standard deviation*

SDS ..... *sodium dodecyl sulfate*

SDS–PAGE ..... *sodium dodecyl sulphate polyacrylamide gel electrophoresis*

SEM ..... *standard error of mean*

SG ..... *stress granule*

SMN ..... *survival of motor neuron*

SNP ..... *single nucleotide polymorphism*

SOD1 ..... *superoxide dismutase 1*

SQSTM1 ..... *sequestosome-1*

TAR ..... *transactivation response region*

TARDBP ..... *transactive response DNA binding protein 43 kDa (gene)*

tardbpl ..... *TAR DNA binding protein, like*

TDP-43 ..... *TAR DNA-binding protein 43 kDA (protein)*

Tris ..... *tris(hydroxymethyl)aminomethane*

TSE buffer ..... *tris sucrose EDTA buffer*

UBQLN2 ..... *ubiquilin-2*

UTR ..... *untranslated region*

UV ..... *ultraviolet*

VCP ..... *valosin-containing protein*

3. Summary

Amyotrophic lateral sclerosis (ALS) is the most frequent form of motor neuron disease and the third most common neurodegenerative disease after Alzheimer and Parkinson with an estimated incidence of 2.6/100.000 per annum. It is characterized by a loss of motor neurons in the brain and spinal cord leading to a fatal paralysis and death within 1 to 5 years. During the last years, it became clear that ALS is a clinical manifestation of genetic disorders in various genes, affecting multiple cellular pathways and leading to heterogeneous disease pattern. Most incidences of ALS are sporadic (sALS) but approximately 10 percent of patients have a family history (fALS) of the disease. Mutations in the *TARDBP* gene have been identified in about four percent of fALS and less than one percent of sALS, though TDP-43 pathology is a consistent feature in all sALS cases and the majority of fALS cases. TDP-43 pathology is characterized by aberrant cytoplasmic TDP-43 inclusions with distinct nuclear clearance in effected neurons, accompanied by a protein truncation, ubiquitination and hyperphosphorylation. However, the functional consequences of TDP-43 mutations triggering the disease remain unknown. Strikingly, pathological TDP-43 aggregates are also reported for ~50% patients with of frontotemporal degeneration (FTD), including most of the patients who develop FTD in combination with amyotrophic lateral sclerosis.

In order to unravel the pathomechanisms underlying TDP-proteinopathies, we generated and analysed TDP-43 transgenic animals expressing four different constructs covering overexpression of wild type human TDP-43, the ALS-related mutations M337V and G348C as well as an altered nuclear localization signal,

inducing cytoplasmic translocation with comparable expression levels. We could demonstrate that expression of TDP-43 species with human pathogenic mutations or forced cytoplasmic mislocalization of TDP-43 do not per se induce disease-related phenotypes in our transgenic lines. This argues against a toxic gain-of-function mechanism of human pathogenic mutations and increased levels of cytoplasmic TDP-43.

Animals of our wild type line (hTDP-43 WT-7) line showed a pathological phenotype, as they die premature after 3 to 6 months from a gut phenotype, resulting from a dilated ileum and colon. This is accompanied by a decreased number of ganglion cells in the Auerbach´s plexus (myenteric plexus) of the colon. WT-7 animals showed no motoric constraint or pathological changes in the CNS, speaking for a detrimental effect of TDP-43 overexpression with the enteric nervous system being the most vulnerable cell population. Remarkably, the observed phenotype was not associated with pathological inclusions.

Furthermore, we noticed a high gender discrepancy of the life span with an earlier onset in hTDP-43 WT-7 males. We were able to abolish this difference by ovariectomy of hTDP-43 WT-7 females and administration of 17β-estradiol to ovariectomized females resulted in a partial extension of the life span, thus indicating a beneficial effect of female sex hormones in TDP-43 mediated toxicity, suggesting potential for future treatment in human TDP-43 proteinopathies.

In summary, we could demonstrate that comparable levels of human wild type TDP-43 is more toxic *in vivo* compared to human pathogenic mutations and cytoplasmic TDP-43. While the hTDP-43 WT-7 mice do not reflect characteristical

histological features of human TDP-43 proteinopathies, they will be valuable tools to further dissect the role of TDP-43 in neurons.

4. Zusammenfassung

Amyotrophe Lateralsklerose (ALS) ist die häufigste neurodegenerative Erkrankung des motorischen Nervensystems und die dritthäufigste neurodegenerative Erkrankung nach Alzheimer und Parkinson, mit einer geschätzten Inzidenz von 2.6/100.000. Sie ist durch einen Verlust der motorischen Nervenzellen in Gehirn und Rückenmark gekennzeichnet, der innerhalb von 1 bis 5 Jahren nach Diagnose zum Tod durch Atemlähmung führt. Forschungen der letzten Jahre haben gezeigt, dass ALS von Mutationen in verschiedenen Genen hervorgerufen werden kann. Die entsprechenden Proteine sind an unterschiedlichen zellulären Prozessen beteiligt, so dass ALS, auch aufgrund der heterogenen Krankheitsausprägung, eher als klinische Manifestation unterschiedlicher Proteinopathien verstanden werden kann. Zumeist tritt ALS als sporadische Erkrankung (sALS) auf; aber etwa 10 Prozent der Fälle sind auf vererbte Genveränderungen zurückzuführen (fALS). Mutationen im Gen *TARDBP* wurden in etwa vier Prozent der fALS-Patienten und weniger als ein Prozent der sALS-Patienten als Krankheitsursache identifiziert. TDP-43 Pathologie ist jedoch in allen bisher beschriebenen sALS Fällen und dem überwiegenden Teil der fALS Fälle beobachtet worden. Merkmale der TDP-43 Pathologie sind die Bildung von Proteinaggregaten im Zytoplasma betroffener Neuronen und das Auftreten verkürzter, ubiquitinierter und hyperphosphorylierter TDP-43 Proteine. Die genauen funktionellen Veränderungen durch TDP-43 Mutationen und ihr Beitrag zur Pathogenese sind allerdings unklar. Pathologische TDP-43-Aggregate finden sich

interessanterweise auch in ~50 % der Fälle von Frontotemporaler Degeneration (FTD), unter ihnen auch ein Großteil der Patienten mit einer überschneidenden ALS-Diagnose.

Zur Aufklärung der zugrundeliegenden Pathomechanismen bei TDP-43 Proteinopathien haben wir transgene Mäuse generiert und untersucht, die vier verschiedene TDP-43 Konstrukte mit annährend gleichem Proteinlevel exprimieren. Dazu gehört die Überexpression des humanen Wildtyp TDP-43, humanes TDP-43 mit den ALS-auslösenden Mutationen M337V bzw. G348C sowie humanes TDP-43 mit einem veränderten Kernlokalisierungssignal zur erzwungenen zytoplasmatischen Translokation. Wir konnten zeigen, dass die alleinige Expression von TDP-43 mit humanpathogenen Mutationen oder die Lokalisation von TDP-43 im Zytoplasma in unseren transgenen Linien nicht ausreicht um einen krankheitsassoziierten Phänotyp hervorzurufen. Diese Ergebnisse sprechen gegen einen Gain-of-function Mechanismus durch humanpathogene Mutationen oder erhöhte zytoplasmatische TDP-43 Level.

Mäuse der Linie hTDP-43 WT-7, die den humanen Wildtyp überexprimiert, zeigen einen pathologischen Phänotyp: innerhalb eines Zeitraums von 3 bis 6 Monaten versterben sie auf Grund einer gastrointestinalen Mobilitätsstörung, charakterisiert durch eine Erweiterung von Ileum und Colon. Dies geht einher mit einer Reduktion der Ganglienzellen im Auerbach Plexus des Colon (myenterischer Plexus). Im Gegensatz dazu zeigen hTDP-43 WT-7 Mäuse auch kurz vor dem Tod keine motorischen Einschränkungen oder pathologische Veränderungen im ZNS. Dies deutet auf einen negativen Effekt der TDP-43 Überexpression hin, der auf besonders anfällige Zellpopulationen im enterischen Nervensystem begrenzt ist.

Wir konnten darüber hinaus bei WT-7 Weibchen eine signifikant höhere Lebenserwartung im Vergleich zu Männchen beobachten. Das Entfernen der Eierstöcke reduzierte die Lebenserwartung der Weibchen, während die Gabe von 17β-estradiol an kastrierte Weibchen zu einer partiellen Lebensverlängerung führte, was für einen positiven Effekt weiblicher Geschlechtshormone spricht und das Potential für zukünftige Therapien humaner TDP-43 Proteinopathien aufzeigt.

Zusammenfassend können wir schlussfolgern, dass humanes Wildtyp TDP-43 *in vivo* toxischer ist als ein vergleichbares Level von TDP-43 mit humanpathogenen Mutationen oder zytoplasmatischem TDP-43. Obwohl die hTDP-43 WT-7 Mauslinie nicht die histologischen Charakteristika humaner TDP-43 Proteinopathien zeigt, kann sie doch in Zukunft ein wichtiges Modell zur Aufklärung der generellen Funktion von TDP-43 in Neuronen sein.

5. Introduction

5.1. TDP-43, a key player in the pathology of amyotrophic lateral sclerosis and frontotemporal lobar degeneration

Over the last decade, there has been growing evidence that two formerly unrelated neurodegenerative diseases show a clinical overlap and share genetically and pathological similarities.

Frontotemporal lobar degeneration (FTLD) is the second most common type of dementia after Alzheimer's disease in patients less than 65 years of age with an estimated prevalence of 15 per 100.000 and tends to occur at a younger age compared to Alzheimer's disease [1, 2]. FTLD represents a group of different disorders, characterized by atrophy in the frontal and temporal lobe of the human brain with neuronal loss and astrocytosis. Personality, behaviour and language can change in various degrees, resulting in a clinical syndrome called frontotemporal dementia (FTD), which is further subdivided by distinctive clinical impairments, determined through differences in the affected brain regions. Approximately 10% to 30% of FTLD cases have an autosomal dominant pattern of inheritance, indicating a significant genetic influence [3]. Currently, there are six genes known carrying mutations linked to FTLD: *MAPT*, *GRN* and *C9ORF72* have emerged as common FTLD genes, whereas *TARDBP*, *VCP*, *FUS*, and *CHMP2B* have been identified as rare genetic causes [4].

Amyotrophic lateral sclerosis is the most frequent form of motor neuron disease and the third most common neurodegenerative disease after Alzheimer´s disease and Parkinson´s disease with an estimated incidence of 2.6 per 100.000 [5]. It is characterized by a loss of motor neurons in the brain and spinal cord leading to a fatal paralysis and death within 1 to 5 years [6]. The famous French neurologist Jean-Martin Charcot initially described it in the year 1869, discovering that lesions within the lateral column in the spinal cord resulted in chronic progressive paralysis and contractures (without atrophy of muscles), while lesions of the anterior horn of the spinal cord resulted in paralysis without contractures (with atrophy of muscles). He recognized that the motor component of the spinal cord consists of a two-part system, and that the location of the lesion results in a varying clinical presentation [7]. Comorbidity of ALS and FTLD symptoms is estimated to occur in roughly 50% of the patients [8-11]. ALS can be split into two groups: sporadic ALS (sALS) accounts for 90-95% of ALS cases, with patients having no family history of ALS and familial ALS (fALS) with a hereditary pattern. Currently, the genetic etiology of two-thirds of fALS cases and about 11% of sALS cases is known [12] caused by mutations in eight confirmed ALS-associated genes: *SOD1*, *TARDBP*, *FUS*, *OPTN*, *SQSTM1, VCP*, *UBQLN2*, *C9ORF72* and *PFN1* [13-22]. sALS and fALS are clinically similar, but clinical comparison of the various fALS associated genes showed differences in site of onset (predominantly lower limbs for *SOD1* and upper limbs for *TARDBP* mutations), age of onset (younger with *FUS* mutations), and in lifespan (shorter for *FUS* carriers) [23]. However, the clinical phenotype varies greatly, e.g. a difference in disease onset of more than 30 years within a family and duration of illness varying from 6 months to 5 years [24].

The detection of differently shaped ubiquitinated protein aggregates in sporadic and familiar ALS in the early 1990s was a major finding, speaking for accumulations of altered or abnormal neuronal proteins resistant to degradation via the ubiquitin proteolytic pathway [25, 26]. Likewise, the most common neuropathological subtype of FTD has been characterized by ubiquitin-positive but tau- and α-synuclein-negative inclusions and was therefore named Frontotemporal lobar degeneration with ubiquitin-positive inclusions (FTLD-U) [27]. However, the ubiquitinated protein(s) itself remained unknown.

In 2006, TAR DNA-binding protein 43 (TDP-43) was described as the principal component of the ubiquitinated inclusions in the vast majority of FTLD and ALS cases [14], now labelled as FTLD-TDP and ALS-TDP [28]. The discovery of TDP-43 as a pathological protein set a genetic link between ALS and FTLD. TDP-43 pathology is present in almost all patients with FTD associated with ALS, in a significant proportion of FTD patients without overt motor neuron disease and in most patients with sporadic and familial ALS. The distribution of TDP-43 pathology tends to correlate with brain areas of atrophy, the stage of dementia and motor impairments in FTLD and ALS, allowing a further subtyping of FTLD-TDP by pathological characteristics of TDP-43 [29, 30]. In ALS, pathological TDP-43 is mainly present pyramidal motor system, but is also observed in multiple brain areas to a variable extent [31].

The discovered clinical and pathological similarities between most cases of FTLD and ALS resulted in major rearrangements in the pathological classification system. FTLD-U and ALS with ubiquitin-positive inclusions are now reclassified under the umbrella term TDP-43 proteinopathies, covering a group of disorders exhibiting

heterogeneous clinical phenotypes [28]. The distribution of TDP-43 pathology tends to correlate with brain areas of atrophy, the stage of dementia and motor impairments in FTLD and ALS, allowing a further subtyping of FTLD-TDP by pathological characteristics [29, 30]. In ALS, pathological TDP-43 is mainly present pyramidal motor system, but is also observed in multiple brain areas to a variable extent [31].

Interestingly, TDP-43 inclusions were absent in patients affected by gene mutations in the first discovered ALS-associated gene, *SOD1*, speaking for a different molecular mechanism [32]. This is an important finding as many scientists used SOD1 animals as a model for amyotrophic lateral sclerosis.

Under normal conditions, TDP-43 is mainly localized to the nucleus, but neurons with aberrant cytoplasmic TDP-43 inclusions in FTLD-TDP and ALS-TDP show a distinct nuclear clearance, accompanied by protein truncation and hyperphosphorylation [14, 33]. Plenty of causative mutations in *TARDBP*, the gene encoding TDP-43, were reported in patients with either ALS-TDP or FTLD-TDP, indicating a direct link between mutations in *TADBP* and disease [15, 34-36]. Some of these mutations like M337V and G348C are inherited following an autosomal dominant trait of inheritance and can be traced throughout unrelated fALS families, supporting the assumption of an autosomal dominant trait [34, 37-39]. However, only a small minority of 4% of fALS patients, an even smaller number of sALS patients and rare cases of FTLD carry coding mutations in the *TARDBP* gene, while the vast majority of ALS-TDP and FTLD-TDP cases occur in the absence of *TARDBP* mutations [40, 41]. Aggregation and nuclear depletion of wild type TDP-43 is a constant feature associated with

mutations in other genes like *GRN* and *VCP* and the newly found *C9orf72* hexanucleotide expansion [4, 12].

Remarkably, pathological TDP-43 aggregations are not restricted to FTLD-TDP and ALS-TDP: secondary TDP-43 accumulations occur also in multiple other neurodegenerative disorders and were even infrequently reported for brains of control subjects over 65 years without mental retardation [1, 42, 43]. TDP-43 pathology is detected in 25% to 50% of AD cases with a higher probability in those with more a severe clinical phenotype and greater Alzheimer type pathology [44]. Some patients with Lewy body disorders also develop TDP-43 pathology, with estimated 7.2% in Parkinson's disease without dementia and 19% in Parkinson's disease with dementia, while dementia with Lewy bodies exhibited no TDP-43 pathology [45]. These data suggest that TDP-43 pathology may have co-morbid effects in some neurodegenerative diseases.

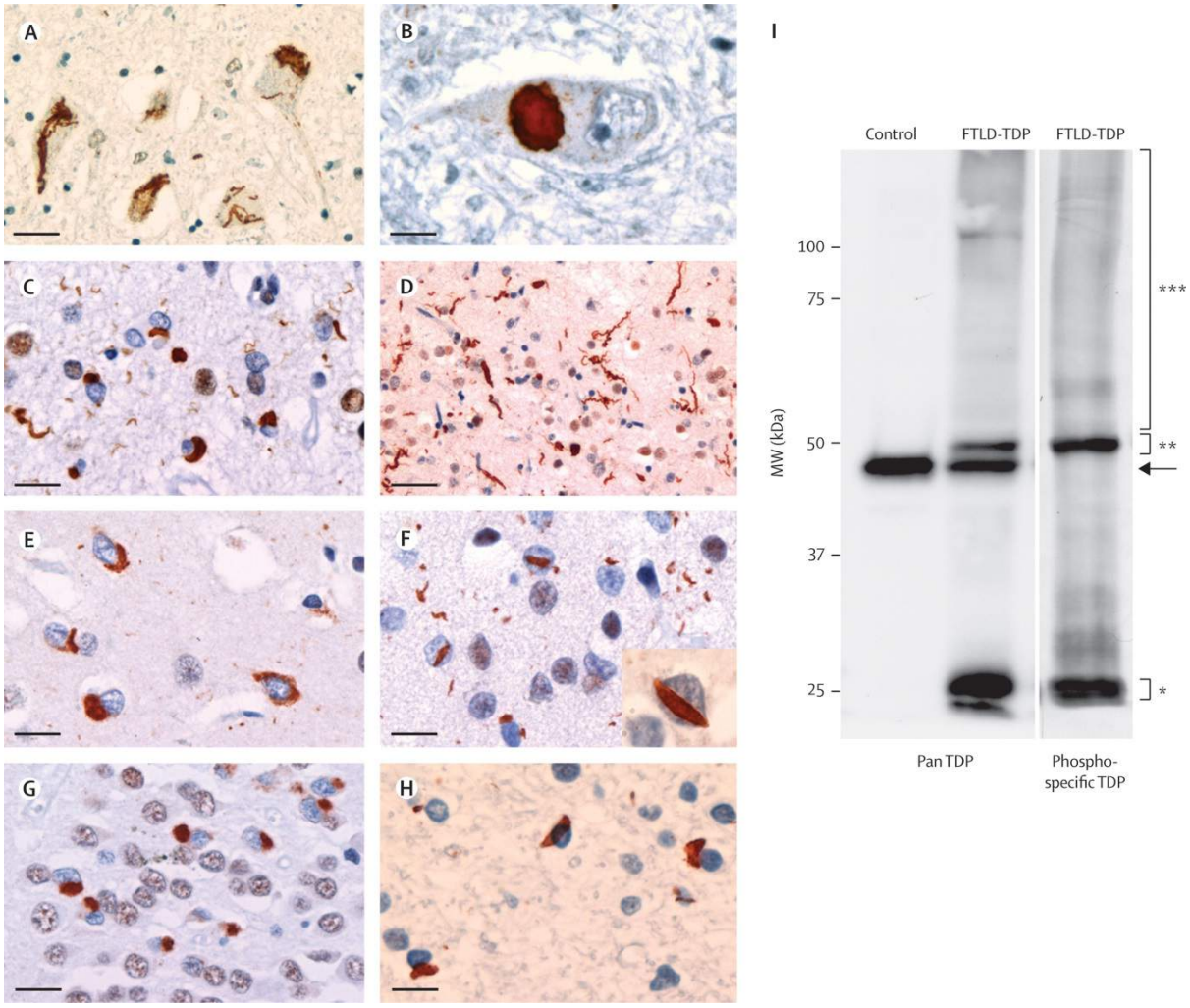

Figure 1. Pathological features in ALS-TDP and FTLD-TDP. TDP-43 immunohistochemistry on paraffin-embedded tissue showing (A) TDP-43-immunoreactive skein-like and (B) round inclusions in motor neurons in ALS-TDP. FTLD-TDP pathology is subdivided into four distinct morphological subtypes: (C) type 1 is characterized by compact neuronal cytoplasmic inclusions and short neurites; (D) type 2 is characterized by long neurites; (E) type 3 is characterized by compact and granular cytoplasmic inclusions; and (F) type 4 is characterized by numerous neuronal intranuclear inclusions. (G) Cytoplasmic inclusions in the dentate granule cells of the hippocampus. Nuclear staining is absent in inclusion-bearing cells. (H) Glial cytoplasmic inclusions. Scale bars: 40 µm (D), 20 µm (A, C, G), 15 µm (E, F), and 10 µm (B, H). (I) Immunoblot analysis of urea fractions isolated from brain tissue, showing the highly characteristic biochemical signature of TDP-43 in FTLD-TDP, with pathological bands of approximately 25 kDa (*) and 45 kDa (**), and a high-molecular-weight smear (***) that are not detected in controls. The arrow indicates the wild-type 43 kDa TDP-43 band present in controls and in patients with FTLD-TDP. Notably, only pathological TDP-43 is detected by a phosphorylation-specific TDP-43 antibody against phosphorylated serine residues 409 and 410. (from Mackenzie et al. 2010, [28])

5.2. Protein structure and functions of TDP-43

Since its first description, TDP-43 has not attracted much attention in the scientific community for a decade. In 1995, Ou et al. characterized a novel transcriptional repressor binding chromosomally integrated TAR DNA and repressing HIV-1 transcription. They named it TAR DNA-binding protein 43 (TDP-43) [46]. Six years later Buratti et al. identified TDP-43 as the factor binding specifically to the splice sites in the cystic fibrosis transmembrane conductance regulator (CFTR), promoting exon skipping at exon 9. This was the first description of RNA binding by TDP-43 and its relevance for pre-mRNA splicing [47]. Similar observations were reported for the apolipoprotein A-II (APOA2) transcript, survival of motor neuron (SMN) and serine/arginine-rich splicing factor 2 (SC35) [48-50]. After identification of TDP-43 as a pathological protein in ALS and FTLD in 2006 great efforts were made to understand physiological functions and structural determinants of TDP-43.

TDP-43 is a highly conserved member of the hnRNP protein family with a nuclear localization signal at the N-terminus, two RNA recognition motifs named RRM1 and RRM2, later bearing a nuclear export signal [51]. Both RRMs have the ability to bind nucleic acids but only RRM1 appears to be essential for RNA splicing [47]. TDP-43 preferentially binds UG repeats, but is also found to be associated with non-UG repeat sequences [47, 52, 53]. High-throughput sequencing of RNA isolated by crosslinking immunoprecipitation (HITS-CLIP) showed that TDP43 binds to a large proportion of the transcriptome (more than 6,000 RNA species), preferentially localizing to introns (including deep intronic sites), 3′ untranslated regions (UTRs) and non-coding RNAs [54, 55]. Functional classification of TDP-43 RNA targets from cortical neurons revealed a significant number of targets related to neuronal

development and axon guidance [56]. Furthermore, TDP-43 is a component of neuronal mRNA transport granules and supports trafficking of its mRNA targets to neuronal distal compartments [57].

TDP-43 acts as part of multiprotein-RNA complexes, binding both RNA and protein partners of the hnRNP family including hnRNP A2/B1, hnRNP A1, hnRNP C1/C2 and hnRNP A3 [56, 58-62]. The glycine-rich C-terminal domain mediates protein-protein interactions and contains most of the disease causing mutations. It has also properties of a Q/N-rich 'prion domain' similar to those observed in yeast prions [63, 64].. Recent studies indicated prion-like properties of TDP-43 with intracellular TDP-43 exhibiting seed-dependent and self-templating aggregation [65], although there are conflicting results about amyloidic properties of TDP-43 aggregates [66-68]. The results of Nonanka et al. also suggest the possibility that exosome may contribute to the release of intracellular TDP-43 aggregates, allowing cell-to-cell transmission of aberrant TDP-43 species [69]. TDP-43 self-aggregation is supposed to be regulated by chaperone availability [70]. However, both the N-terminus and the two RNA-recognition motifs have been implicated in regulating inclusion formation, suggesting an additional effect of RNA binding on the pathogenesis [71-75]. Additionally, TDP-43 species can form homodimers mediated by the N-terminus [76]

TDP-43 is a splice regulator, but it also influences the mRNA levels of various genes: TDP-43 depletion increases the levels of cyclin-dependent kinase 6 (CDK6) and reduces the levels of Futsch (the *Drosophila melanogaster* homologue of microtubule-associated protein 1B (MAP1B)) and histone deacetylase 6 (HDAC6) [77-79].

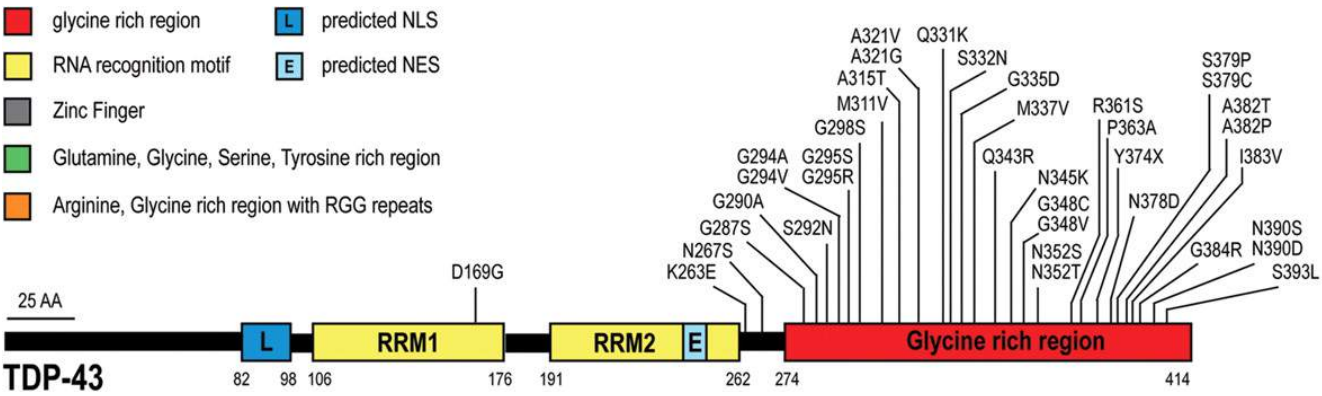

Figure 2. TDP-43 protein structure and mutations in ALS and FTLD patients. Thirty-eight dominant mutations have been identified in TDP-43 in sporadic and familial ALS patients and in rare FTLD patients, with most lying in the C-terminal glycine-rich region. All are missense mutations, except for the truncating mutation TDP-43 Y374X. NLS: nuclear localization signal; NES: nuclear export signal. Domains have been defined according to http://www.uniprot.org and http://www.cbs.dtu.dk/services/NetNES. (from Lagier-Tourenne et al. 2010, [40])

Intriguingly, HDAC6 is a critical component of stress granules (SG) involved in the stress response, mediating the motor-protein-driven movement of individual SG components along microtubules [80]. SGs are cytoplasmic RNA-protein complexes, which temporarily assemble in response to stress-induced translational arrest [81]. Together with other members of the hnRNP family, TDP-43 can become part of SGs, where it contributes to both the assembly and maintenance of SGs [82].

TDP-43 also regulates microRNA (miRNA) biogenesis, as it localizes to the perichromatin fibres in which miRNA biogenesis is thought to occur, becoming part of the primary miRNA processing Drosha complex [83]. Consequently, knockdown of TDP43 alters the level of several miRNAs [59, 84-86].

Due to its diverse functions in different RNA-processing steps TDP-43 expression levels are tightly controlled by an autoregulatory feedback mechanism, preventing TDP-43 expression by a nuclear retention mechanism after TDP-43 binding to its own 3′ untranslated region (UTR) [87].

Normal TDP-43 shows a predominantly nuclear localization, but continuously shuttles between nucleus and cytoplasm in a transcription-dependent manner, mediated by its nuclear localization signal and nuclear export signal [51].

5.3. Evidence for a loss-of-function mechanisms in TDP-43 proteinopathies

The nuclear clearance of TDP-43 observed in inclusion bearing cells in FTLD and ALS patients argues a loss-of-function mechanism due to protein mislocalization with subsequent alterations at the level of gene transcription, pre-mRNA splicing, microRNA production, mRNA stability and mRNA translation **(Figure 3)**.

In support of this, knockout approaches in rodents had been lethal in early embryonic stage and targeted depletion of murine TDP-43 in spinal cord resulted in an ALS-like phenotype [88] [89]. Consistently, knockout of TDP-43 in mouse postnatal motor neurons using the inducible Cre/loxp system resulted in progressive weight loss and motor impairment accompanied by neuropathological alterations [90]. However, another study using mice with a conditional knockout of TDP-43 reported a significant loss of body weight but without significant FTLD/ALS symptoms [91]. A modest knockdown of TDP-43 protein in the periphery and the central nervous system of mice is sufficient to induce progressive neurological phenotypes [92]. Knockdown of TDP-43 in mice also results in a large change in gene expression pattern, probably linked to neurodegeneration [54, 55]. This notion is supported by experiments where TDP-43 knockdown causes morphological abnormalities and cell death in cultured neurons [93-95].

Most TDP-43 knockout non-mammalian models did not cause embryonic lethality. *C. Elegans* TDP-43 deletion mutants are viable, but exhibit a low fertility, slow growth

and locomotor defects [96]. TDP-43 loss-of-function models of Drosophila show a high mortality in the embryonic stage such that few survive into the adult stage. Surviving knockout Drosophilae developed severe motor dysfunction in adulthood similar to those in ALS, potentially linked to alterations in motor neurons development [79, 97-99]. In zebrafish, two TDP-43 homologs were identified: loss-of-function mutants for either *tardbp* or *tardbpl* gene resulted in motor dysfunction [100] [101]. However, in another report, only doubly knocked-out genes resulted in muscle degeneration and significant motor deficits in zebrafish [102].

Disease-related mutations are mainly localized in the C-terminal glycine-rich region which is important for protein-protein interactions. Whether mutations are pathogenic by disruption of normal interactions is not known, but recent studies revealed functional deficits directly linked to TDP-43 mutations. Arnold et al. reported enhanced activity of mutant TDP-43 for facilitating splicing of some RNA targets, but “loss-of-function” for others in a transgenic mouse model overexpressing TDP-43 with a Q331K mutation, uniquely dependent on the mutation [103]. ALS-causing mutations in *TARDBP* also impair the axonal mRNA transport in mRNA granules containing mutant TDP-43 protein both in *in vivo* models as well as in stem cell-derived motor neurons from ALS patients bearing different TDP-43 mutations [57]. Interestingly, other studies showed no alteration in the direct protein-protein interactions by TDP-43 with pathogenic mutations [58, 60, 62]. Likewise, the autoregulatory properties of mutant TDP-43 remains unchanged despite FTLD or ALS-associated mutations, demonstrated by various transgenic mouse models [104-106]. D169G, the only ALS-linked TDP-43 mutation identified that lies in the RRM1,

binds RNA- and DNA-binding as effective as wild type TDP-43, but it is more resistant to thermal denaturation [107, 108].

5.4. Evidence for gain-of-function mechanisms in TDP-43 proteinopathies

In the disease state, pathological TDP-43 is not just redistributed to the cytoplasm but it is also ubiquitinated, cleaved and phosphorylated and forms insoluble cytoplasmic aggregates. A hypothesis says that these aggregates might exhibit a toxic gain-of-function mechanism. (**Figure 3**).

The consequences of cytoplasmic redistribution of TDP-43 were addressed by *in vitro* and *in vivo* studies using TDP-43 with a modified NLS-sequence, resulting in an impaired nuclear uptake. In 2008, Winton et al. showed in different cell culture models that expression of mutant TDP-43 with defective nuclear localization signals perturbs endogenous TDP-43 trafficking and aggregate formation in neuronal perikarya and neurites [109]. Increased cytoplasmic TDP-43 is toxic in primary cortical neurons unrelated to aggregate formation. Remarkably, Barmada et al. also reported an increased cytoplasmic mislocalization for the TDP-43 A315T mutant resulting in a decreased survival [110]. Overexpression of either human TDP-43 with modified NLS or the human wild type TDP-43 in mice led to neuron loss in selectively vulnerable forebrain regions, corticospinal tract degeneration, and motor spasticity recapitulating FTLD and ALS features [111]. Expression of human TDP-43 with modified NLS in the CNS of rats by an adeno-associated virus gene transfer method resulted in motor impairments, but did not induce mortality [112]. Mislocalization of exogenous TDP-43 results in a degenerative phenotype in the Drosophila eye, whereas eyes of flies expressing normal TDP-43 appear

morphological normal [113]. However, both nuclear and cytoplasmic accumulations of TDP-43 in adult neurons lead to reduction of lifespan in Drosophila, accompanied by an abnormal phosphorylation on the disease-specific Ser409/Ser410 site [114]. Overexpression of TDP-43 with a mutated NLS induced degenerative phenotypes in most of the model systems unrelated to TDP-43 aggregate formation.

Pathological C-terminal fragments of TDP-43 (CTFs) are a key feature of TDP-43 proteinopathies with the potential for a gain-of-function mechanism. Expression of CTFs in cell culture resulted in cytoplasmic aggregates that are ubiquitinated and abnormally phosphorylated and splicing abnormalities [115]. Furthermore both N- and C-terminal fragments were prone to aggregate in cultured neurons and may impair neuronal differentiation by dominant-negatively interfering with the function of the full length TDP-43 [93]. Expression of 25 kDa C-terminal proaggregatory fragment of TDP-43 in mice resulted in a pronounced forelimb impairment compared to TDP-43 with NLS mutation [112], whereas TDP-43 CTFs expression in Drosophila is less severe than TDP-43 with NLS mutation or wild type TDP-43 expression [74].

In a majority of animal model systems, overexpression of both TDP-43 with disease-associated mutations and wild type TDP-43 leads to a neurodegenerative phenotype [104-106, 116-119]. However, these models only partially recapitulate key features of TDP-43 proteinopathies: wild type and mutant TDP-43 is diffusely distributed in the cytoplasm of neuronal cells of the CNS, sometimes accompanied by nuclear and cytoplasmic TDP-43 inclusions, phosphorylated TDP-43 and increased ubiquitin staining. Some models also develop motor deficits and cognitive impairments correlating with the general TDP-43 protein levels. The toxic potential of mutated TDP-43 remains unknown, as differences in the expression strength account for

observed phenotypical alterations. The previous studies suggest that TDP-43 aggregation and hyperphosphorylation are associated with the cell death process rather than being a direct cause, supported by experiments showing that blocked TDP-43 aggregation does not prevent its cytotoxicity [120].

While TDP-43 is evidently a stress responsive protein, it is not clear whether pathological TDP-43 inclusions arise from SGs, but sALS motor neurons clearly show a colocalization of TDP-43 positive inclusions with SG markers [121-123]. Furthermore, TDP-43 appears to be a crucial player in stress granule dynamics as TDP-43 mutations were linked to a loss-of-function mechanism in the SGs assembly and disassembly [82, 124]. Accordingly, disease-linked mutations increased TDP-43 stress granule assembly in the presence of sodium arsenite [122]. These mutations are all localized in the Q/N-rich region, mediating protein-protein interactions. A repeat extension of the wild type Q/N-rich region results in an increased aggregate formation [125].

There are strong arguments for a loss-of-function as well as a gain-of-function mechanism, but most likely they cannot be seen as independent, single events and a combination of disease mechanisms might be involved. A hot topic currently under debate is the so-called “two-hit” or “multiple-hit” hypothesis. It assumes that TDP-43 proteinopathies depend on cascade of cellular events starting with cytoplasmic mislocalization and an independent hit inducing the formation of cytoplasmic aggregates that may sequester TDP-43, disrupt RNA processing and initiate neuron degeneration. These secondary hits can include different forms of cellular stress or genetic risk factors, finally leading to ALS and FTLD pathology [126, 127].

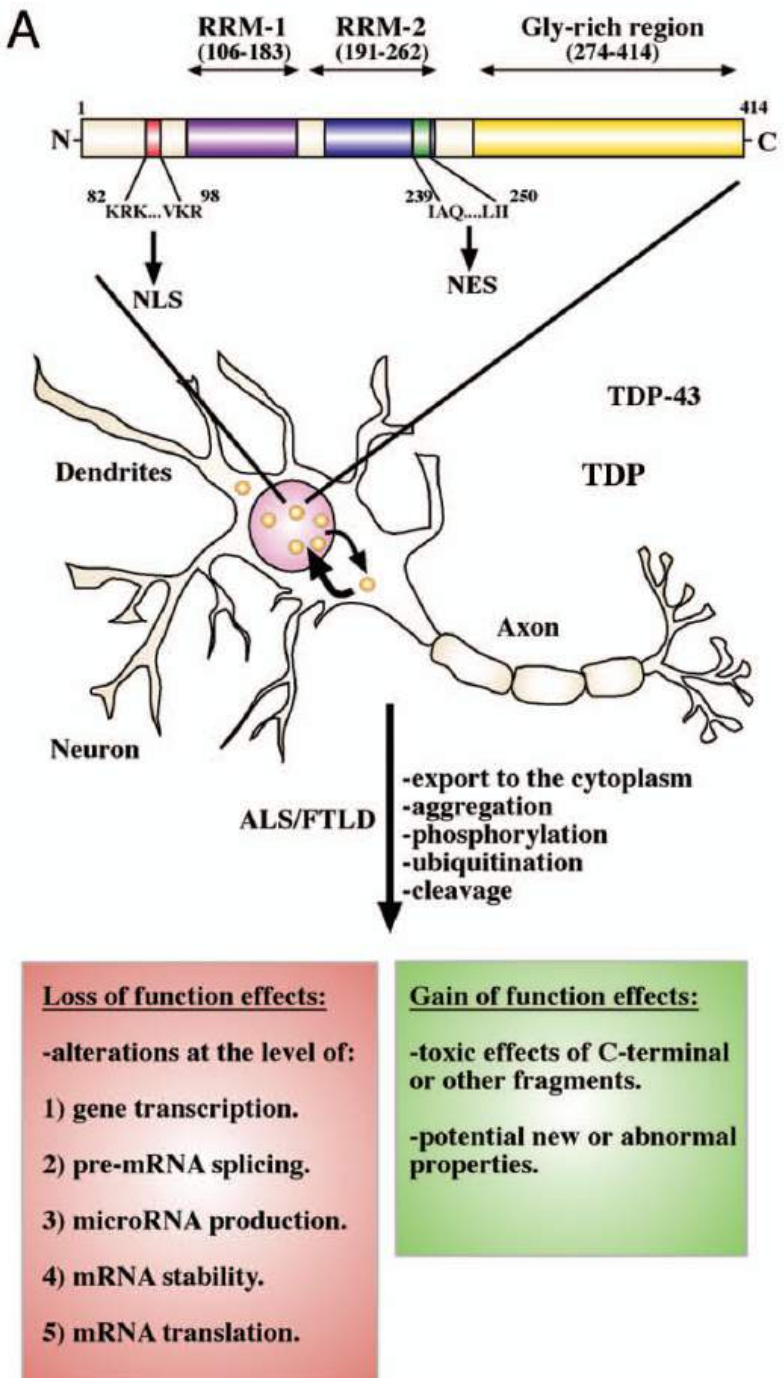

Figure 3: Mechanisms of TDP-43 mediated neurodegeneration. The upper diagrams show a schematic representation of the TDP-43 protein structure reporting the major domain sequences determining nuclear/cytoplasmic localization (NLS and NES) or important for binding to RNA (RRMs), and potential protein-protein interactions (Gly-rich region). The lower panel shows the normal localizations of these proteins in the cellular environment (normally nuclear). In normal conditions, TDP-43 is continuously shuttling between the nucleus and the cytoplasm but is predominant in the nuclear compartment. In the disease state, it is ubiquitinated, cleaved, phosphorylated and exported to the cytoplasm to form insoluble aggregates.

The possible disease mechanisms (gain- or loss-of-function models) for either protein that may lead to neuronal loss are summarized in the bottom panels (from Buratti et. al. 2010 [128])

5.5. Scientific aims

The underlying mechanisms of TDP-43 associated cell death are unclear. To further elucidate a potential gain-of-function mechanism, the major questions I wanted to address in my thesis are:

- Is overexpression of wild type human TDP-43 sufficient to induce a neurodegeneration and a pathological phenotype similar to FTLD or ALS, including nuclear clearance and TDP-43-positive protein aggregates, hyperphosphorylation and truncation?
- Are fALS-associated mutations in the human TDP-43 associated with a toxic gain-of-function?
- Are increased level of cytoplasmic TDP-43 necessary and sufficient to induce neurodegenerative effects?

In order to address these questions *in vivo*, we generated and analysed human TDP-43 transgenic animals utilizing the widely used prion protein promoter with four different constructs covering overexpression of wild type human TDP-43, the ALS-related mutations M337V and G348C as well as an altered nuclear localization signal, inducing cytoplasmic translocation.

6. Materials and Methods

6.1. Generation of human TDP-43 transgenic mice

Human *TARDBP* cDNA (National Center for Biotechnologie Information Sequence NM_007375) was amplified by PCR from human brain cDNA and cloned into the pCR2.1-TOPO vector (Invitrogen). Mutations for M337V, G348C and a modified nuclear localization signal (NLS) [K82A;R83A;K84A] were inserted by site-directed mutagenesis using the QuickChange Site-Directed Mutagenesis Kit (Agilent Technologies/Stratagene). The cDNA fragments *TARDBP* WT, M337V, G348C and NLS were subcloned in the "half-genomic" Prnp vector phgPrP described earlier [129]. After removal of most of the vector backbone, DNA fragments consisting of the promoter sequence and the cDNA fragments were microinjected into fertilized oocytes of C57BL/6JOlaHsd background. The embryos were implanted in pseudo pregnant mothers in collaboration with the Max Planck Institute of Molecular Cell Biology and Genetics in Dresden. Founders were identified by PCR analysis of tail DNA and bred with C57BL/6JOlaHsd mice. The newly generated mice were named according to the standard nomenclature for genetically modified mice, e.g. C57BL/6JOlaHsd-/Tg(Prnp-human TDP-WT)7, abbreviated WT-7. Out of 24 transgene positive founders, seven mouse strains with human TDP-43 overexpression were established and maintained in hemizygous state: human TDP-43 WT-2, WT-7, M337V-3, M337V-5, G348C-4, NLS-4 and NLS-6. The mice were group housed under a 12-h light/dark cycle with access to food and water at all times. All mouse experiments were performed according to Swiss federal guidelines ('Ethical

Principles and Guidelines for Experiments on Animals' 3rd edition, 2005) and were approved by the Animal Experimentation Committee of the Canton of Zurich (permit 200/2007).

6.2. Genotyping of human TDP-43 transgenic mice

Weaned animals were marked by clipping small tissue pieces from the ears. Biopsies were lysed for genotyping according to the following protocol: 2µl proteinase K (Roche), 180µl distilled H_2O, 20µl 10x lysis buffer [5ml 1M Tris-HCl pH9.0, 25ml 1M KCl, 2.5ml Nonident P40, 2.5ml Tween20, 15ml distilled H_2O]. Samples were incubated for at least 3h or overnight at 55°C with 700-800rpm on a heat block, following heat inactivation (15min 95°C). For transgenic human TDP-43 the following primers were used: Forward primer: 5'-CAACCGAGCTGAAGCATTCTGC-3'. Reverse primer: 5'-TCCACAAAGAGACTGCGCAATC-3'. A single PCR reaction contained 9µl distilled H_2O, 0.25µl forward primer (100 pmol/µl), 0.25µl reverse primer (100 pmol/µl), 12.5µl REDTaq Readymix PCR Reaction Mix (Sigma-Aldrich) and 3µl lysate. The following PCR conditions were established on a TProfessional Thermocycler/Standard (Biometra): 95°C 5min initial denaturation; 95°C 30s denaturation; 57°C 30s annealing; 72°C 80s elongation; 35 cycles.

PCR products were separated on a 2% agarose gel (TAE-buffer) containing ethidiumbromide (0.1µg/ml) by electrophoresis. Exposition to UV-light in a Gel DOC XR+ (Bio-Rad Laboratories) showed a single DNA band in transgenic mice of 801 base pairs.

6.3. RIPA lysates

Organ samples were collected, cleaned in PBS if necessary and stored at -20°C. Collected tissue was weighed and homogenized in ice-cold radioimmunoprecipitation assay (RIPA) buffer (50mM Tris–HCl, 150mM NaCl, 5 mM EDTA, 1% NP-40, 0.5% sodium deoxycholate, 0.1% sodium dodecyl sulfate) freshly supplemented with complete Protease Inhibitor Cocktail (Roche) and PMSF by glass homogenizer (5x volume/weight), followed by sonification (Bioruptor, Diagenode). The RIPA homogenate was centrifuged for 5min at 10,000g. The protein concentration of the supernatants was determined by a BCA protein assay (Thermo Scientific). 5x SDS–PAGE sample buffer was added to all samples and heated up to 95°C for 5min.

6.4. Subcellular fractionation protocol

Cytoplasmic and nuclear fractions from brain hemispheres were prepared as described earlier [130]. Briefly, fresh tissue was weighed and homogenized in buffer containing 10mM Hepes, 10mM NaCl, 1mM KH_2PO_4, 5mM $NaHCO_3$, 5mM EDTA, 1mM $CaCl_2$, 0.5mM $MgCl_2$ (10× volume/weight). After 10min on ice, 2.5M sucrose (0.5 volume/weight) was added. 2ml of homogenate were centrifuged at 1,000 × g for 10min at 4°C. Supernatant was collected as cytoplasmic fraction. The remaining pellet was washed three times in 1.5 ml TSE buffer (10mM Tris, 300mM sucrose, 1mM EDTA, 0.1% Nonidet P-40), homogenized by sonification, and centrifuged at 4,000 × g for 5min. Finally, the pellet was resuspended in 200µl RIPA buffer with 2% SDS as the nuclear

fraction. Protease Inhibitor Cocktail (Roche) and PMSF had been added to all buffers prior use. 5x SDS–PAGE sample buffer was added to all and samples were boiled for 5min. SDS-PAGE gels were loaded with a 10 times more volume for cytoplasmic fraction than nuclear fraction for ratio adjustment. AIDA Biopackage (Raytest) was used for densiometric analyses.

6.5. SDS-PAGE and immunoblot

A 10% SDS-PAGE was used to separate denatured proteins by their electrophoretic mobility according to published procedures **(Table 1)** [131]. Protein homogenates or samples from the subcellular fractionation protocol were mixed with a 5x SDS-PAGE sample buffer and loaded into pockets of stacking gel. By voltage application, negatively charged proteins were separated by the polyacrylamide matrix in a vertical electrophoresis unit (SE260, Hoefer). The fractionated proteins in the polyacrylamide gel were transferred to a PVDF membrane (Hybond-P, Amershan) by semi-dry-blotting (TE77Xp, Hoefer). Nonspecific binding sites were blocked by incubation with 3% milk powder in Tris-buffered saline (TBS). The membranes were probed overnight with primary antibodies in blocking buffer at 4°C; horseradish peroxidase (HRP)-labeled secondary antibodies were applied in blocking buffer for 1h at room temperature. Blots were developed by Lumina Forte Western HRP Substrate (Millipore) and digital images were acquired using a Stella 3200 (Raytest). AIDA Biopackage (Raytest) was used for densiometric analyses.

Table 1. Composition of 10% SDS-PAGE gels.

Materials	10% Separation gel (30ml)	Stacking gel (4.96ml)
Distilled H2O	15.57ml	3ml
1.5M Tris HCl pH8.8	7.5ml	-
0.5M Tris HCl pH6.8	-	1.25ml
40% Polyacrylamide solution	7.5ml	0.6ml
10% Sodium dodecyl sulfate solution (SDS)	0.3ml	0.05ml
10% Ammonium persulfate solution	0.090ml	0.045ml
Tetramethylethylenediamine (TEMED)	0.050ml	0.015ml

6.6. Antibodies

6.6.1. In-house antibodies

Monoclonal antibodies targeting pan-TDP-43 (human and murine TDP), murine TDP-43 and phosphorylated TDP-43 were produced by standard procedures in collaboration with E. Kremmer, Institute of Molecular Immunology, Helmholtz Center Munich [132]. The anti-pan-TDP-43 mouse monoclonal antibody detecting both murine and human TDP-43 was designated TAR5-6D6 (epitope: SMDSKSSGWGM), used 1:10 for immunoblots. The murine TDP-43-specific rat monoclonal antibody was designated TAR-M-12B4 (epitope: EDMTAEELQQFFCQYGEVVDVFI), used 1:5 for immunoblots and 1:10 for immunofluorescence. The rat monoclonal antibody TAR5p-1D3 was described earlier [132] and detects phosphorylated serine-residues at the TDP-43 C-terminus (epitope: SMDSKpSpSGWGM) and was used 1:500 for immunohistochemistry.

6.6.2. Commercial antibodies

In addition, commercial antibodies were used. Anti-Human TDP-43-specific TARDBP mouse monoclonal antibody (Proteintech), was used 1:5,000 in immunoblots and 1:20,000 for immunohistochemistry and

immunofluorescence. Anti-α-tubulin rabbit polyclonal antibody (abcam), was used 1:5,000 in immunoblots. Anti-Histone H3-HRP rabbit polyclonal antibody (abcam) was used 1:500,000 for immunoblots without secondary antibody. Anti-CD117 clone ACK2 monoclonal rat antibody (Millipore) was used 1:500 for immunofluorescence. Anti-ubiquitin rabbit polyclonal antibody (DAKO) was used 1:1,000 for immunohistochemistry. Anti-GFAP mouse monoclonal antibody (NeoMarkers) was used 1:4,000 for immunohistochemistry. Anti-Iba-I rabbit polyclonal antibody (Wako) was used 1:3,000 for immunohistochemistry. Secondary antibodies for immunoblotting were HRP-coupled goat anti-mouse, anti-rabbit (both Promega) and goat anti-rat IgG (Cell Signaling). For immunohistochemistry, Alexa-488, Alexa-555 or Alexa 647-conjugated goat anti-mouse and anti-rat IgG (Invitrogen) were used as secondary antibodies.

6.7. RNA Extraction and TaqMan qRT-PCR

RNA was isolated from mouse brain hemispheres (200-250mg) with the RNeasy Maxi Kit (Qiagen) after overnight incubation with RNA stabilization reagent RNAlater (Qiagen) according to manufacturer's protocol. The concentration of each sample was measured by a NanoDrop 2000 spectrophotometer (Thermo Scientific). 300ng of RNA was reverse transcribed using the QuantiTect Reverse Transcription Kit (Qiagen). 2ng cDNA was used for TaqMan qPCR amplification by a TaqMan® Gene Expression Master Mix specific assays (human TDP: Hs00606522_m1; mTDP: Mm00523866_m1; mFUS: Mn00836363_g1; GAPDH: 4352339E, Life Technologies). The reactions were run in single-plex assays as technical

duplicate, performed on a 7500 Fast Real-Time PCR System (Applied Biosystems), using the manufacturer's recommended standard protocol. Relative gene expression was calculated by the ΔΔCt method [133]. The Ct (Cycle Threshold*)* values of both the calibrator (cDNA of non-transgenic animals) and the samples of interest were normalized to the relative abundance of the mouse GAPDH transcript. The normalized Ct values of the samples of interest were compared with normalized Ct of non-transgenic animals as calibrator.

6.8. Motor and cognitive tests

The assessment started at 2 months of age (WT-7, twice weekly) or 10 months of age (G348C-4 and M337V-5, every second week) for 4 months or 10 months respectively. The motoric abilities of WT-7, G348C-4 and M337V-5 were assessed with three different tests. Each mouse underwent three trails per test with the highest score used for analysis. Prior motoric testing, body weight was measured. The last recorded weight was set as 0 for statistical analysis. The different tests were performed in a consecutive manner with at least 10min rest period for each mouse.

Cognitive abilities were assessed starting with 2 months of age (WT-7, or 10 months of age (G348C-4 and M337V-5) by two different tests according to published procedures at the Division of Psychiatry Research, University Zurich [134, 135]. Only one cognitive test per day was conducted and motor tests and cognitive tests were performed on different days.

All tests were carried out at the Division of Psychiatry Research, University Zurich.

6.8.1. Rotarod performance test

Each test session started with a rotarod performance test for motor coordination (Ugo Basile). In this test, 5 mice were placed on a rod of 3cm diameter, separated by opaque plastic walls. The rod accelerated linearly from 4 to 40rpm within 180s. Mice dropping off the rod activated a switch recording time point and current acceleration.

6.8.2. Paw Grip Endurance (PAGE)

A Paw Grip Endurance (PAGE) was performed by placing mice upside-down on a wire grid, holding tight with all four limbs. The time was recorded until the mouse lost its grip. Otherwise, the test was stopped after 120s.

6.8.3. Grip strength

Grip strength of maximal muscle strength of combined forelimbs and hind limbs was assessed by a grip strength meter (Ugo Basile). The mice were allowed to peg to a wire grid which is connected to a force sensor. By pulling the mice backwards at the tail, they instinctively applied a counteracting force. The grip strength meter recorded the highest applied force in grams.

The assessment started at 2 months of age (WT-7, twice weekly) or 10 months of age (G348C-4 and M337V-5, every second week) for 4 months or 10 months respectively.

6.8.4. Novel Object Recognition Test (NORT)

Single mice were placed in the centre of a brightly-lit white Plexiglas box (50x50cm^2), and their movements (distance travelled, maximum speed, immobile time and time spend in centre) were tracked using ANY-maze video tracking software (Stoelting) for 15min during habituation period. Center area was defined as the area 5cm away from the walls. After habituation period, the mice were removed from the box for 2min. The box included two circles of 10cm diameter in diagonally opposite corners named object zones. Two simple objects of the same color and shape were placed in the object zones. The mice were placed in the centre of the box for a 5min familiarization period. Object interaction was assumed when the head of a mouse entered an object zone. After familiarization period, the mice were removed from the box for 2min. A differently colored and shaped object of the same size replaced one of the two objects. The mice got 5min time for interaction with the now different objects, one familiar and one unfamiliar. The ratio between novel object and familiar object was divided by the *same object ratio* gained in the familiarization period to calculate the *novel zone preference* unaffected by general object preference.

6.8.5. Y-Maze

Spatial working memory was assessed in mice using the Y-Maze (Y-shaped plastic maze, with 40 × 20 × 10cm^3 arm sizes). During a 5min trial, the sequence of arm entries as well a maximum speed, immobility time and traveled distance were recorded using the ANY-maze Video Tracking System

(Stoelting). The percentage alternation was calculated as the ratio of actual to possible alternations (defined as the total number of arm entries 2) × 100%.

6.9. Histology, immunohistochemistry and double-label immunofluorescences

Collected tissue was immediately placed in 10% formalin solution and fixed for at least for 24h. Immunohistochemistry (IHC) was performed on 5-µm thick sections of formalin-fixed paraffin-embedded tissue on glass slides. The procedure for DAB staining followed the protocol provided with the NovoLink Polymer Detection Kit (Leica): Sections were de-paraffinized in xylene and re-hydrated through graded alcohols finalized by distilled water. For antigen retrieval, the sections were boiled for 5x 3min in citrate buffer pH6.0 using a microwave oven, followed by a wash step with distilled water and 10-15min of hydrogen peroxide treatment with 3% (v/v) solution in distilled water and consecutive wash steps with PBS. Sections were blocked for 30min with 1% BSA, 0.5% Triton-X in PBS. Primary antibodies were applied for 24h at 4°C in 0.5% BSA, 0.25% Triton-X in PBS. After consecutive wash steps with PBS, the sections were incubated with Post Primary solution (included in the kit) for 30min. After consecutive wash steps with PBS, the sections were incubated with Novolink Polymer (included in the kit) for 30min, followed by consecutive wash steps with PBS. The polymer is linked with peroxidase. DAB working solution was applied on the sections, resulting in a brownish precipitate by oxidation of DAB. The reaction was stopped with PBS after 1 to 5min of incubation. Finally, the sections were dehydrated in graded alcohols and mounted with a cover slip using HICO-MIC embedding medium (Hirtz). IHC

images were obtained with a DM100 LED light microscope, equipped with a DFC295 camera (both Leica).

Double-label immunofluorescence (IF) on paraffin embedded tissue samples was performed according to a similar protocol without hydrogen peroxide treatment. Sections were incubated with secondary fluorescence antibodies for 2h. Hoechst 33342 (1:5000) was used for nuclear counterstaining and Fluorescence Mounting Medium (Dako) for final mounting. IF images were obtained with a DM5000B fluorescence microscope system, equipped with a DFC345FX camera (both Leica).

6.10. Morphometric analysis of intestine

Intestines were fixated in 10% formalin solution. Six transverse, consecutive sections of 5mm were taken from the proximal part of the duodenum, the terminal ileum and the proximal colon, paraffin-embedded, cut and stained with H&E. Slides were scanned with a Nanozoomer C9600virtual slide light microscope scanner (Hamamatsu). The circumference of each section as well as the muscle thickness of the longitudinal and circular muscle were assessed on digital slides. The diameter of each sample was calculated from the circumference, whereas the muscle thickness was measured at three triangular points using the NDP.view program (Hamamatsu).

6.11. Whole mount preparation of myenteric plexus, Azure II-staining and ganglion cell counting

Fresh terminal ileum and proximal colon, each 3cm long, were opened along the mesenteric border, cleaned in cooled PBS and mounted with needles on a polystyrene block. Three animals had been used per genotype. Fixation was done for 45min in 10% formalin solution. Samples were rinsed with PBS and mucosal layer was removed under a stereomicroscope. Cleaned muscle layers containing the myenteric plexus were air-dried on glass slides with the circular muscle facing up for 30min. Azure II (Sigma-Aldrich) was prepared as 0.2% solution in distilled water and filtered by a syringe-mounted 0.40µm filter. Slides were placed on preheated hot plate (70°C) and immediately incubated with the Azure II solution for 20s and stopped by a wash step with PBS. Wash steps were performed with 70% ethanol and PBS, ending with a final dehydration in 100% ethanol and mounting with a glass coverslip.

Azure II-stained cells were manually counted using a bright field light microscope DM100 LED (Leica) at 100x magnification representing 3.547 mm^2 as following: four consecutive fields of view were selected starting at the proximal end of the specimen with the anti-mesenteric border as midline. To correct for the intestinal dilatation in the WT-7 lines, numbers were divided by the circumference ratio compared to non-transgenic controls.

6.12. “Swissrole technique” for histological analysis of acetylcholine esterase activity and c-Kit immunoreactivity

Longitudinal specimen of the intestine were prepared as described earlier [136]. Briefly, freshly dissected small intestine and colon were cleaned in

PBS and opened along the mesenteric border. The tissue was cut into 10cm parts, rolled up with the mucosa facing out and quick-frozen for cryo-sectioning.

Acetylcholine esterase activity was determined as described before [137]. Thawed specimen were fixated with 10% formalin solution with 1% (w/v) calcium chloride for 30s and washed with tap water. The specimens were incubated with a 1:1 mix of two solutions, adjusted to pH6.0: solution A (0.1M sodium acetate, 0,1M sodium citrate, 30mM cupric sulfate solution, 4mM iso-OMPA (tetraisopropylpyrophosphoramide), 0.005% (w/v) acetylcholine iodide, diluted in ddH_20) and solution B (0.165% (w/v) potassium ferricyanide in ddH_20) for 1h on 37°C.

After washing with ddH_20 and incubation with 1% (w/v) ammonium sulfate solution, the specimens were washed with tap water and ddH_20, followed by 1min incubation with 0.1% (w/v) silver nitrate solution and another wash step with ddH_20. The specimens were fixed with 10% formalin solution for 5s, washed with tap water and ddH_20 and finally counterstained by 1min incubation with haematoxylin solution and washed with ddH_20 and tap water.

The product of the cholinesterase activity, thiocholine, reduces ferricyanide to ferrocyanide, which precipitates as copper ferrocyanide directly at the site of enzymatic activity. Images were obtained with a DM100 LED light microscope, equipped with a DFC295 camera (both Leica).

c-Kit immunofluorescence on cryo-sections was done as following: The “Swissrole technique” intestinal specimens were thawed for 25min, following 5min fixation with cooled aceton and 10min of air dry. They were treated with 0.1M Tris-HCL pH7.5 for 5min and incubated with anti-c-KIT antibody in 0.1M

Tris-HCL pH7.5 + 2% FBS for 1h. A wash step with 0.1M Tris-HCL pH7.5 for 5min was repeated 3 times, followed by 1h incubation with the secondary antibody in 0.1M Tris-HCL pH7.5 +2% FBS. Nuclear counterstaining was achieved by 10min incubation with Hoechst 33342 diluted 1:5000 in 0.1M Tris-HCL pH7.5. IF images were obtained with a DM5000B fluorescence microscope system, equipped with a DFC345FX camera (both Leica)

6.13. Surgery and 17β-estradiol treatment of WT-7 animals

WT-7 male and female mice (n=11/12) were castrated at 28 to 37 days of age and compared to sham operated human TDP-43 WT-7 mice (n=12/12). Anesthesia and surgery was performed according to established methods (2-5% Sevoflurane, pain treatment with Carprofen twice daily for 3 days) followed by daily monitoring for general movement, body shape and clinical symptoms. End stage animals are defined by 7% weight loss over 7 days, a hunchback and a reduced motility (2 of 3 criteria need to match) **(Table 2)**.

Furthermore, female human TDP-43 WT7 mice were ovariectomized and administered 17β-estradiol using 90-days' time release pellets with two different concentrations (high dose: 0.002mg/day (n=12); low dose: 0.004mg/day (n=6); Innovative Research of America, USA). As controls WT-7 females (n=12) animals underwent placebo treatment. The successful abolishment of gonadal steroids by ovariectomy and the reconstitution via of 17β-estradiol administration was controlled by measuring the uterus wet weight.

Table 2. Control criteria for transgenic WT-7 animals to define clinical endpoint

Symptoms	Result/Action	Score (total ≥2 = endpoint)
Spontaneous and provoked movement (tactile stimulation)?	Reduced motility? = 1 No motility? = 2	0, 1 or 2
Roundish body shape; expanded belly?	If yes: 1	0 or 1
Unexpected clinical symptoms, indicating pain, burden or disease?	Veterinary clarification; control twice daily as long as the problem persist	0 or 2
Body weight	Loss of body weight within a week by >7%? = 2	0 or 2

6.14. Statistical analysis

The statistical analysis were performed with Graphpad Prism, Version 6.01, using statistical methods described here [138].

One-way-ANOVA was used to compare three or more unmatched groups. The Dunnett´s-test was used was used as a multiple comparison post-test to compare the mean of each column to the mean of a control column. Tukey's test was used for multiple comparisons when comparing each group with each other group. An unpaired Student´s t-test (two-sided) was used to compare two groups. For longitudinal studies, two-way-ANOVA with Sidak's multiple comparison post-test was used.

The nonparametric Log-rank (Mantel-Cox) test was used to compare the survival distributions of survival curves.

Significance levels were set at $p<0.05$ for all analyses. Data are presented as means ± standard deviation (SD) if not marked differently.

The statistical test, *p*-values and the n for each statistical analysis are indicated in each of the corresponding figure legends.

7. Results

7.1. Generation of human TDP-43 transgenic mouse lines

At first, transgenic mice with a comparable expression level and expression pattern of human TDP-43 had to be generated. Four different transgenic constructs were created by integrating the cDNA sequence of human wild type TDP-43 (WT), human TDP-43 bearing ALS-associated mutations (M337V, G348C) or human TDP-43 with a disrupted NLS-sequence (NLS) in the phgPrP Vector. M337V and G348C are two TDP-43 mutations associated with fALS and TDP-43 proteinopathies **(Figure 4)** [15, 34, 38, 39, 139-142]. We utilized the prion protein (Prnp) promoter known for a strong and persistent expression in neurons and a subset of glial cells of the central and peripheral nervous systems, accompanied by an expression in non-neuronal tissue such as liver, spleen and intestine [129, 143]. The Prnp-promoter human TDP-43 constructs were linearized and microinjected into C57BL/6JOlaHsd oocytes and implanted into pseudopregnant females at the Transgenic Core Facility, Max Planck Institute of Molecular Cell Biology and Genetics, Dresden.

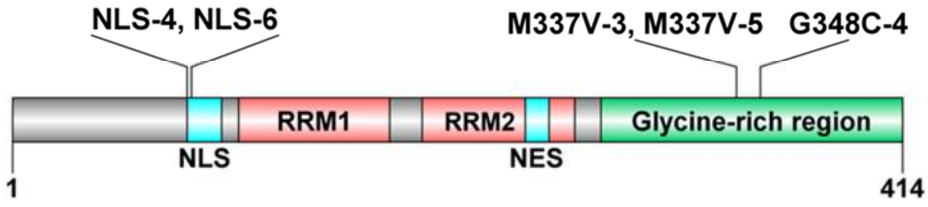

Figure 4. Functional elements of the human TDP-43 protein and inserted mutations. Schematic diagram of the TDP-43 protein domain structure showing the mutated sites in the human TDP-43 of generated TDP-43 transgenic animals. M337V and G348C are human pathogenic ALS-associated mutations whereas NLS refers to a disrupted nuclear localization signal (NLS). The nuclear export signal (NES) remained unchanged in all transgenic lines.

PCR analysis of genomic DNA from offsprings for positive integration of the transgenes revealed eleven founders for the human TDP-43 WT, five founders for human TDP-43 M337V, eight founders for human TDP-43 G348C and eight founders for human TDP-43 NLS constructs **(Table 3)**. Germline transmission of the transgene was confirmed for 15 founder mice by breeding the founder mice with C57BL/6JOlaHsd mice.

Offspring from each founder were investigated by immunohistochemistry and immunoblot analysis using a human TDP-43 specific antibody to select for those with comparable transgene expression levels and expression patterns for the four different TDP-43 constructs. One WT line (WT-7), two M337V lines (M337V-3, M337V-5), one G348C line (G348C-4) and two NLS lines (NLS-4, NLS-6) were successfully established, characterized by germline transmissibility and ubiquitous pan-neuronal human TDP-43 protein expression in the central nervous system (CNS) with comparable expression levels **(Figure 5)**. G348C-6 shared the same features, but could not be established as strain because of breeding difficulties. Since Prnp-driven expression of a transgene has been reported in different tissues besides the CNS we also investigated for transgene expression in other organs **(Figure 5 A)**. All lines showed a similar expression pattern of human TDP-43 transgene at the age of 2- to 3-month with a high expression in the central nervous system represented by brain and spinal cord as well as high but more variable TDP-43 levels in the cecum and colon, speaking for a strong expression in the enteric nervous system. Expression in other organs or tissues was not detectable.

Other lines with germline transmission only revealed a mosaic expression pattern in a subset of neurons in the brain or no transgene expression and were therefore not

further established. WT-2 showed only weak expression in the CNS and strong expression in the skeletal muscles not seen in the other mouse lines and was therefore not included in the future studies.

Table 3. Human TDP-43 transgenic founder mice with the seven established transgenic mouse lines highlighted in grey.

Founder name (short form)	Germline transmissible	human TDP-43 protein in the CNS
WT-1 (1st injection)	yes	no
WT-2 (1st injection)	no	
WT-3 (1st injection)	no	
WT-4 (1st injection)	no	
WT-2 (2nd injection)	yes	yes, but very weak
WT-3 (2nd injection)	no offspring	
WT-4 (2nd injection)	no	
WT-5 (2nd injection)	founder died	
WT-6 (2nd injection)	no	
WT-7 (2nd injection)	yes	yes
WT-8 (2nd injection)	yes	no
NLS-1	no	
NLS-2	no	
NLS-3	yes	yes, but weak and focally
NLS-4	yes	yes
NLS-5	no	
NLS-6	yes	yes
NLS-7	no	
NLS-8	no	
G348C-1	no	
G348C-2	yes	no
G348C-3	yes	no
G348C-4	yes	yes
G348C-5	no offspring	
G348C-6	yes, but bad breeding	yes
G348C-7	founder died	
G348C-8	yes	yes, but weak and focal
M337V-1	no offspring	
M337V-2	no offspring	
M337V-3	yes	yes
M337V-4	yes	yes, but only single cells
M337V-5	yes	yes

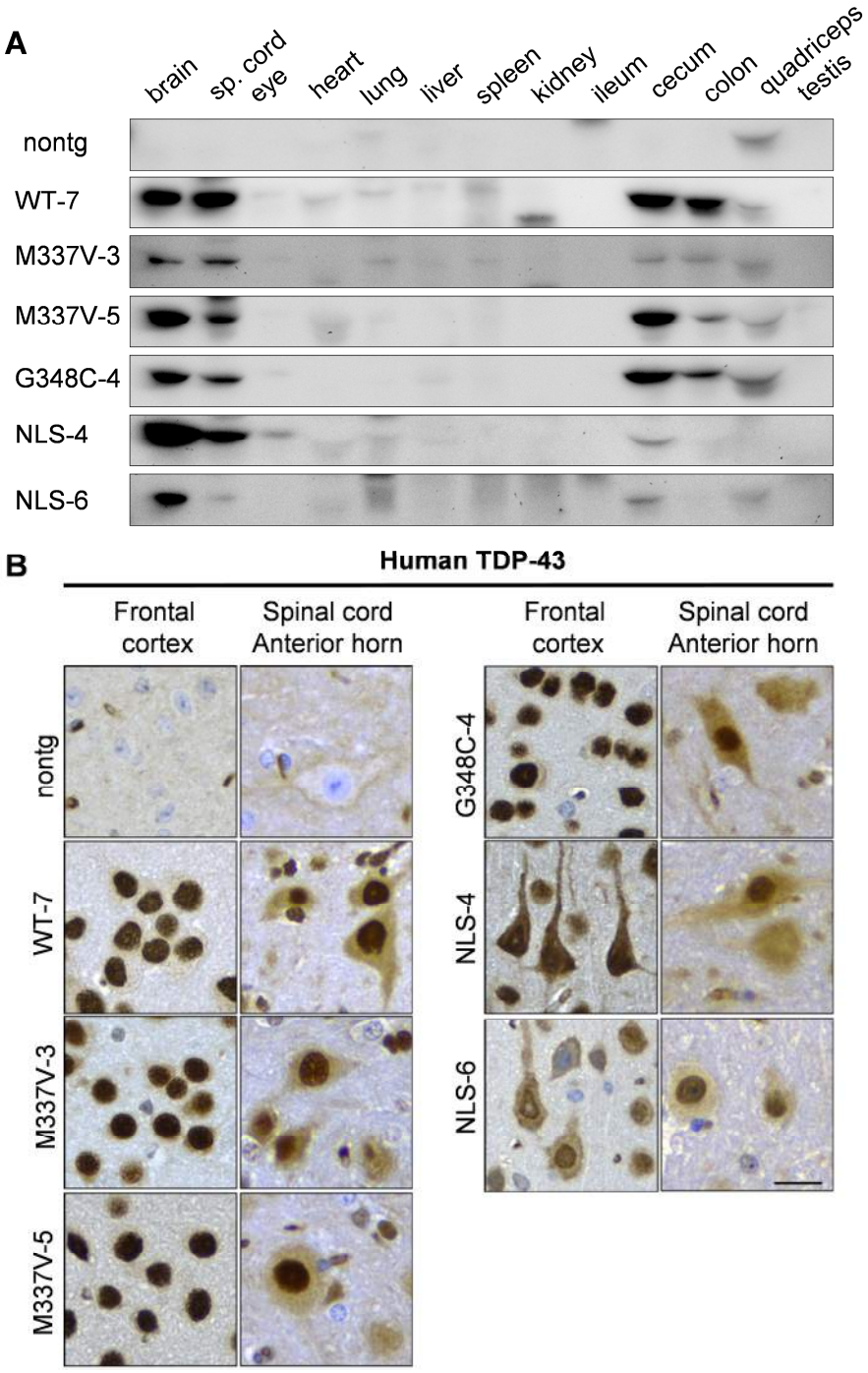

Figure 5. Expression of human TDP-43 in different organs of human TDP-43 transgenic mice.

(A) Immunoblot analysis with a human TDP-43 specific antibody in different organs of 2- to 3-month-old transgenic males. All lines show a similar expression pattern with high human TDP-43 levels in brain and spinal cord and a more variable expression in the cecum and colon. 50 µg of RIPA lysate were loaded.

(B) Immunohistochemistry with a human TDP-43 specific antibody illustrates the panneuronal Prnp-promoter driven expression of human TDP-43 expression in brain and spinal cord of 6-month-old females. In cortical neurons, human wild type TDP-43 and TDP-43 with M337V and G348C mutation is largely localized to neuronal nuclei. The two NLS-mutant lines both show a strong shift to the cytoplasm in addition to a nuclear expression. In motor neurons in the anterior horn of the spinal cord, all lines show a strong nuclear and weak cytoplasmic immunoreactivity. Scale bar: 20µm

7.2. Subcellular localization of transgenic and endogenous TDP-43

We performed immunohistochemistry staining on brain and spinal cord material with a human specific TDP-43 antibody to assure pan-neuronal transgene expression in all established lines and to examine the subcellular distribution of TDP-43. Both genders have been included in a longitudinal analysis ranging from 1 to 24 months. We did not observe an influence of gender or age on the expression pattern or localization of human TDP-43. Selected images represent adult 6-month-old females **(**

Figure 5 B).

In the transgenic mouse lines WT-7, M337V-3, M337V-5 and G348C-4, human TDP-43 is predominantly localized to the nucleus in most of neuronal cells, resembling the localization of endogenous TDP-43 in humans and mice. The motor neurons in the anterior horn showed an increased cytoplasmic immunoreactivity compared to other transgene-expressing cells. However, it is probably not a pathogenic redistribution as TDP-43 accumulation in the cytoplasm of motor neurons has been observed in aging non-transgenic mice [144].

Disruption of the human TDP-43 NLS-sequence in the NLS-4 and NLS-6 mouse lines resulted in a strong cytoplasmic immunoreactivity for human TDP-43 in all transgene-expressing neurons in addition to nuclear localization. Notably, nuclear localization of TDP-43 was not fully abolished by the three amino acid substitution in the NLS *in vivo* in contrast to results observed in cultured cells [109], but in line with studies in other rodent models [111, 112]. This might be explained by dimerization of

TDP-43 with NLS mutation and wild type TDP-43 and subsequent nuclear uptake [76].

The human TDP-43 both in the nucleus and in the cytoplasm was diffusely distributed without indication of a pathological nuclear clearance of TDP-43 or the formation of TDP-43 aggregates.

At next, we wanted to confirm and quantify the subcellular distribution pattern of TDP-43 biochemically by subcellular fractionation and immunoblots using brain homogenates. In particular, we were also interested to analyse the distribution of endogenous murine TDP-43 to see weather transgenic TDP-43 expression might influence endogenous TDP-43. This required an antibody targeting specifically the endogenous murine TDP-43. Since no commercial murine TDP-43 specific antibody was available we generated own monoclonal antibodies. The human and mouse TDP-43 protein share a sequence identity of 96.1%, making the generation of a discriminating antibody challenging. In collaboration with Elisabeth Kremmer, Institute of Molecular Immunology, Helmholtz Center Munich, rats were immunized with a peptide corresponding to amino acids 201 to 223 of the murine TDP-43 protein sequence. This region has a lower similarity between human and murine amino acid composition with only 69.6% sequence identity with 7 different amino acids. 180 hybridoma subclones were tested for the production of a monoclonal murine specific TDP-43 antibody by immunoblot. One clone (TAR-M-12B4) was identified being able to discriminate between murine and human TDP-43 with a detection of a band at 43kDa in mouse brain tissue but not in human HEK293T cells.

(

Figure 6). This result was confirmed by IHC staining using paraffin-embedded mouse and human brain tissue (not shown).

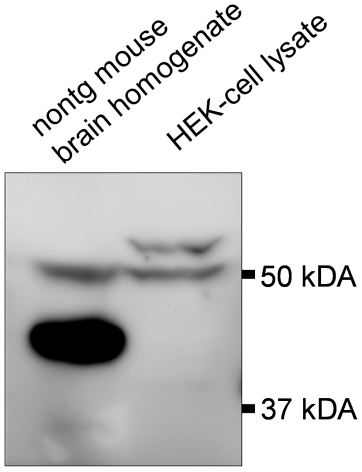

Figure 6. TAR-M-12B4 recognizes murine TDP-43 but not human TDP-43. Immunoblot probed with the TAR M-12B4 antibody comparing non-transgenic mouse brain homogenate and human embryonic kidney (HEK-293) cell lysate. Murine TDP-43 appears in the mouse brain homogenate at 43kDa while human TDP-43 is not detected. 80µg of RIPA lysates were loaded.

We performed a subcellular fractionation protocol using total brain homogenates of 2-month-old males of each mouse line to separate nuclear and cytoplasmic TDP-43 and performed immunoblots analysis using the antibodies TAR5-6D6, Anti-Human TDP-43-specific TARDBP mouse monoclonal antibody (Proteintech) and TAR-M-12B4 to detect total, human and mouse TDP-43, respectively **(Figure 7 A)**. The correct subcellular fractionation was verified with antibodies against histone H3 as marker for the nuclear fraction and tubulin as marker for the cytoplasmic fraction.

The cytoplasmic/nuclear ratios of human TDP-43, endogenous murine TDP-43 and total TDP-43 were comparable in the mouse lines WT-7, M337V-3, M337V-5, G348C-4, revealing a much lower TDP-43 concentration in the cytoplasm compared to the nucleus **(Figure 7)**. Neither did the ALS-associated mutations negatively influence nuclear uptake of human TDP-43 nor did the general overexpression of TDP-43 change the subcellular localization of endogenous TDP-43. Accordingly,

pan-TDP-43 and endogenous TDP-43 ratios of WT-7, M337V-3, M337V-5 and G348C-4 were not changed compared to non-transgenic controls.

Altering the NLS resulted in a significant increase (~8 fold, $p<0.05$) of the cytoplasmic/nuclear ratio of human TDP-43, compared to the mouse lines WT-7, M337V-3, M337V-5 and G348C-4 **(Figure 7 C)**, in line with an inhibited nuclear uptake of human TDP-43 bearing a mutated NLS-sequence. Consequently, the pan-TDP-43 cytoplasmic/nuclear ratio increased significantly (~2.5 fold, $p<0.0001$ **Figure 7 B**), while the cytoplasmic/nuclear ratio of murine TDP-43 remained unaffected compared to non-transgenic controls **(Figure 7 D)**, speaking against a retention effect of NLS-mutated human TDP-43, i.e. increased cytoplasmicTDP-43 did not entrap endogenous TDP-43 or a disturb of the nuclear uptake mechanism due to overexpression of a protein with an altered NLS.

By the previous experiments, we could exclude an influence of human TDP-43 expression on the subcellular localization of endogenous murine TDP-43.

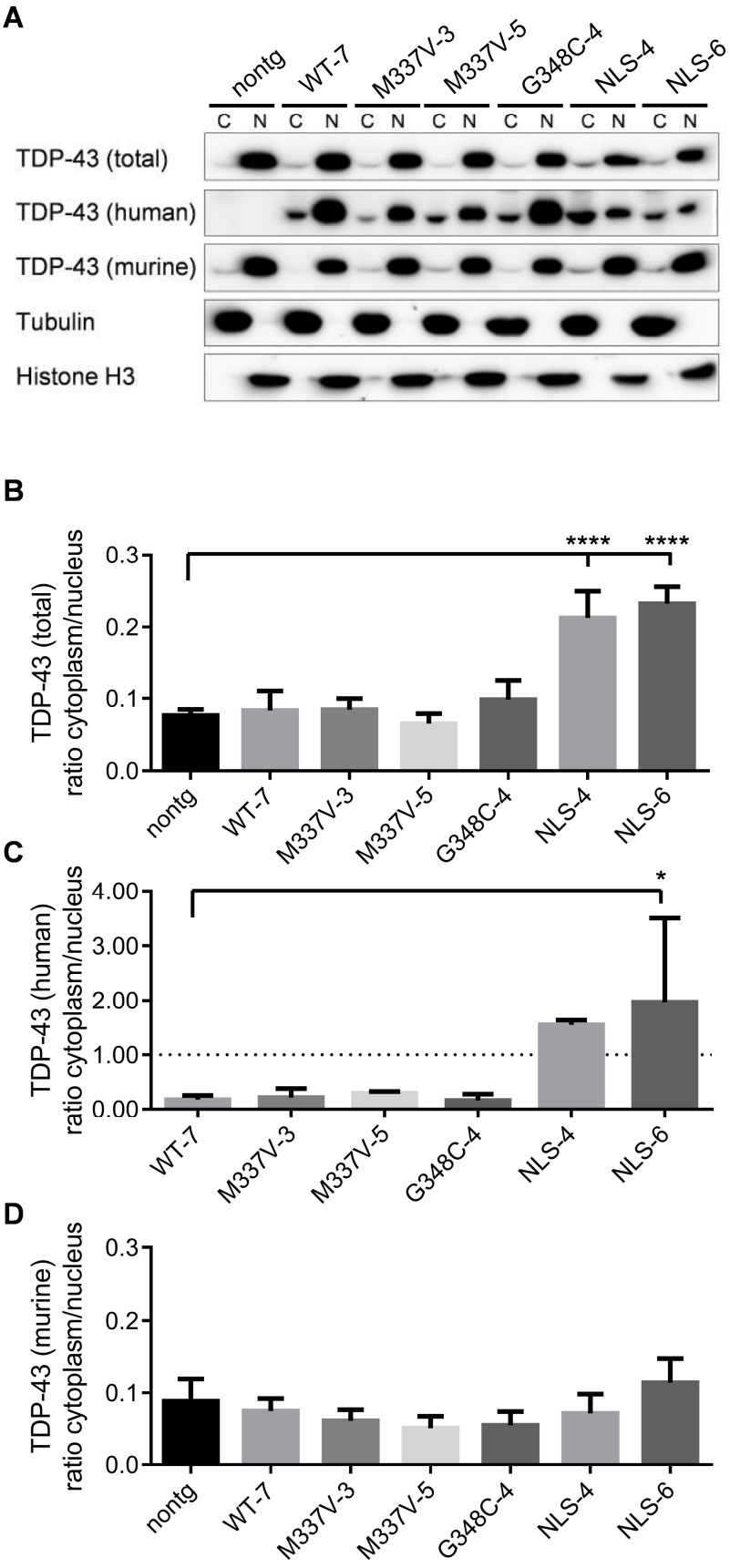

Figure 7. NLS mutation leads to a cytoplasmic shift of human TDP-43. Immunoblots using ratio-adjusted subcellular fractionations of total brain homogenate of 2-month-old males probed with antibodies detecting total TDP-43, human TDP-43 murine TDP-43, respectively. **(B)** A densiometric analysis of band intensities showed a comparable total TDP-43 cytoplasmic/nuclear ratio of ~0.08 in non-transgenic, WT-7, M337V-3, M337V-5 and G348C-4, while significant decrease up to ~0.2 is seen for NLS-4 and NLS-6. **(C)** Both NLS mutant lines show a ~8-fold higher level of human TDP-43 in the cytoplasm compared to WT-7, M337V-3, M337V-5 and G348C-4. **(D)** Similar cytoplasmic/nuclear rations are observed for all transgenic lines and non-transgenic controls demonstrating that the redistribution of human TDP-43 in the NLS-lines does not affect the cytoplasmic/nuclear ratio of murine TDP-43. Tubulin is used as cytoplasmic marker; histone H3 as nuclear marker. Data are based on triplicates and shown as means ± SD; One-way-ANOVA with Dunnett`s multiple comparisons; *p<0.05, ****p<0.0001 compared to non-transgenic controls (total TDP-43; murine TDP-43) and WT-7 (human TDP-43) respectively.

7.3. Downregulation of endogenous TDP-43 upon transgenic TDP-43 expression is independent of *TARDBP* mutations and subcellular localization

It was demonstrated *in vitro* that the TDP-43 protein is able to bind specific regions in its own 3'UTR, activating a normally silent intron 7 in the 3′-UTR, leading to an altered subcellular distribution of the *TARDBP* mRNA that is mostly retained in the nucleus and degraded [145, 146]. The TDP-43 protein levels are thereby tightly regulated by an autoregulatory feedback mechanism. We therefore investigated a possible regulatory effect of transgenic human TDP-43 on the expression levels of endogenous TDP-43 *in vivo*.

First, we compared the mRNA expression levels by quantitative reverse transcriptase-PCR (qRT-PCR) using RNA extracted from brains of 3-month-old males. We utilized human and murine *TARDBP*-specific TaqMan probe sets, based on the detection of fluorogenic labels during PCR amplification. GAPDH was used for normalization. The highest human TDP-43 mRNA expression was observed in the WT-7 line, compared to ~50% in the other transgenic lines **(Figure 8 A)**. Non-transgenic animals were negative for human TDP-43 (not shown). In line with the described autoregulation of TDP-43 expression *in vitro*, we observed a significant decrease of the endogenous murine TDP-43 transcript by 40% ($p<0.05$ / $p<0.01$) with the exception of the M337V-3 and NLS-6 with ~10% and ~30% ($p>0.05$), respectively, in the brains expressing the human transgene compared to non-transgenic controls, independent of human TDP-43 localization or ALS-associated mutations **(Figure 8 B)**.

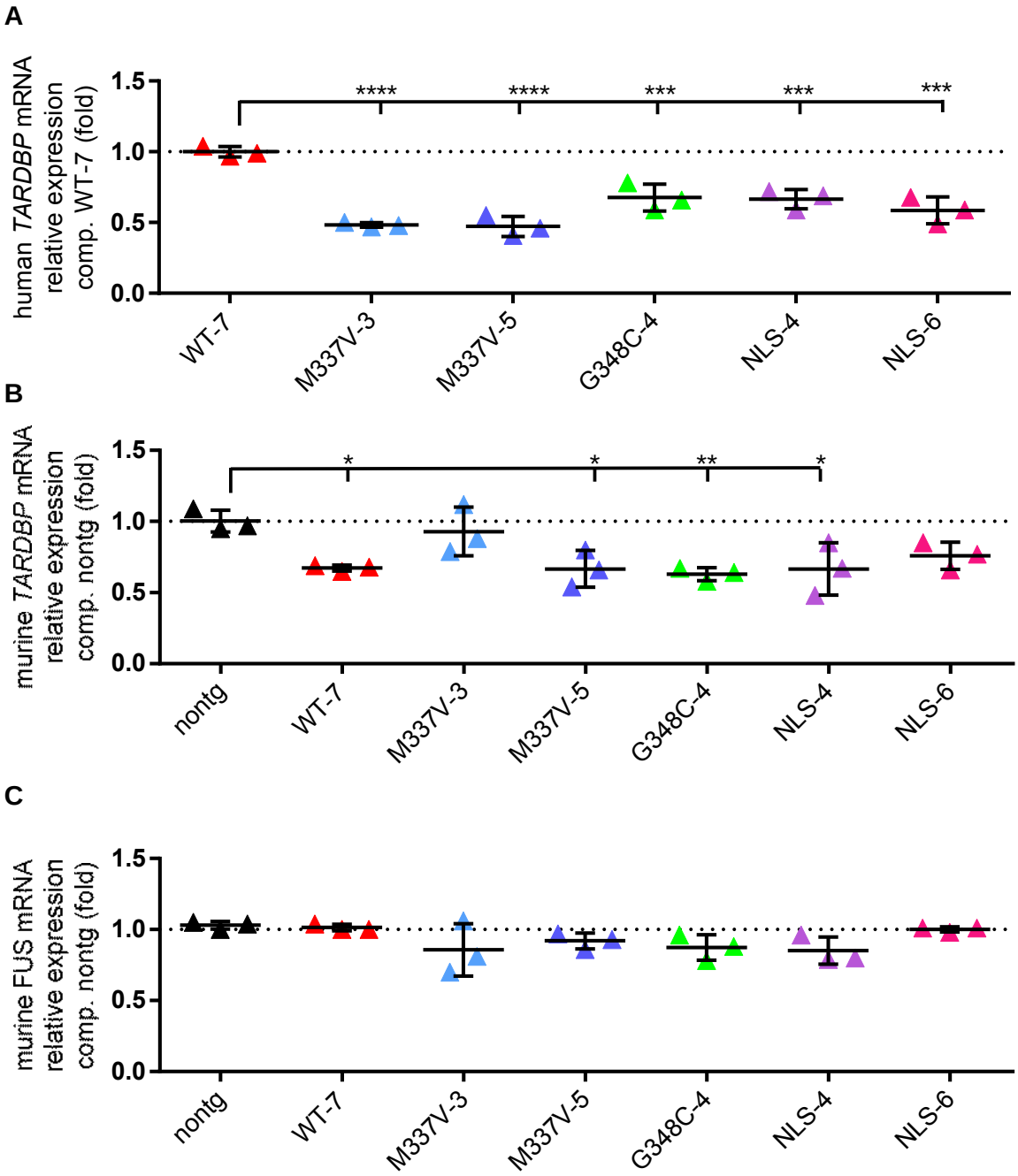

Figure 8. Human TDP-43 overexpression down regulates endogenous murine TDP-43 but does not alter FUS expression. qRT-PCR using mRNA isolated from whole brain tissue. (A) The WT-7 line shows the highest mRNA levels for transgenic human TDP-43 (B) Expression of human TDP-43 results in a decrease of murine TDP-43 mRNA in WT-7, M337V-5, G348C-4, NLS-4 and NLS-6. (C) Expression of different human TDP-43 proteins does not influence the expression levels of FUS/TLS transcript. GAPDH used for normalization; 3 males per genotype, 3-month-old; Data are means ± SD; One-way-ANOVA with Dunnett´s test multiple comparisons *p<0.05, **p<0.01, ***p<0.001, ****p<0.0001

The ALS-associated protein FUS/TLS (Fused in Sarcoma / Translocated in Liposarcoma) has a high structural similarity to TDP-43, both implicated in a wide range of cellular activities, including transcription, alternative splicing, mRNA stability, and RNA-protein granule formation [147]. The 3′UTR of *FUS* mRNA and introns 6 and 7 contain TDP-43 binding sites [55]. TDP-43 binding potentially alters transcript stability and translation rate. We therefor quantified the *FUS* mRNA levels in the same samples used for *TARDBP* mRNA comparisons to investigate potential alterations of FUS expression; however, no differences in *FUS* mRNA expression were detectable in our human TDP-43 transgenic mice **(Figure 8 C)**.

To investigate the autoregulatory effects of TDP-43 on protein level, brain homogenates of 3- to 5-month-old human TDP-43 transgenic males and non-transgenic controls were used to quantify total, human and murine TDP-43 levels in the different transgenic mouse lines by immunoblots. The newly generated antibody TAR-M-12B4 was used to detect the murine TDP-43. For densitometric analysis bad intensities of TDP-43 were normalized to tubulin **(Figure 9 A)**.

WT-7 and G348C-4 showed the highest expression levels of human TDP-43 protein with G38C-4 reaching 80% of the WT-7 level ($p>0.05$). M337V-3, M337V-5, NLS-4 and NLS-6 expressed ~25% of the WT-7 human TDP-43 level respectively ($p<0.0001$) **(Figure 9 B)**. No human TDP-43 was detected in non-transgenic animals. However, the protein levels of total TDP-43 remained comparable between the transgenic lines and non-transgenic males of the same age suggesting that transgenic TDP-43 expression lowers the murine TDP-43 protein levels. This was confirmed by immunoblots with the murine TDP-43 specific antibody showing a reduction of murine TDP-43 in all transgenic lines compared to non-transgenic mice.

The reduction of endogenous TDP-43 was strongest in the WT-7 line (~77%, p<0.0001), followed by M337V-3, G348C-4 and NLS-6 (~40%, p<0.05 / p<0.01%). Therefore WT-7 showed the highest expression of human TDP-43 and the strongest downregulation of endogenous murine TDP-43.

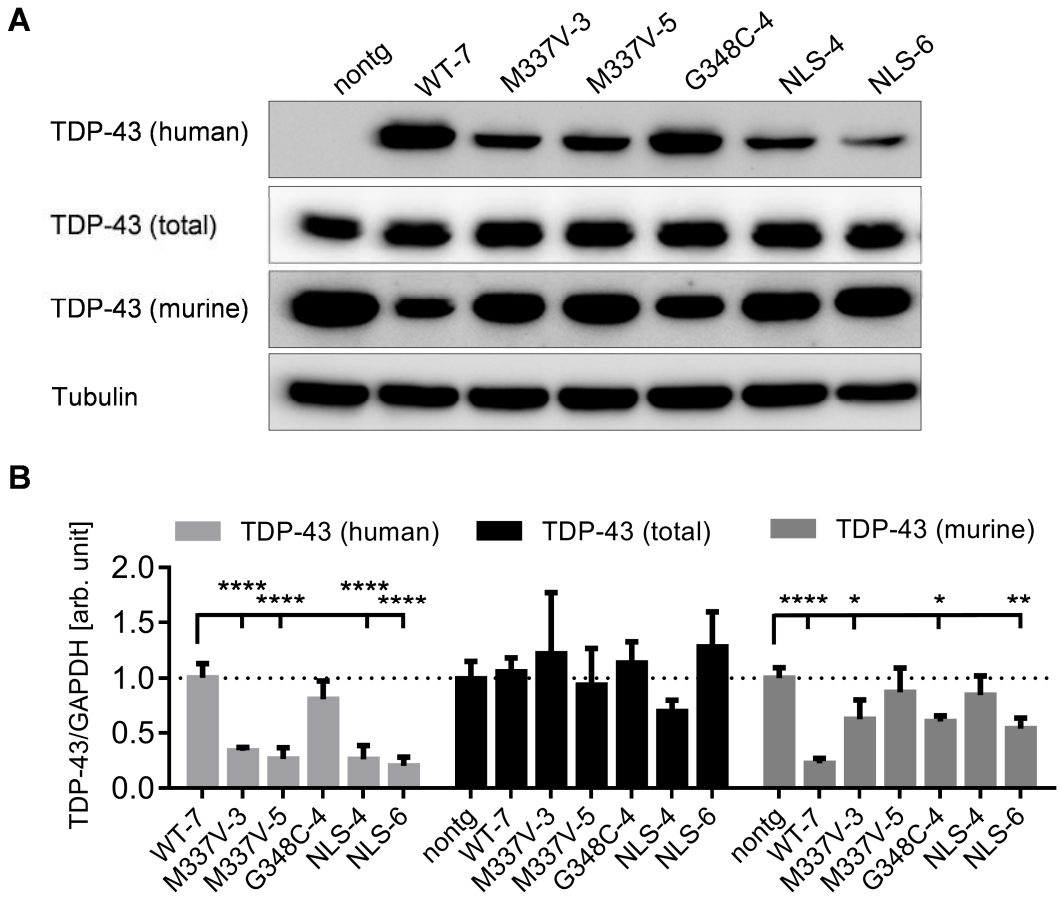

Figure 9. TDP-43 protein levels in the brain of human TDP-43 transgenic mice. (A) Brain homogenates of 2- to 5-month-old males expressing human TDP-43 under the control of the PrnP-promoter probed with antibodies detecting total TDP-43, human TDP-43 or murine TDP-43 respectively. 35µg of RIPA extract are loaded. **(B)** A densitometric analysis of immunoblots using 3 individuals per genotype shows that the WT-7 line has the highest expression of human TDP-43, followed by G348C-4 with ~80% and M337V-3, M337V-5, NLS-4 and NLS-6 with ~25% compared to WT-7. All transgenic lines have comparable levels of total TDP-43 levels between 69 and 128% compared to non-transgenic controls. WT-7 shows the strongest reduction of endogenous murine TDP-43 of ~77% speaking for a correlation with the human TDP-43 expression. Data are means ± SD; One-way-ANOVA with Dunnett´s test multiple comparisons *p<0.05, **p<0.01, ****p<0.0001

The expression level dependent autoregulation of murine TDP-43 was confirmed on a cellular level by double label immunofluorescence staining with mouse and human TDP-43 specific antibodies in brain tissue of the M337V-5 founder with a mosaic expression pattern **(Figure 10)**. The expression of high levels of human TDP-43 resulted in a strong reduction of murine TDP-43.

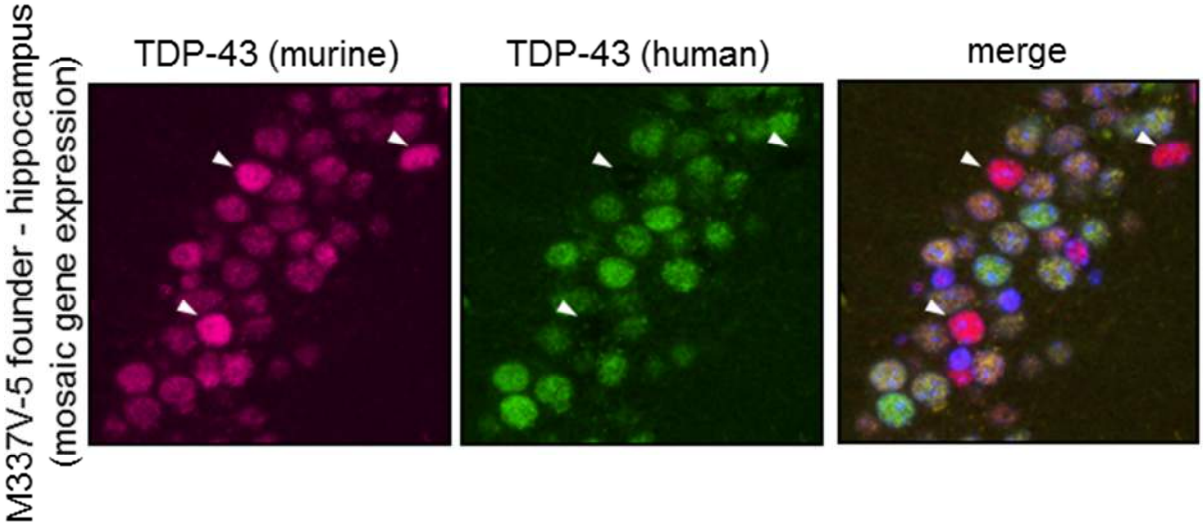

Figure 10. Autoregulatory effect of human TDP-43 on the murine TDP-43 expression. Comparison of human and murine TDP-43 expression in the hippocampal neuron nuclei of the human TDP-43 M337V-5 founder animal with mosaic expression pattern by double label immunofluorescence. In the absence of transgenic human TDP-43, endogenous TDP-43 levels are higher compared to cells expressing transgenic human TDP-43.

In summary, the results demonstrate an autoregulatory effect of transgenic human TDP-43 protein expression on the endogenous murine *TARDBP* transcript and protein levels *in vivo* thereby confirming previous *in vitro* studies. Notably, the downregulation of endogenous TDP-43 is dependent on the protein levels of transgenic TDP-43 but not obviously affected by human pathogenic *TARDBP* mutations and the subcellular distribution of transgenic TDP-43.

7.4. Overexpression of human wild type TDP-43 leads to premature death in WT-7

To investigate functional consequences of human TDP-43 expression, we performed longitudinal studies by a frequent monitoring program, including the ability and willingness to move, the body shape and body weight control. Furthermore, we conducted motoric and cognitive tests at different time points. We observed a premature death in the WT-7 line compared to non-transgenic controls with a mean lifespan of 133.6±39.7 days ($p<0.0001$). The life expectancy of the other human TDP-43 transgenic lines remained unchanged compared to non-transgenic controls **(Figure 11 A)**. End stage WT-7 animals revealed a swollen abdomen, a hunchback appearance and a reduced activity compared to non-transgenic littermates **(Figure 11 B)**. By breaking down the survival data of WT-7 animals according to the gender, we observed a significant gender-dependent difference in survival times (mean lifespan: 103±16.7 days in males compared to 157.5±33.4 days in females, $p<0.0001$) (**Figure 11 C**). Both genders of WT-7 showed a tendency towards a lower body weight during the presymptomatic phase and a significant loss of body weight during the weeks before death (**Figure 11 D**). The altered body shape and reduced activity were observed in both genders. Based on these findings, we modified the health monitoring of the WT-7 line with defining termination criteria based on the body shape, activity and body weight loss within one week **(Table 2)**. Given that WT-7 develops its characteristic phenotype quite rapidly, we monitored the animals on a daily basis starting with the age of 60 days for males or 95 days for females. Animals reaching the defined endpoint criteria were euthanized.

None of the other human TDP-43 transgenic lines showed a pathological phenotype or an altered lifespan similar to WT-7. Both genders were indistinguishable from non-transgenic littermates.

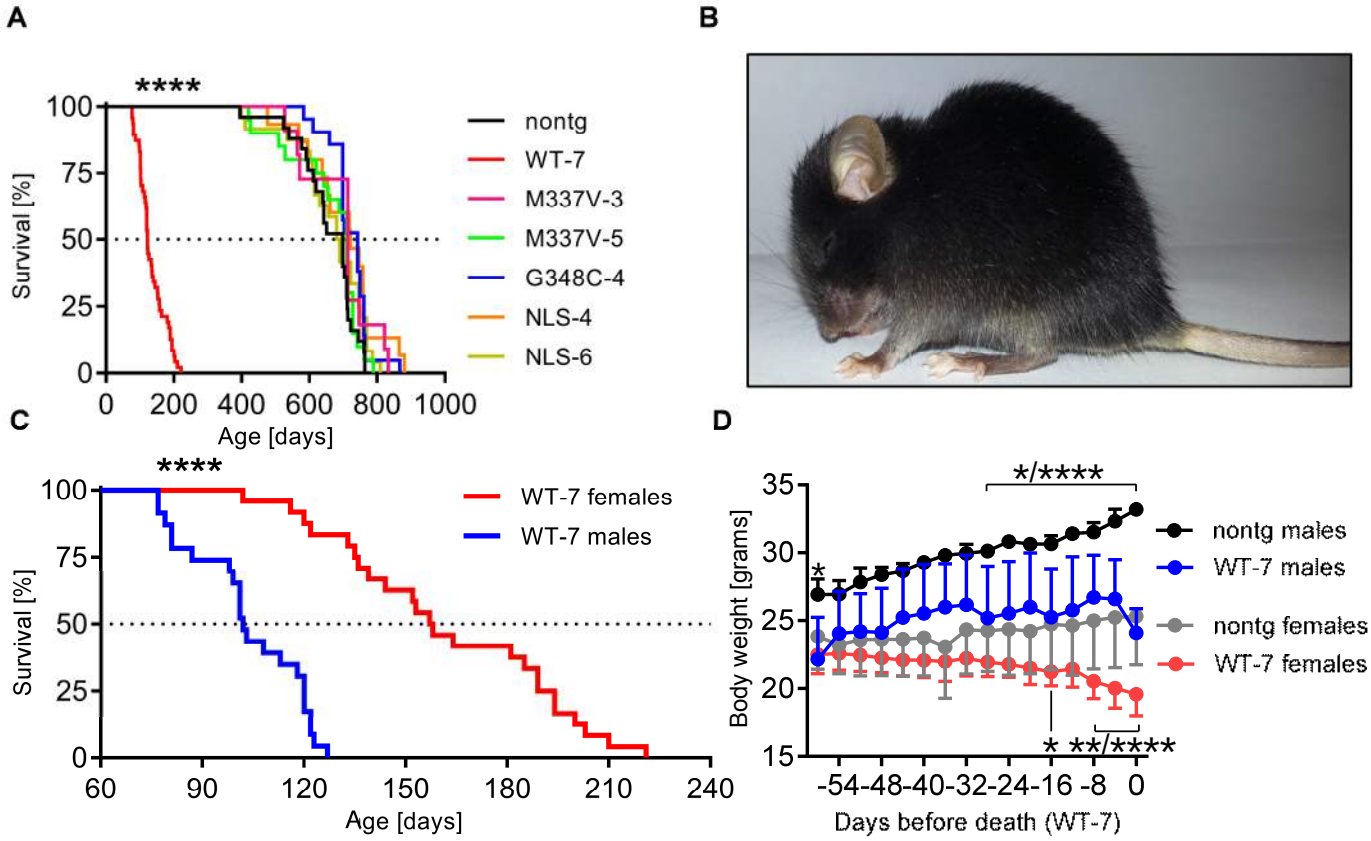

Figure 11. WT-7 animals die premature compared to the other human TDP-43 transgenic animals with an earlier onset in males and weight loss prior death (A) WT-7 animals die premature with an mean lifespan of 133.6±39.7 days in contrast to the other transgenic lines showing a normal life expectancy compared to non-transgenic littermates (WT-7 n= 47; nontg n=25; G348C-4 n=21; M337V-3 n=11; M337V-5 n=20; NLS-4 n=15; NLS-6 n=24; including both males and females). **(B)** End stage female mouse, 69 days old, showing a hunchback appearance with a swollen abdomen, reduced motoric activity and rapid weight loss over 2 to 3 days. The end stage phenotype is identical in males and females. **(C)** WT-7 males show a significantly reduced life span compared to transgenic females (mean lifespan: 103±16.7 days compared to 157.5±33.4 days, n=23/24). **(D)** A reduced body weight is observed in WT-7 animals of both genders compared to non-transgenic littermates with a significant drop close to death. Survival data are analysed by Log-rank (Mantel-cox) test; body weight by Two-way-ANOVA with Sidak multiple comparisons. Bars represent means ± SD; *p<0.05, **p<0.01, ****p<0.0001

7.5. Phenotype in WT-7 is due to alterations of the gut

End stage WT-7 animals showed a swollen abdomen. Closer examination at autopsy revealed a consistent dilatation of the lower ileum, cecum and upper colon in both genders, all filled with intestinal contents (**Figure 12 A**). To quantify these alterations, the circumference and thickness of the muscular layers were measured on six consecutive sections of the proximal duodenum, distal ileum and proximal colon of formalin-fixated, paraffin-embedded tissue from end stage WT-7 males and non-transgenic littermates.

We observed a strong dilatation of the ileum and a less pronounced dilatation of the duodenum and colon of WT-7 males shown by an increase in diameter compared to non-transgenic littermates (duodenum: 2597.88±364.44 µm vs. 2314.26±226.10 µm, $p<0.01$; ileum: 4273.73±406.19 µm vs. 2255±281.83 µm, $p<0.0001$; colon: 3909.60±1107.77 µm vs. 2813.34±615.09 µm, $p<0.01$) **(Figure 12 B)**. A muscular hypertrophy was seen in the circular and longitudinal muscle layers of the ileum (circular muscle: 43.66±13.94 µm vs. 26.58±9.35µm, $p<0.0001$; longitudinal muscle: 28.52±10.02µm vs. 18.05±8.24µm, $p<0.05$) as well as in the longitudinal muscle of the colon (22.36±10.91µm vs. 17.27±9.06µm, $p<0.01$) **(Figure 12 C)**, while both muscle layers in the duodenum and the circular muscle layer in the colon revealed no changes in muscle thickness (duodenum circular muscle: 18.07±6.11µm vs. 20.02±7.30µm, $p=0.1351$; duodenum longitudinal muscle: 12.96±4.60µm vs. 13.93±5.28µm, $p=0.3075$; colon circular muscle: 73.88±35.05µm vs. 67.34±25.21µm, $p=0.2680$)

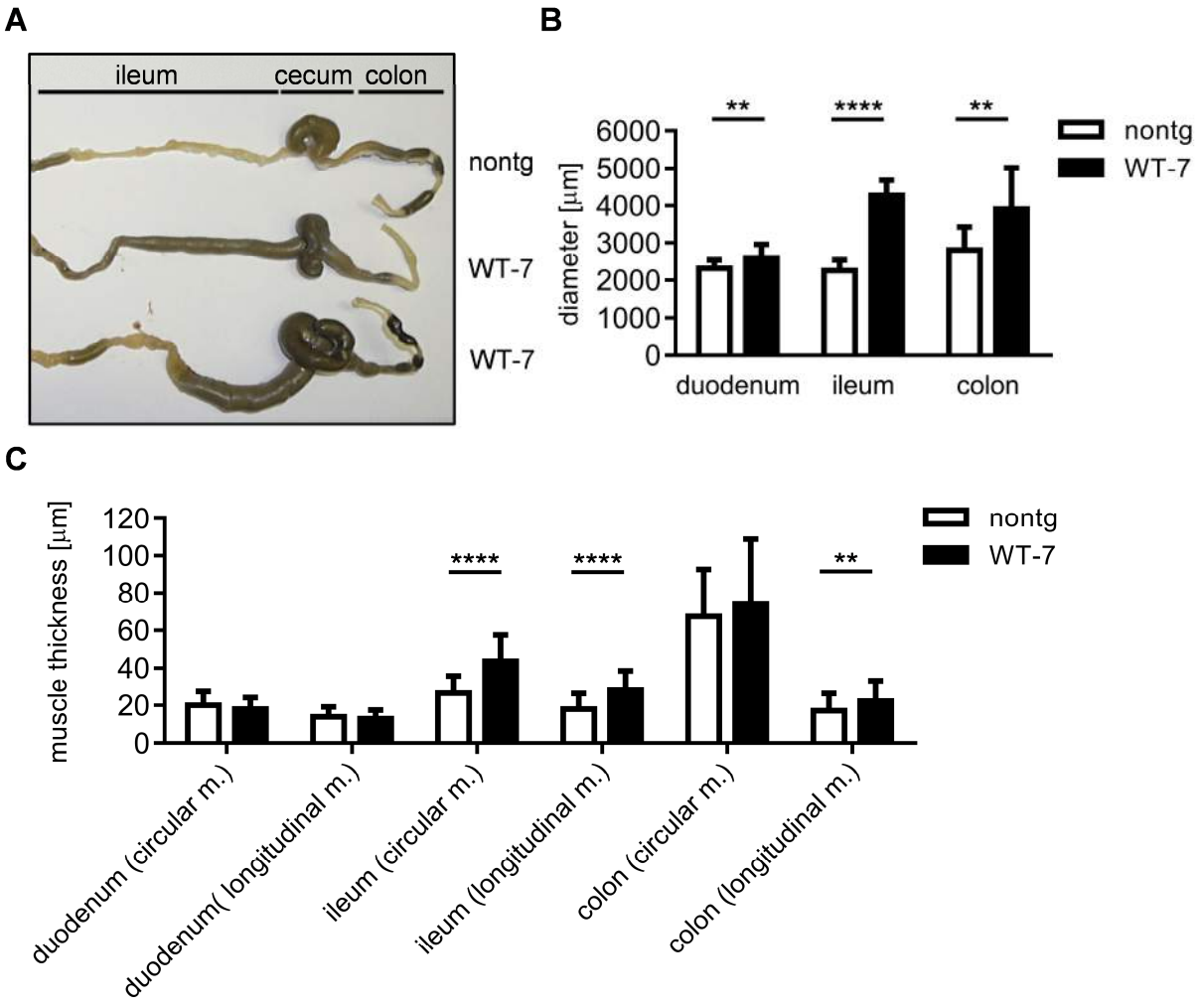

Figure 12. End stage WT-7 animals have an increased intestinal diameter in the duodenum, ileum and colon and thickened muscular layers in the ileum and colon. (A) End stage WT-7 animals of both genders have a dilated ileum, cecum and colon. **(B)** End stage WT-7 males show an increased diameter of the duodenum, the distal ileum and the proximal colon, more pronounced in the ileum **(C)** Muscle hypertrophy was observed in the circular and longitudinal muscle layer of the ileum as well as in the longitudinal muscle layer of the colon. Data are analysed by unpaired t-test; bars represent means ± SD; **p<0.01, ****p<0.0001

The data argue for alterations of the gut motility in WT-7. As demonstrated by immunoblots in **Figure 5**, all transgenic lines showed human TDP-43 expression in the gastrointestinal system. To further examine the cell types expressing human TDP-43, we performed IHC-staining on the ileum and colon of 6-month-old females, including end stage WT-7 females. All our transgenic lines showed an expression of human TDP-43 mainly restricted to ganglia cells in the myenteric plexus

(Figure 13 A), localized between the circular and longitudinal muscular layer in the gastrointestinal tract. The myenteric plexus forms a crucial part of the enteric nervous system (ENS) as it innervates both muscle layers and controls the gastrointestinal tract motility autonomously. We concluded that the phenotype of the WT-7 mice is most likely due to dysfunction of the ENS. Importantly, the presence of transgenic TDP-43 expression in the ENS in all transgenic mouse lines excludes that the phenotype in the WT-7 is due to a unique expression pattern in this line and argues for a specific dysfunction of the ENS upon human wild type TDP-43 expression.

To investigate whether the phenotype is associated with a reduction of neurons, we quantified the number of neurons in the myenteric plexus in 3 months old end stage WT-7 animals compared to non-transgenic littermates and age-matched males of the mouse lines M337V-5 and G348C-4. Distal ileum and proximal colon samples were gathered from three animals per group. The fixed muscular layers including the myenteric plexus were separated from the mucosa layers and stained as partial whole-mount with Azur II for investigation of neurons. We adjusted the numbers of neurons/mm^2 to the ileum and colon circumference of the non-transgenic males to control for dilatation.

We observed a strong decrease of ~50% in ganglia cell density in the proximal colon of end stage WT-7 males (249±59 vs. 436±94 per mm^2, $p<0.0001$) and a slight reduction in the G348C-4 line (359±43 vs. 436±,94 per mm^2, $p<0.05$) compared to non-transgenic littermates **(Figure 13 B and C)**.

These results suggest a dysregulation of the enteric nervous system by a decreased number of ganglia cells due to human wild type TDP-43 overexpression, resulting in an altered gastrointestinal motility. Furthermore, the dysfunction of gastrointestinal motility appears to originate from the colon.

Both TDP-43 hyperphosphorylation and an increased ubiquitin-staining in the CNS are frequent features of TDP-43 proteinopathies. In particular, phosphorylation of S409/410 of TDP-43 is consistently observed in all sporadic and familial forms of TDP-43 proteinopathies whereas ubiquitination might indicate abnormal accumulations of TDP-43 or other proteins [132]. Therefore, we analysed the tissue slide sets of the 6-month-old females with an antibody detecting phosphorylated TDP-43 at S409/410 sites and an antibody targeting ubiquitin. Ganglia cells showed no indication for phosphorylated TDP-43 species **(Figure 14 A)**. Ubiquitin-positive staining was present in the ganglia of both transgenic animals and non-transgenic controls without aggregate formation. We concluded that the remaining ganglia cells in the colon of end stage WT-7 animals do not show features frequently seen in TDP-43 proteinopathies.

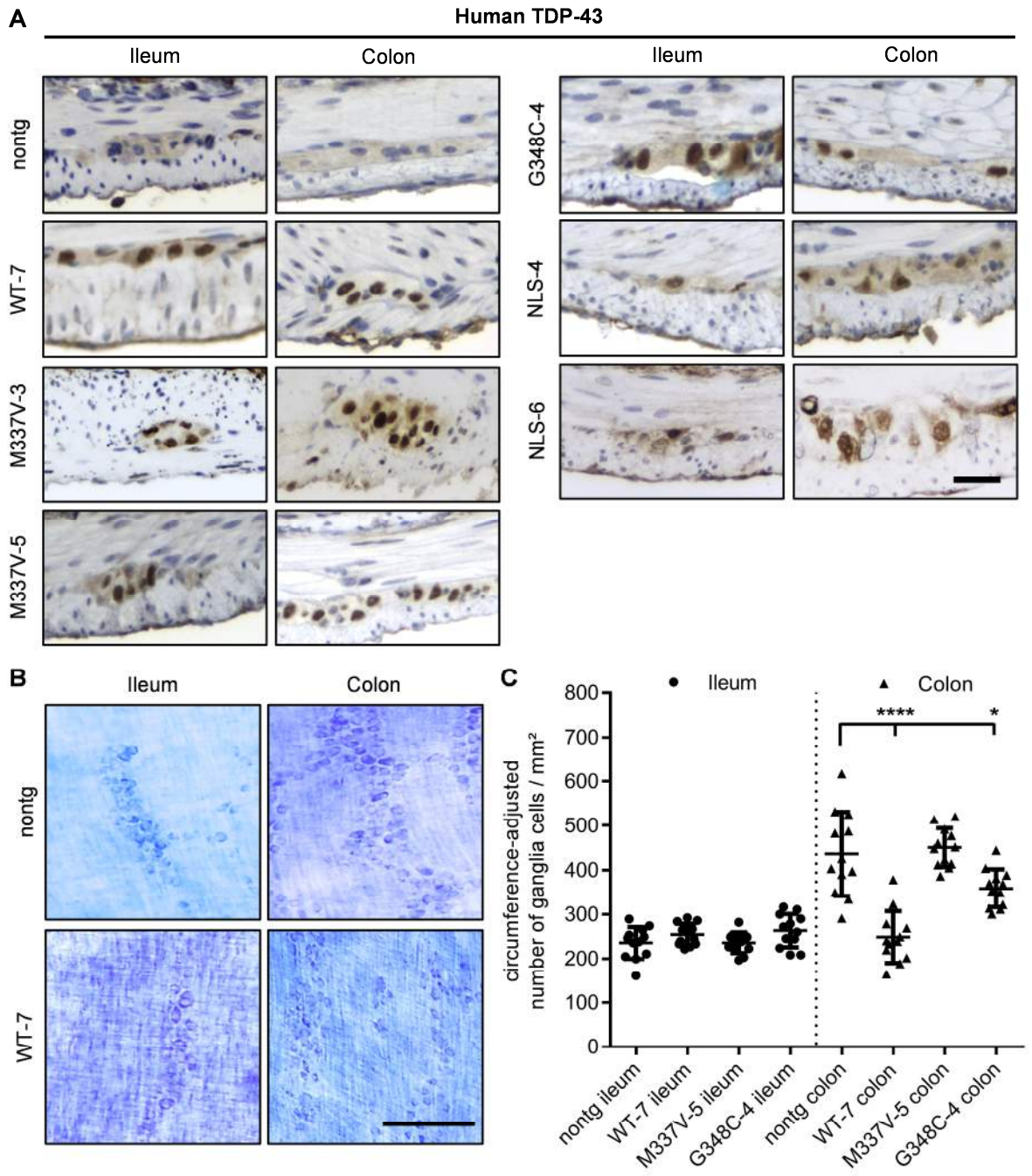

Figure 13. Human TDP-43 is expressed in the enteric nervous system of all human TDP-43 transgenic lines; in WT-7 mice, the ganglia cell density is reduced at the clinical endpoint. (A) Expression of human TDP-43 in ganglion cells in the myentric plexus of ileum and colon of 6-month-old female mice shown by IHC with a human TDP-43 specific antibody. Human TDP-43 is mainly localized in the nucleus similar to the CNS apart from the NLS-mutants with cytoplasmic and nuclear localization. Scale bar 25µm **(B)** Azur II stained ganglia cells of the myenteric plexus. Scale bar 50 µm. **(C)** Counting of the ganglia cells and adjustment to the circumference ratio revealed a strongly reduced ganglia cell density in the WT-7 colon, a slight reduction in G348C-4 and no changes in M337V-5 compared to non-transgenic animals. 3 animals per group, 3-month-old. Data are analysed by One-way-ANOVA with Dunnett´s test multiple comparisons; bars represent means ± SD; *p<0.05, ****p<0.0001

A loss of ganglia cells can be associated with an increased acetylcholinesterase (AChE) activity, as demonstrated in Hirschsprung's disease [148]. We performed enzyme histochemistry on frozen sections, covering the distal half of the small intestine and full colon and rectum of 3-month-old end stage WT-7 males and non-transgenic littermates using the "Swiss-role" technique. Both intestinal segments showed no evidence for an increased AChE activity in the WT-7 tissue **(Figure 14 B)**.

An alternate explanation for intestinal dysmotility is a lower density of the interstitial cells of Cajal (ICC) as seen in human slow transit constipation [149]. As pacemaker cells, they regulate the contraction of the intestinal smooth muscles by creating a periodical bioelectrical slow wave potential and therefor setting the basal electrical rhythm of the intestine. We performed immunofluorescence staining on frozen sections mentioned before using a c-Kit (CD-117) antibody, targeting a cytokine receptor abundant in ICCs. We observed comparable numbers of ICCs based on semi-quantitative assessment in the small intestine and colon of WT-7 males and non-transgenic controls. Furthermore, the localization of ICC subtypes in different tissue layers appeared to be unchanged **(Figure 14 C)**.

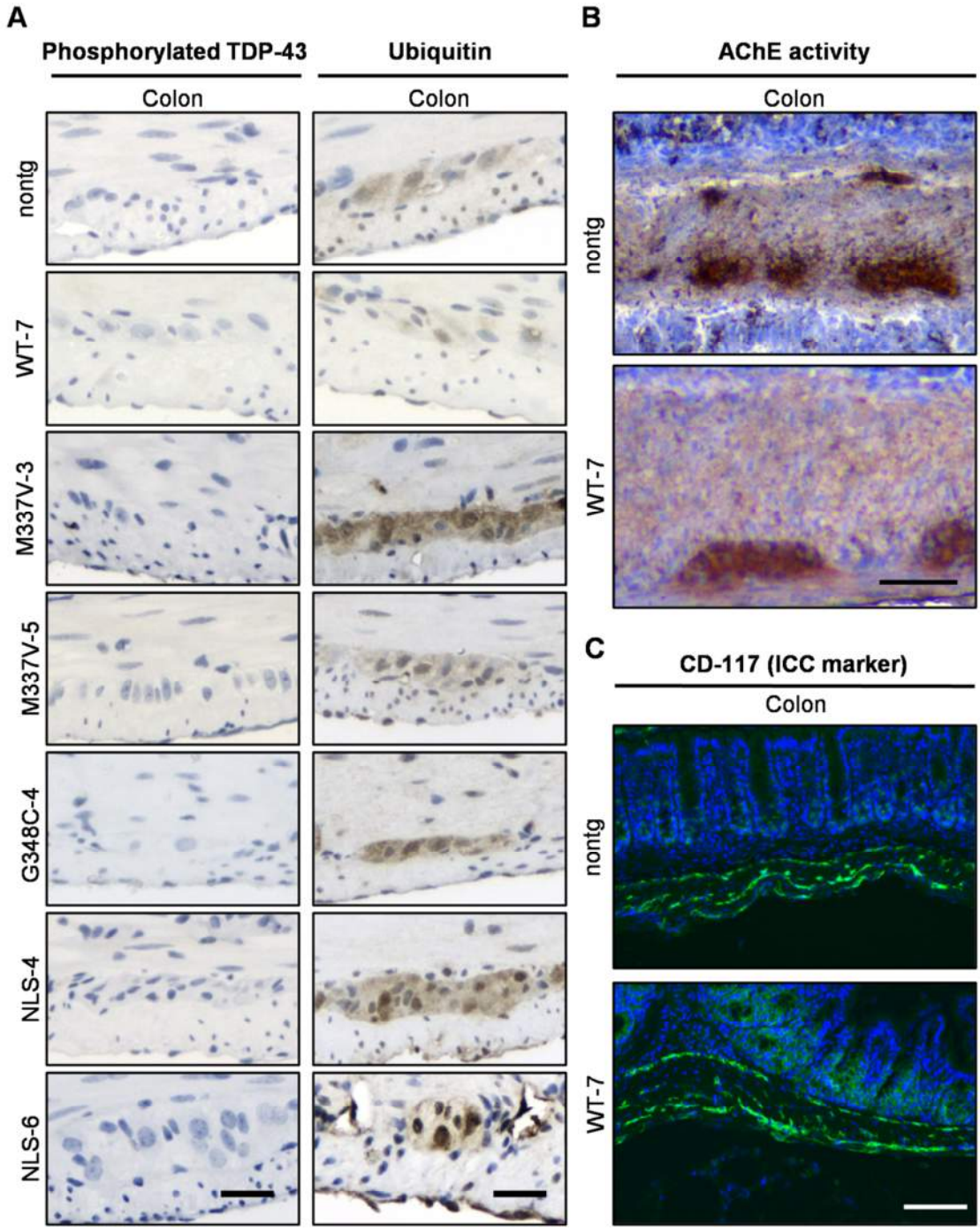

Figure 14. TDP-43 overexpression in the ENS does not induce hyperphosphorylation, increased ubiquitin staining, increased AChE-activity or adisruption of the ICC pattern. (A) IHC staining for phosphorylated TDP-43 and ubiquitin in ganglion cells of the ileal and colonic myentric plexus of 6-month-old mice. None of the TDP-43 transgenic mice or the non-transgenic controls showed phospho-TDP-43-positve inclusions using the antibody TAR5p 1D3 for the phosphorylated sites pS409/410. Diffuse staining for ubiquitin indicated the existence of ubiquitin-mediated proteolysis without major differences between the strains. Ubiquitin-positive inclusions are not observed. **(B)** 3-month-old end stage WT-7 males showno increase of acetylcholine esterase activity in “swiss role” frozen sections of the colon. **(C)** The distribution and density of intestinal cells of Cajal remains unchanged in the colon of 3-month-old end stage WT-7 males. Scale bar 25 µm.

7.6. Motor performance and cognitive tests

Important clinical hallmarks of human TDP-43 proteinopathies are motor function deficiencies caused by a progressive loss of motor neurons in ALS or worsening cognitive capabilities resulting from a loss of cortical neurons in FTLD. The effect of human TDP-43 expression on the locomotive abilities was monitored in females of the WT-7 line ranging from 50 to 200 days of age and in females of the G348C-4 and M337V-5 lines within an age range of 300 to 600 days **(Figure 15)**. The motoric tests persisted of rotarod, paw grip endurance and grip strength measurements and have been performed twice weekly (WT-7) or biweekly (G348C-4 and M337V-5). These tests cover motor coordination, endurance and the maximal muscle strength of the limb muscles. All monitored lines showed no locomotive constraint compared to non-transgenic littermates speaking against pathological changes in the motor nervous system. Notably, WT-7 animals in the early pathological stage marked by a swollen abdomen showed an unchanged motoric performance in the described tests.

We performed two different tests to assess the cognitive abilities of WT-7, M337V-5 and G348C-4 animals, novel object recognition test (NORT) and Y-maze, both supported by a video-based animal tracking system (**Figure 16**). The WT-7 animals were tested between the age of 56 to 146 days, the M337V-5 and G348C-4 between the age of 335 and 558 days. NORT based on the spontaneous tendency of rodents to spend more time exploring a novel object than a familiar one based on learning and recognition memory. The Y-maze consisted of three opaque arms arranged in a star-like manner, allowing to test for alterations in the spatial memory.

WT-7, M337V-5 and G348C-4 showed similar results for distance, immobile time and maximum speed when compared to non-transgenic controls in both NORT and Y-maze. Furthermore, they showed no indication for a higher anxiety in the NORT environment (data not shown). We observed a couple of significantly altered results at different time points. In particular, we did not observe age dependent differences, speaking against an overall trend to cognitive decline during aging. However, these conclusion needs to be treated with caution because of high variability in the results.

The absence of a motor phenotype or cognitive deficits made a major pathological alteration in the CNS unlikely. All transgenic lines were screened by IHC for presence of phosphorylated TDP-43 (**Figure 17**), reactive gliosis using GFAP as marker, activation of microglia and macrophages using IBA1 as marker and presence of ubiquitin aggregates in the CNS (**Figure 18**). Brain and spinal cord tissue was collected from males and females every second month of age starting with at one month of age up to the age of 12 or 13 months. Furthermore, sample tissue was collected from 24 or 25 months old geriatric mice. An exception was the short living WT-7 line with the oldest animals of 3 months (males) and 6 months (females) respectively. Consistent with results for motor dysfunction and cognitive impairment, none of the transgenic lines showed aggregates incorporating phosphorylated TDP-43 or ubiquitin-positive proteins. No evidence for neurodegeneration in the CNS with absence of astrogliosis and microgliosis was observed.

Thus, the lethal WT-7 phenotype appears to be caused by toxic effects of TDP-43 expression in the nervous system, suggesting that these neuron populations are the most vulnerable in our mouse model.

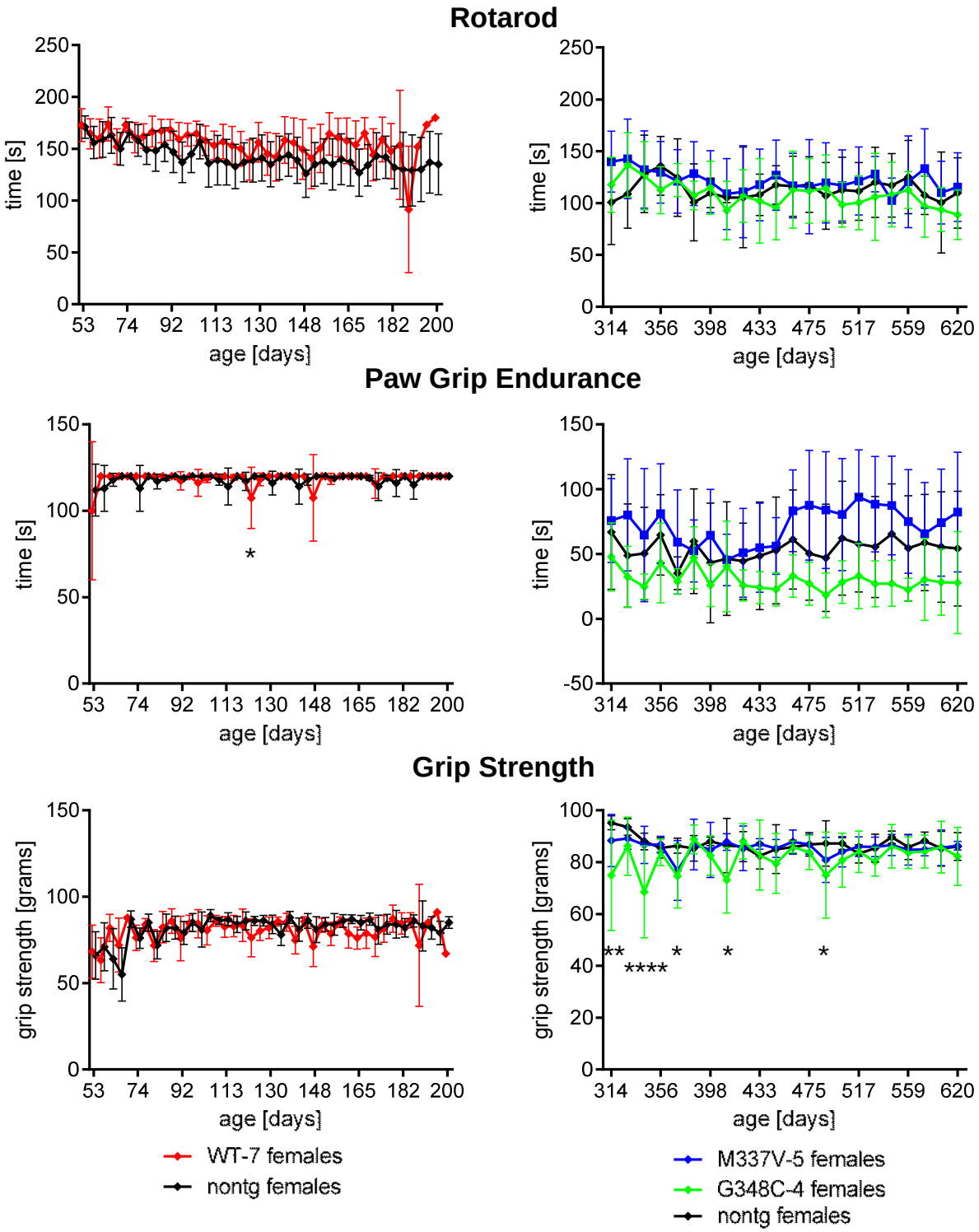

Figure 15. Motoric tests show no locomotive constraint in WT-7, M337V-5 and G348C-4 females compared to non-transgenic littermates. Forced motor activity was tested with the rotarod performance test. Paw grip endurance (PAGE) as well as the grip strength test show no constraints regarding the endurance or maximum applicable force of the limbs. n=13 for transgenic WT-7 females, n=14 for non-transgenic WT-7 littermates; n=9 for M337V-5 females, n=8 for G348C-4 females, n=6 for non-transgenic littermates of the same age (3x M337V-5 nontg; 3x G348C-4 nontg); Data are analysed by Two-way-ANOVA with Sidak multiple comparisons, bars represent means ± SD; *p<0.05, **p<0.01, ****p<0.0001.

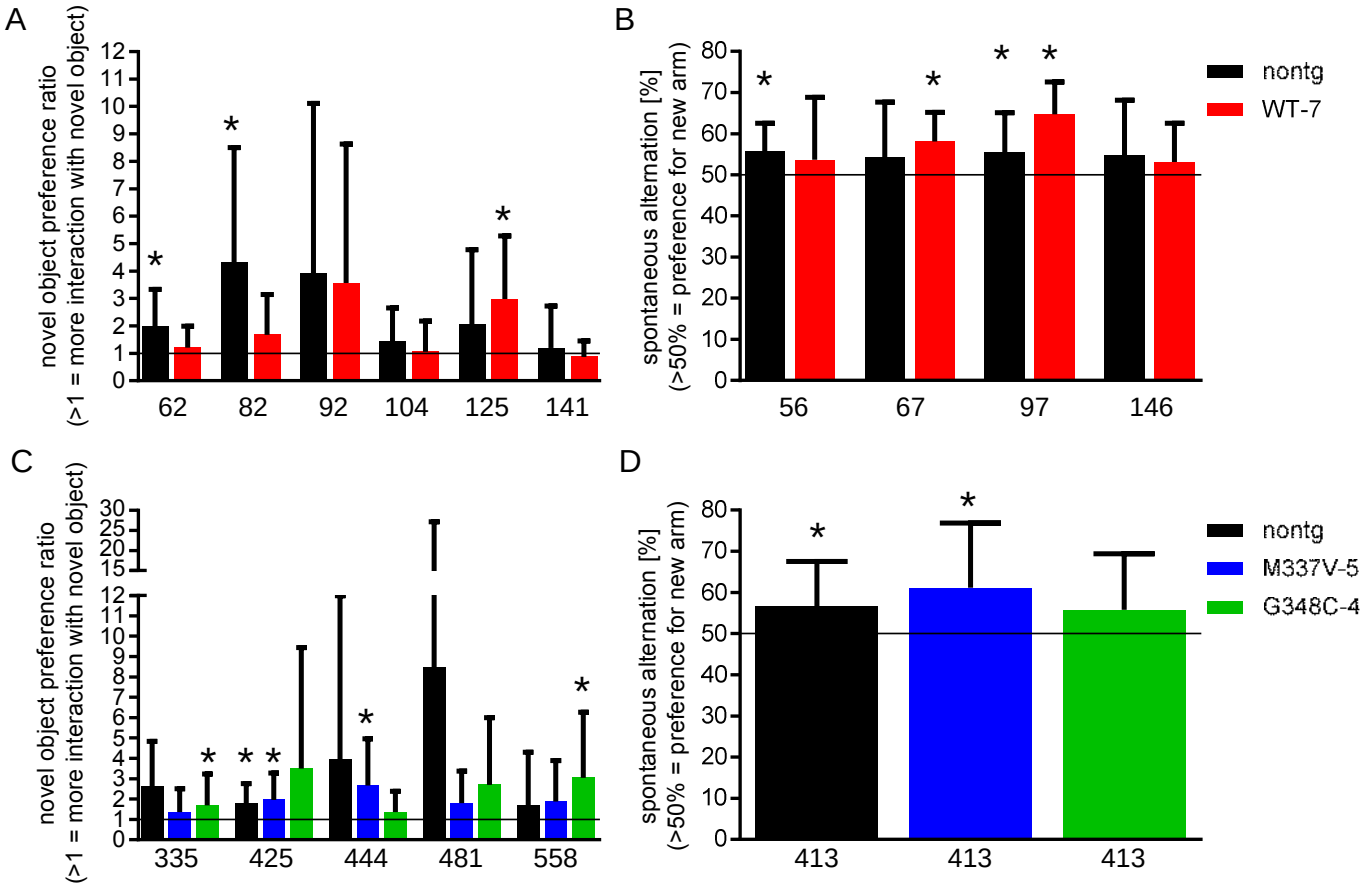

Figure 16. Behavioural tests reveal no cognitive deficits in WT-7, M337V-5 and G348C-4 animals compared to non-transgenic animals. (A) No significant cognitive deficit was observed in WT-7 animals of both genders tested by a novel object recognition test (NORT). **(B)** WT-7 animals showed the same preference for a new arm in a left–right discrimination paradigm of a Y-maze as non-transgenic controls. **(C and D)** Aged M337V-5 and G348C-4 animals show the same cognitive performance in the NORT and Y-maze as non-transgenic controls. n=7 for transgenic WT-7 (3 males / 4 females), n=14 for non-transgenic WT-7 littermates (6 males / 8 females); days 125 and 141 do not include WT-7 males. n=13 for M337V-5 (9 females; 4 males), n=15 for G348C-4 (7 males / 8 females), n=16 for non-transgenic littermates of the same age (11 males / 5 females); Data are analysed by One-Sample t-test against 1 (NORT) or 50 (Y-maze), one-tailed, bars represent means ± SD; *p<0.05.

.

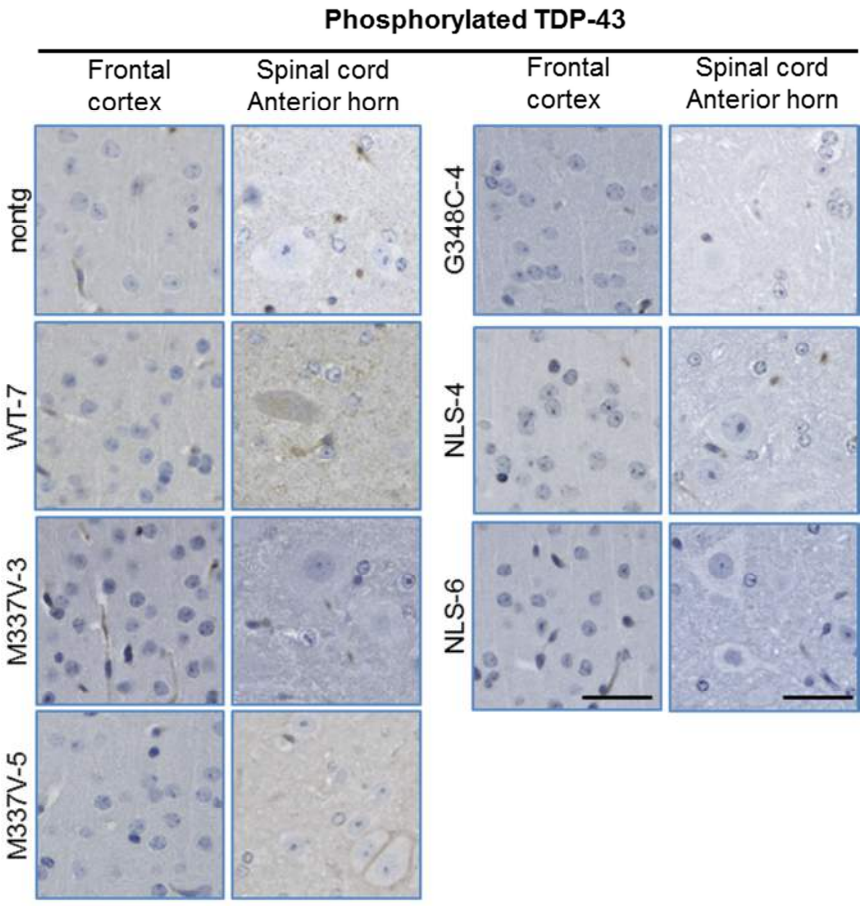

Figure 17. TDP-43 is not hyperphosphorylated in our human TDP-43 mouse models. IHC with an antibody detecting phosphorylated TDP-43 sites at the C-terminus (pS409/410) on brain and spinal cord tissue of 3-month-old males. None of the transgenic lines show nuclear or cytoplasmic inclusions positive for phosphorylated TDP-43, a consistent feature in all sporadic and familial forms of TDP-43 proteinopathies. Scale bar: 20 µm.

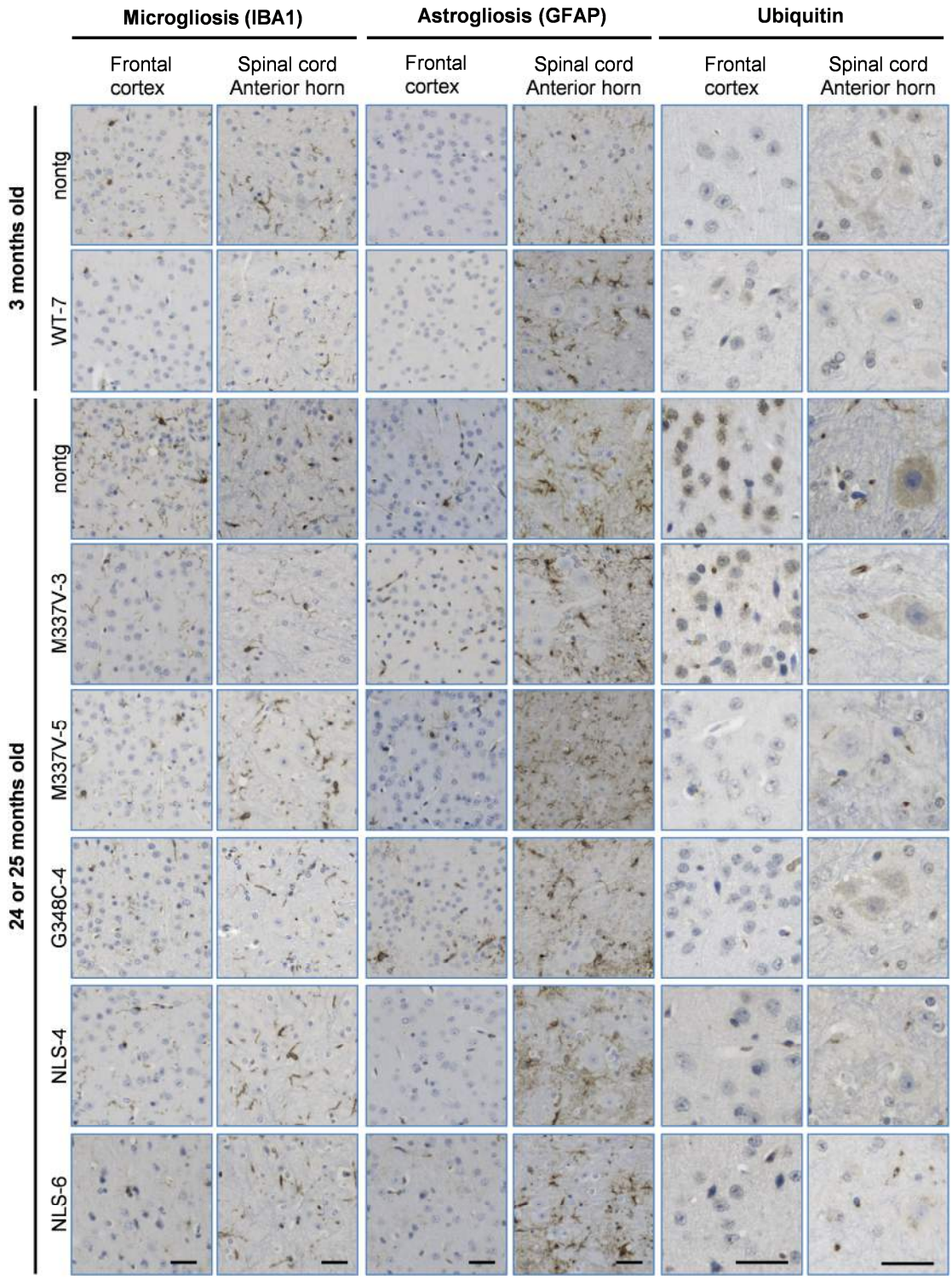

Figure 18. Brain and spinal cord of human TDP-43 expressing mice show no indications for neuroinflammation or impaired protein degradation. IHC with an antibody against IBA1, a marker for microgliosis, GFAP, a marker for astrogliosis, and ubiquitin. 3-month-old end stage WT-7 males and aged males of the other human TDP-43 transgenic lines show no signs of neurodegeneration in the CNS compared to non-transgenic animals. There is no evidence for an accumulation of ubiquitin-positive protein aggregates, speaking against an inhibition of protein degradation or an increase of aberrant protein species. Scale bar: 20 µm.

7.7. Gender-dependent life span discrepancy in WT-7 animals is estrogen dependent

WT-7 mice showed premature lethality with a striking gender difference for survival times (average life span: 103±16.7 days compared to 157.5±33.4 days; p<0.0001) **(Figure 11 C**).

A possible explanation for the gender difference would be a beneficial or detrimental effect of sex specific hormones. To investigate this, we castrated WT-7 males and ovariectomized WT-7 females shortly before sexual maturation at the age of 30 to 35 days. The mice were closely monitored and euthanized when the terminal stage was reached, defined by the WT-7 control sheet **(Table 2)**. Ovariectomized WT-7 females showed a reduced life span compared to sham operated WT-7 control females (mean age at terminal endpoint: 113.4±10.9 days vs. 128.8±17.3 days, p=0.0114) **(Figure 19 A)**. In contrast, castration of WT-7 males did not alter the life span compared to sham operated WT-7 control males (mean age at terminal endpoint: 109.9±24.2 days vs. 100.9±11.9 days, p=0.4170) **(Figure 19 B)**. The groups of sham operated mice included of 12 animals of females and males respectively. 6 sham females and 7 sham males obtained an additional placebo pellet without hormones to exclude a general effect of subdermal implants on the life span. The life span of sham operated mice with a placebo pellet was equal to mice with sham surgery without placebo pellet (mean age at terminal endpoint females: 134.5±19.91 vs. 123.20±13.67 days, p=0.2771; mean age at terminal endpoint males: 97.86±13.70 days vs. 105.20±8.44 days, p=0.3160; t-test). Therefore, all sham operated animals with placebo pellet were treated as sham operated mice for further investigations.

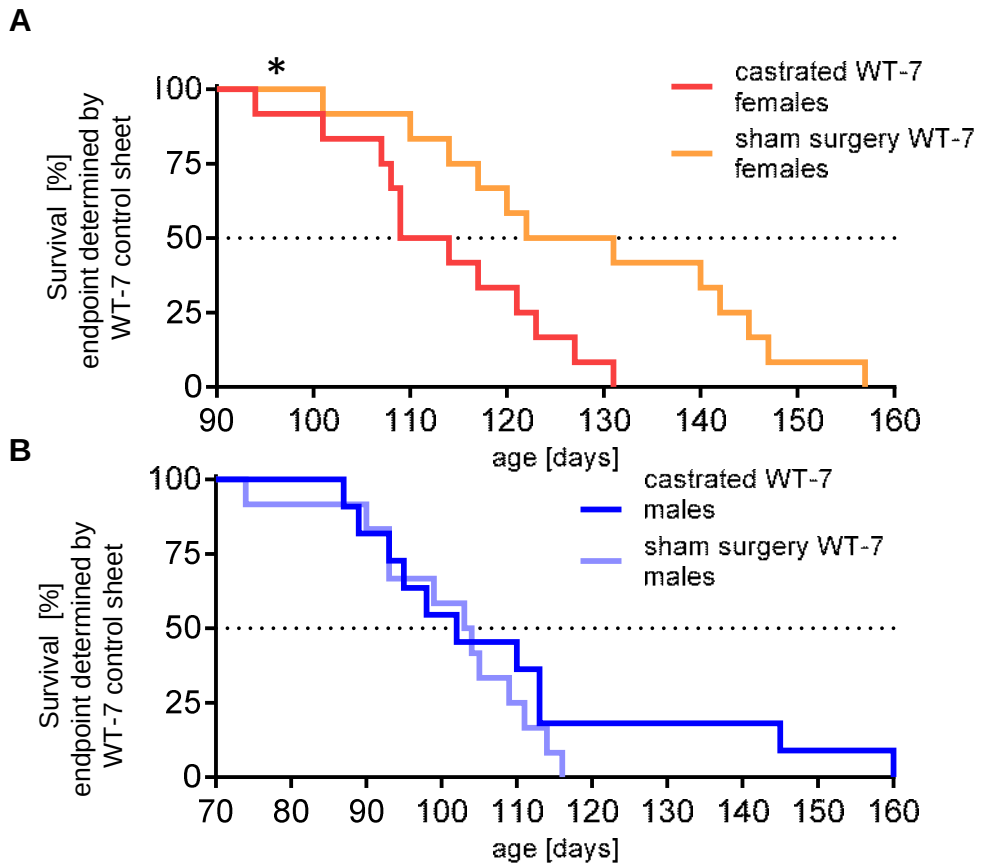

Figure 19. Gender-depended life discrepancy is mediated by female sex hormones (A) Ovariectomy of human TDP-43 WT-7 females leads to a reduced life span compared to sham operated WT-7 females (mean life span: 113.4±10.9 days to 128.8±17.3 days; n=12; SD, p=0.0114). **(B)** In contrast, castration of human TDP-43 WT-7 males by orchiectomy does not alter the lifespan compared to sham operated WT-7 males (mean life span: 109.9±24.2 days to 100.9±11.9 days; n=11/12; SD, p=0.4170). Data are analysed by Log-rank (Mantel-cox) test; *p<0.05

The results from the previous experiments argue for a beneficial effect of female sex hormones without major influence of male sex hormones. To further address the role of female sex hormones, we implanted subcutaneous pellets releasing 17β-estradiol, the most potent female sex hormone [150], in ovariectomized WT-7 females. The pellets provided a constant hormone substitution for 90 days and have the advantage of lower stress levels compared to daily injections and a higher consistency then dilution in drinking water. Two concentrations were administered: high dose (HD) 17β-estradiol pellets (0.002 mg/day) pellets or low dose (LD) pellets (0.0004 mg/day). The 17β-estradiol concentrations have been selected according to

published experiments using pellets of the same manufacturer to avoid over- or underdosage [151-154]. To maintain treatments over a 4 months period, animals were delivered a second pellet 3 months after the initial pellet if necessary. Castrated human TDP-43 WT-7 females with 17b-estradiol supplement showed a trend towards a dose dependent life span extension compared to castrated animals, but do not reach the life span of mice after sham surgery **(Figure 20)**.

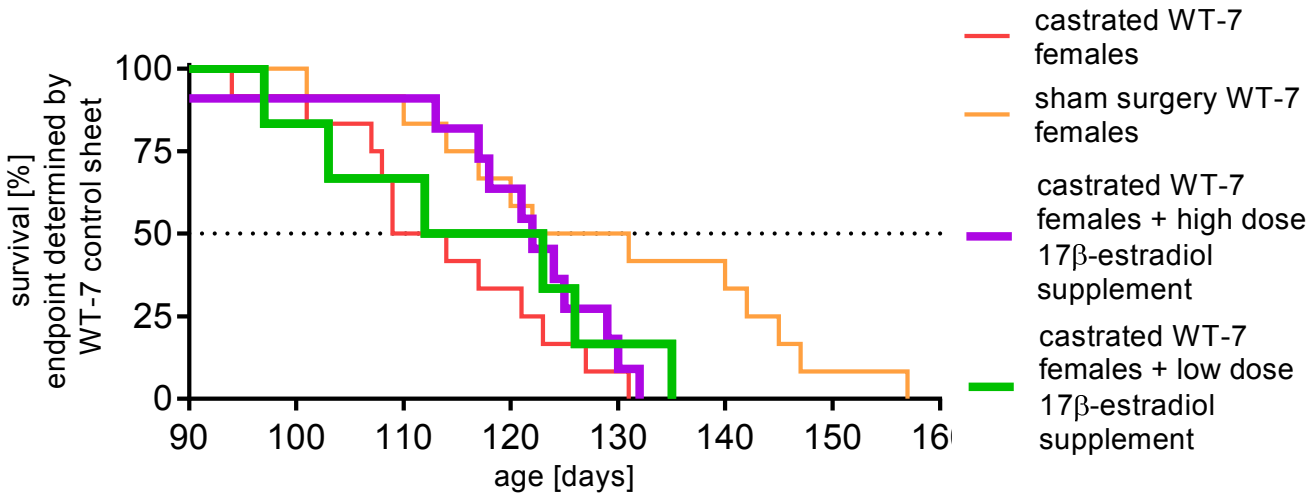

Figure 20. 17β-estradiol treated castrated females show a trend towards a life extension. 17β-estradiol supplemented castrated females showed a trend towards a dose dependent life span extension compared to castrated females without treatment (mean life span: castrated females 113.4±10.9 days n=12; castrated females with low dose supplement 116±14.5 days n=6; castrated females with high dose supplement 117.8±18.6 days n=11; females with sham surgery: 128.8± 17.3 days n=12; SD). Data are analysed by Log-rank (Mantel-cox) test.

The uterus wet weight was used as a control for a successful removal of sex-hormone releasing tissue and hormone supplementation in female mice **(Figure 21 A and B)**. Ovariectomized WT-7 females showed a significantly reduced uterus weight compared to sham operated females, lacking the growth stimulus of endogenous sex hormones (13.6±3.4 mg vs. 23.73±4.5 mg, $p<0.0001$) **(Figure 21 A)**. 17β-estradiol treatment of ovariectomized WT-7 females resulted in a significant increase of uterus wet weight compared to sham operated females. High

dose treated females had the highest uterus weight, indicating that the uterine cells underwent hypertrophy and/or hyperplasia following extensive 17β-estradiol exposition (mean uterus wet weight: females with sham surgery 23.73±4.5 mg, castrated females with high dose supplement 47.9±14.3 mg, castrated females with low dose supplement 27.8±18.2 mg) **(Figure 21 B)**. The results demonstrate that the 17β-estradiol releasing pellets have reconstituted the basal hormone status seen in mice who were undergoing sham surgery. However, both pellet supplemented cohorts of ovariectomized animals showed a higher variability in the uterus wet weight, speaking for some variability in hormone release. Likewise, constant hormone supply is not able to reconstitute the complexity of the estrous cycle.

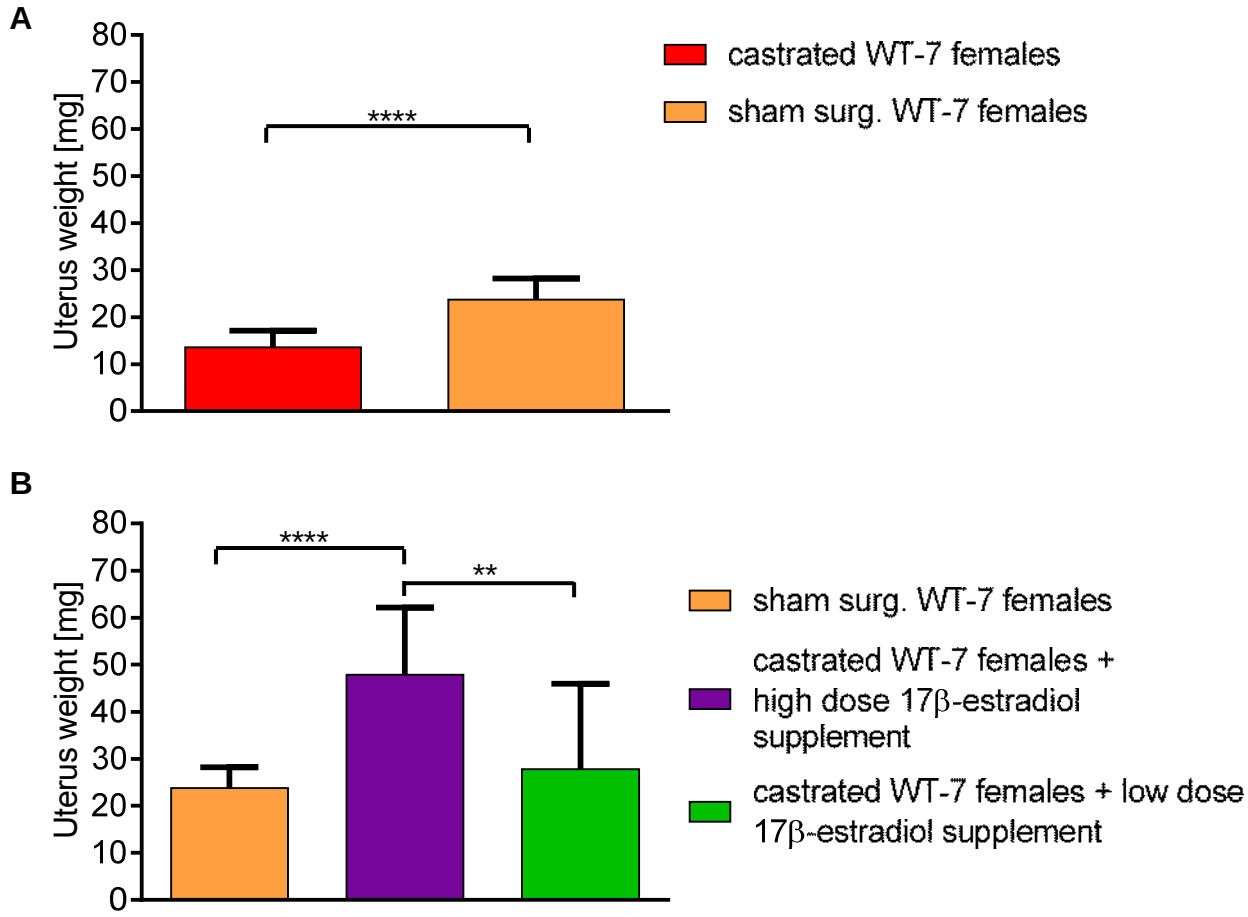

Figure 21. Increased uterus weight indicates successful 17β-estradiol administration in castrated WT-7 females. (A) Measurements of the uterus wet weight after death show a decreased uterus weight in females with ovariectomy compared to sham operated female controls: 13.6±3.4 mg vs. 23.73±4.5 mg. Data were analysed by t-test, ****p<0.0001. **(B)** High dose treatment with 17β-estradiol resulted in an increased uterus weight compared to sham operated females without treatment. (castrated females n=8, females with sham surgery n=7, castrated females with high dose supplement n=12, castrated females with low dose supplement n=6) Data are analysed by One-way-ANOVA with Tukey's test multiple comparisons; bars represent means ± SD; **p<0.01, ****p<0.0001

8. Discussion

Over the last decade, TDP-43 has been identified as a major pathological protein in ALS and FTLD-TDP, however the mechanism leading to cell death and its exact function in the CNS remain unclear. Transgenic mouse models might be powerful tools to explore the mechanisms in TDP-43 proteinopathies resulting in a fatal clinical phenotype in humans. However, results from transgenic mouse models so far are quite inconsistent; no model fully recapitulates human pathology. The interpretation of results is hampered by the fact that TDP-43 is a tightly autoregulated protein and that reported phenotypes are strongly linked to expression levels of TDP-43 transgenes. Furthermore, several studies do not include comparison of wild type TDP-43 and TDP-43 with human pathogenic mutations, leaving important questions unanswered.

In order to unravel the pathomechanisms underlying TDP-43 proteinopathies, we generated and analysed TDP-43 transgenic animals expressing four different constructs covering overexpression of wild type human TDP-43, the ALS-associated mutation M337V and G348C4 as well as an altered nuclear localisation signal, inducing cytoplasmic translocation with comparable expression levels, that allowed us to address the specific questions on weather overexpression of wild type TDP-43 is toxic, weather fALS-associated mutations in the human TDP-43 are associated with a toxic gain-of-function and weather increased levels of cytoplasmic TDP-43 are sufficient to induce toxicity.

8.1. Comparable levels of wild type TDP-43 are more toxic than TDP-43 with human pathogenic mutations

Comparing mouse lines expressing human wild type TDP-43 or human TDP-43 with pathogenic mutations with comparable expression levels as well as the expression patterns revealed striking differences with the wild type line WT-7 developing a pathological lethal phenotype in contrast to lines expressing different human pathogenic mutations (M337V and G348C).

The phenotype in the WT-7 line consists of a sex-dependent premature death (mean age at death: 133.6±38.7 days) originating from a gut motility deficit, related to gastrointestinal alterations including an increased intestinal diameter, an ileal smooth muscle thickening and a loss of enteric neurons in the myenteric plexus in the colon of end stage mice. Neither motor deficits nor cognitive impairments were observed and end stage WT-7 mice developed no pathological changes like TDP-43 aggregation, ubiquitination and phosphorylation, astrocytosis or activation of microglia in the CNS.

Demonstrating that the transgenic human wild type TDP-43 and the mutated human TDP-43 reduce the levels of endogenous murine TDP-43 by an autoregulatory mechanism in a comparable way in our mouse lines, an effect due to loss of endogenous TDP-43 is unlikely to explain the difference. Moreover, both WT-7 and the mutant mouse lines express transgenic TDP-43 in the enteric nervous system speaking against an effect of differential expression patterns.

Another potential explanation for a unique phenotype in a single transgenic line could be an integrational artefact, disrupting an endogenous genomic DNA

sequence unrelated to the actual transgene. However, Wegorzewska et al. created a mouse model expressing human TDP-43 with the disease-associated mutation A315T (PrP-TDP-43 A315T) causing a premature death with a mean survival of 153 days [105]. Surprisingly, it took 2 years to discover the main cause of death: PrP-TDP-43 A315T mice develop gastrointestinal complications, associated with TDP-43 aggregation, vacuolization within the myentric plexus and a progressive neurodegeneration, mainly restricted to the colon [155-157]. The phenotypical similarity of WT-7 and PrP-TDP-43 A315T argues strongly against an integrational artefact.

Thus, the striking differences in the phenotype in our lines by expressing comparable levels of wild type human TDP-43 or mutant TDP-43 suggests a more toxic role of wild type TDP-43 and thereby argues against a gain-of-function mechanism of mutations.

8.2. Expression of wild type TDP-43 can induce a gastrointestinal phenotype

The WT-7 line is the first TDP-43 mouse model demonstrating a gut motility defect upon transgenic expression of wild type TDP-43. The previously described PrP-TDP-43 A315T mouse model expressing human TDP-43 with the disease-associated mutation A315T also develops a lethal gut motility defect [155-157]. However, some obvious differences show up: Wegorzewska et al. reported a 3-fold higher expression of transgenic human TDP-43 in the CNS of the PrP-TDP-43 A315T line compared to endogenous TDP-43 in non-transgenic animals, which was later confirmed by Guo et al. [105, 156]. The expression levels of transgenic human TDP-43 in the PrP-TDP-43 A315T line are approximately 3-fold

higher than in our WT-7 line, as the total TDP-43 levels in the brain remained unchanged between WT-7 mice and non-transgenic littermates. It must be pointed out that the expression levels in the intestine were not estimated.

This finding suggests that pathological mutations in *TARDBP* might be partial loss-of-function mutations, so higher expression levels are needed compared to fully functional wild type TDP-43 to induce a similar toxic effect most likely due to altering the normal homeostasis of TDP-43 with downstream dysregulation of RNA processing. Furthermore, our results challenge the conclusions from the previous studies that TDP-43 mutations are associated with a toxic gain-of-function mechanism.

The involvement of the enteric nervous system in ALS and FTLD is not well examined; a single study reported gastrointestinal motor dysfunction in the majority of ALS patients, independent of bulbar involvement, upper motor neuron involvement or disease duration [158]. Furthermore, question surveys showed an increased rate of self-reported constipation [159]. Nevertheless, gastrointestinal dysfunction is a frequent feature in other neurodegenerative diseases, such as Dementia with Lewy bodies (DLB) [160] and Parkinson´s disease (PD) [161, 162]. Notably, recent reports suggest a link between these two diseases and TDP-43 pathology as more than 50% of DLB-patients show pathological phosphorylated TDP-43 in the CNS [163] and genetic data support a potential role of TDP-43 mutations in clinical PD [164, 165]. Furthermore, concomitant expression of wild type human TDP-43 and mutant α-synuclein by crossing transgenic mice indicate a synergistic role of both proteins resulting in more severe loss of dopaminergic neurons [166]. The co-occurrence of TDP-43 pathology in different neurodegenerative diseases characterized by

gastrointestinal dysfunction might indicate an involvement of TDP-43 hitherto not noticed.

The gut phenotype of the WT-7 line resembles some features of the human disorder Hirschsprung´s disease (HD). HD is a congenital disorder, effecting about 1 in 5.000 new-borns. It is characterized by the absence of ganglia cells in the myentric plexus in parts or all of the large intestine, resulting in a severe constipation and distended bowel due to a non-motile colon [167]. Similar to FTLD and ALS, HD is related to mutations in several genes inducing aganglionosis with many of them displaying incomplete penetrance [168]. Most of known HD-associated genes encode members of two main signalling pathways: the RET (proto-oncogene rearranged during transfection) and EDNRB (endothelin receptor, type B) pathways. Both pathways regulate survival, differentiation, migration, and proliferation of neural crest-derived cells [169]. An investigation into the relationship between TDP-43 and RET pathway or EDNRB pathway is to consider as TDP-43 overexpression might interfere with these pathways in TDP-43 transgenic mouse models. Furthermore, differences in the vulnerability of cells in the myenteric plexus of the colon compared to other intestinal segments might explain the restriction to this specific region in HD. For example, diminished *Ret* expression in a HD mouse model compromised neuronal survival in the colon without detectable neuronal loss in the small intestine [170]. A higher vulnerability for TDP-43 mediated toxicity in enteric neurons in the colon could explain the development of a clinical phenotype in the intestine prior detectable pathological changes in the CNS in our TDP-43 WT-7 line.

The intestinal system can be used as a model to study general functions of TDP-43 due to its diverse cell composition similar to the CNS and a high accessibility for drug

administration. However, it remains questionable if the ENS provides a model for human TDP-43 proteinopathies lacking key features of human disease progression.

8.3. Wild type TDP-43 expressing mouse models vary in phenotype

Several TDP-43 animal models were generated in recent years to investigate the consequences of TDP-43 overexpression *in vivo* [171]. Expression of wild type human TDP-43 under the control of the murine PrP-promotor was studied by two research groups [104, 172].

Stallings et al. generated 13 wild type human TDP-43 expressing mice with 9 founders developing a motor phenotype characterized by weakness, spasticity and reduced spontaneous movements with early premature death ranging from 12 to 34 days, correlating with the TDP-43 expression levels in the spinal cord [172]. Motor abilities were studied by a gait analysis and grip strength measurements. Affected founders also manifested a progressive weight loss prior death. Spinal cord pathology was observed in at least one founder with motor neurons in ventral horn appearing hyalinised with amorphous nuclear and cytoplasmic architecture. Three founders survived into adulthood and were established as transgenic mouse lines. Surprisingly, the wild type line with the highest spinal cord expression did not develop a motor phenotype up to 11 month despite the rare appearance of neurons with an increased diffuse ubiquitin staining. Another line with a lower expression in the spinal cord showed a late onset progressive motor phenotype resulting from a progressive myopathy in the skeletal muscle, correlating with increased TDP-43 expression in the muscles. Stallings et al. concluded that overexpression of TDP-43 *in vivo* can lead to the development of progressive motor syndromes in mice with

pathology sharing some similarity to TDP-43 proteinopathies and that a strong TDP-43 overexpression outside of the CNS may also yield disease. Considering our results for the human TDP-43 WT-7 line, a more detailed cause of death analysis, quantification of the total TDP-43 levels and determination of TDP-43 expression beyond CNS and skeletal muscle are advised.

Xu et al. generated a single mouse model with wild type human TDP-43 under the control of the murine PrP-promotor and were able to maintain hemizygous and homozygous breeding [104]. Aged hemizygous TDP-43 mice were phenotypically, histologically, and immunohistochemically indistinguishable from aged non-transgenic controls despite a 1.9-fold increase of total TDP-43 in the brain. The homozygous TDP-43 mice showed a 2.5-fold increase compared to non-transgenic controls. Xu et al. reported TDP-43 truncation as well as intranuclear and cytoplasmic aggregates that were immunopositive for phosphorylated TDP-43 in the CNS. However, human TDP-43 was not ubiquitinated despite increased cytoplasmic and nuclear ubiquitin levels. Reactive gliosis as well as axonal and myelin degeneration were observed in the spinal cord of end stage mice together with an abnormal aggregation but without a loss of neurons via apoptosis. Gait abnormalities occurred and were determined by a motorized treadmill with a video capture system. Homozygous TDP-43 mice died premature with 1 to 2 month of age unable to right themselves. The final cause of death was not determined. The human TDP-43 expression was highest in the brain and spinal cord, with moderate levels in the testis and spleen, and low levels in other tissues, such as the heart, liver, kidneys and stomach. A gastrointestinal phenotype cannot be excluded as expression data for the intestine are missing. Xu et al. showed that even small differences in the

expression level of wild type human TDP-43 result in major differences in the phenotype.

These studies and our results indicate that wild type TDP-43 expressed under control of the murine PrP-promotor is able to induce pathological phenotypes. However, a direct comparison is difficult due to different expression levels resulting in a huge variability in the reported phenotypes.

8.4. Motoric and cognitive phenotypes in TDP-43 transgenic mice correlate stronger with expression level rather than pathological mutations

Our transgenic mouse lines WT-7, M337V-3, M337V-5 and G348C-4 did not exhibit cognitive or motoric alterations or obvious signs of neurodegeneration in the motor system, in contrast to some reports on previously generated TDP-43 rodent lines expressing wild type human TDP-43 or variants with pathogenic mutations [104-106, 111, 116, 117, 172-174]. However, reported onset and manifestation varies greatly between the reported TDP-43 models. Differentiation between important TDP-43-mediated alterations emulating the human disease situation and secondary factors is complicated for various reasons. At first, even a small increase of the total TDP-43 is sufficient to induce lethal phenotypes. Comparison of transgenic mice expressing TDP-43 under different promoters is difficult due to differences in the expression pattern and expression onset during development. Secondly, TDP-43-mediated toxicity is strongly influenced by the genetic background. For example, congenic PrP-TDP-43 A315T with a congenic C57BL/6J background die significantly earlier by the gastrointestinal phenotype than mice of various mixed genetic backgrounds [157]. Likewise, some conclusions made in earlier publications have to be treated

with caution. For example, the original characterization of the PrP-TDP-43 A315T line missed the fact that mice die premature due to gastrointestinal complications rather than CNS and described motoric changes were not fully recapitulated in follow-up studies on these mouse lines [105, 155].

Tests for cognitive impairments and behavioral changes like Barnes maze task, Morris water navigation task, open field test or active and passive avoidance tests were only performed in a minority of reports. Swarup et al. generated mice expressing wild type human TDP-43, A315T or G348C mutant forms under control of the human *TARDBP*-promoter [173]. All three transgenic mouse models exhibited impaired learning and memory capabilities during ageing, as well as motor dysfunction. These lines expressed comparable levels of human TDP-43 mRNA, but the total TDP-43 protein levels were not measured. Impaired learning and memory capabilities and motor impairments were also reported for three transgenic mouse lines expressing mouse wild type TDP-43 under control of the CaMKII-promotor in the forebrain, resulting in a 2-fold increase of total TDP-43 compared to non-transgenic animals [117]. Notably, TDP-43 expression induced impaired cognitive function at 2 month of age and motor dysfunction in the 6 month-old transgenic mice. In contrast, PrP-TDP-43 A315T animals showed not symptoms of cognitive decline prior death due to the gastrointestinal motility defect [175].

Current data argue that the reported motoric and behavioural changes are largely depending on the overexpression level of TDP-43, reaching a neurotoxic threshold. Our transgenic mice showed no motoric and behavioural changes either because the cellular TDP-43 levels in the CNS remained below this neurotoxic threshold or the gastrointestinal phenotype preceded CNS-related changes.

The current overexpression models for disease-associated mutations are not be able to address further questions as changes in the expression level strongly influence the phenotypical outcome. More sophisticated knock-in models are needed to investigate the phenotypical changes induced by disease-related mutations in the endogenous TDP-43 under native expression levels.

8.5. Increased cytoplasmic TDP-43 is not sufficient to induceTDP-43 aggregation and toxicity

Cytoplasmic TDP-43 accumulation with TDP-43 nuclear clearance is a hallmark of TDP-43 proteinopathies. Under normal conditions, TDP-43 is mainly localized in the nucleus, presumably within specific nucleoplasmic domains required for its normal function such as transcriptional repression, pre-mRNA splicing and mRNA transport and stabilization [176]. These observations led to the hypothesis that increased cytoplasmic TDP-43 levels are potentially toxic due to abnormal interactions.

In order to address this hypothesis *in vivo* we generated the transgenic mouse lines NLS-4 and NLS-6 expressing human TDP-43 protein with a modified NLS sequence resulting in a decreased nuclear uptake. We observed a diffuse cytoplasmic distribution of human TDP-43 without aggregate formation, neurodegeneration or a clinical phenotype. Our results show that TDP-43 with a mutated NLS sequence is partially redistributed to the cytoplasm *in vivo*, but that increased levels of cytoplasmic TDP-43 are not sufficient to induce TDP-43 aggregation, sequestering of endogenous TDP-43 and/or a neurodegenerative phenotype in *vivo*.

Other groups have also addressed the question whether cytoplasmic TDP-43 causes protein aggregation and neurodegeneration in rodents: Igaz et al. generated mice

expressing human TDP-43 with mutated controlled by an inducible Tet-Off system in combination with forebrain-specific CaMK2α promoter elements [111]. Transgene expression was inhibited until 28 days of age. They observed a progressive neuron loss in the NLS lines depending on the general expression strength and the selective vulnerability of particular brain regions such as the dentate gyrus. Cytoplasmic expression of human TDP-43 triggered variable accumulation of hyperphosphorylated and ubiquitinated human TDP-43 with mutated NLS in cytoplasmic aggregates. However, the paucity of aggregates in the low expressing line indicated that cytoplasmic inclusions were not required for neuron death. Dayton et. al used a different approach by transducing rats at postnatal day 1 with intravenous administration of an adeno-associated virus (AAV9) gene transfer method in the temporal vein, resulting in a uniform expression of human TDP-43 with a mutation in the NLS controlled by the strong CMV-promotor [112]. Two different AVV9 dosages were used. Transduced animals of the high dose AVV9 group developed a motor impairment within 2 weeks, determined by a hind limb escape reflex test, rotarod and open field test, whereas only 2 of 8 low dose treated rats developed minor signs of limb impairments. However, Dayton et al. were unable to discern any evidence of ubiquitin or p62 immunopositive cytoplasmic aggregates in intravenously transduced rats. Noticeably, with more concentrated AAV9 stereotaxic brain injections, rare TDP-43 aggregates were induced.

There are some explanations for the different phenotype compared to our mouse lines NLS-4 and NLS-6. First, our transgenic mice show a low expression level with total TDP-43 levels quite comparable to non-transgenic mice in contrast to Igaz et al. reporting an 8 to 9-fold overexpression of total TDP-43 in the forebrain of their NLS-

lines. Dayton et al. reported a consistent 2-fold overexpression of total TDP-43 in the cervical and lumbar spinal cord in intravenously transduced rats using high dose AVV9 titers. In our NLS-lines, the total TDP-43 levels remained unchanged. Second, neuronal vulnerability to TDP-43 overexpression is depending on timing of induction due to a high sensitivity of neurons during early development [118]. Gene expression controlled by mouse prion promotor is reported at earliest at embryonic day 13.5, speaking for considerable differences between the model systems [177].

Moreover, in contrast to cell culture models of NLS mutations, all NLS rodent models described show an incomplete cytoplasmic localization of transgenic TDP-43 with NLS mutation with various proportions of transgenic TDP-43 also in the nucleus, possibly explained by dimerization of TDP-43 with NLS mutation and wild type TDP-43 and subsequent nuclear uptake [76, 178]. This raises the question if reported neurotoxic effects in the above mentioned mouse rodent models might be induced by cytoplasmic TDP-43 or result from a small but fatal increase of total TDP-43 in the nucleus.

Reports from other *in vivo* NLS models are ambiguous whether there is a link between increased cytoplasmic TDP-43 and toxic effects: *Caenorhabditis elegans* developed a neurodegenerative phenotype by expression of wild type human TDP-43, whereas expression of human TDP-43 containing point mutations in NLS resulted in cytoplasmic accumulation of both diffuse and aggregated human TDP-43 without neurotoxic effects [179]. In *Drosophila melanogaster*, expressing either wild type human TDP-43 or TDP-43 with mutations in the NLS is neurotoxic [114, 180]. *In vitro* models developed pathological phenotypes, but also missed some key features of TDP-43 proteinopathies: Winton et al. showed that a mutated NLS

restricts human TDP-43 distribution to the nucleus and leads to cytoplasmic retention of the endogenous TDP-43 in TDP-43 aggregates within transfected cell lines [109]. These aggregates also recapitulated the biochemical signature of pathological TDP-43 in FTLD-TDP and ALS, including a high molecular weight smear of ubiquitinated TDP-43 and C-terminal TDP-43 fragments. However, cellular toxicity was not reported. In contrast, Barmada et al. reported a higher cumulative risk of death in primary cultures of rat cortical neurons after transfection with NLS-mutant human TDP-43 compared to wild type TDP-43 transfected cells [181]. The formation of ubiquitin-immunopositive, detergent-insoluble inclusion bodies were observed but not necessary for the toxicity.

Our results for the NLS lines indicate that increased levels of cytoplasmic TDP-43 *per se* are not sufficient to induce neurodegeneration and support the idea of a multiple-hit-model of TDP-43 inclusion body formation [126]. This model implies that TDP-43 inclusion body formation depends on cascade of cellular events starting with cytoplasmic mislocalization (first hit) and an independent second hit inducing the formation of cytoplasmic aggregates that may sequester TDP-43, disrupt RNA processing and initiate neuron degeneration. A proposed step in this cascade is the formation of stress granules (SG), dense aggregations composed of proteins and RNA, initiated by environmental stress triggers, as a precursors for pathological protein aggregates [182, 183]. Cytoplasmic TDP-43 inclusions have been shown to colocalize with several SG markers in cultured cells and primary neurons in response to cellular stress as well as in post-mortem samples from ALS and FTLD patients [184]. However, only a single study claimed that withdrawal of the stressor lead to removal of SGs while TDP-43 positive aggregates remained present [185],

whereas other studies did not observe persistent TDP-43 aggregates after SGs dissociation [183].

A different potential modifier of initial TDP-43 aggregation and propagation is an intrinsic part of the TDP-43 protein structure: recent studies showed that the C-terminal domain, in addition to mediating protein-protein interactions, has properties of a Q/N-rich prion domain [63, 64, 186, 187]. Transduction of cultured cells with insoluble recombinant TDP-43 fibrils triggered the aggregation of intracellular TDP-43 proteins, becoming sarkosyl-insoluble and ubiquitinated [65]. Insoluble TDP-43 aggregates from diseased brains showed the same prion-like properties by inducing seed-dependent and self-templating aggregation of intracellular TDP-43 in the neuroblastoma cell line SH-SY5Y transfected with human TDP-43 [69]. The cells with intracellular TDP-43 released TDP-43 aggregates via exosomes, propagating phosphorylated TDP-43 aggregates between cultured cells, raising the question of a potential transmission via exosomes as an intermediate step during human pathogenesis, a concept already proposed earlier [188].

Our NLS-lines will be valuable tools to further investigate the proposed two-hit-model as well as the role of seeding in TDP-43 proteinopathies as cytoplasmic localization might represent the initial step in a fatal molecular cascade. By applying cellular stressors or insoluble TDP-43 species on primary cortical neurons or organotypic slice cultures of our NLS strains, it can be tested whether they are able to induce pathological changes similar to those seen in TDP-43 proteinopathies.

8.6. Role of estrogen in the phenotype of the TDP-43 expressing mouse line WT-7

The observed life span of male and female WT-7 animals was significantly different with 103±16.7 days in males compared to 157.5±33.4 days in females. Notably, epidemiological studies have shown that both the incidence and prevalence of ALS are greater in men than in women [189]. Female sex hormones might play a beneficial role as women who develop ALS have often had a later menarche and earlier menopause than healthy controls [190] with ALS incidence shifting from a male/female ratio of 4:1 in the second decade to 1:1 at ages above 60 years [191]. We abolished sex hormone release in both genders of WT-7 by ovariectomy or castration prior maturation and later partially reconstituted the hormone status in ovariectomized WT-7.

By abolishing sex hormone release in both genders of WT-7 by ovariectomy or castration prior maturation, we observed a significantly earlier disease onset in ovariectomized WT-7 females compared to sham-operated controls, whereas castration of WT-7 males did not alter disease onset compared to sham-operated controls. Together with the partial rescue upon 17β-estradiol supplementation in ovariectomized WT-7 females, our data exclude a detrimental effect of androgens and provide strong evidence for a beneficial effect of female sex hormones in our mouse model in line with the postulated beneficial role of female sex hormones in ALS patients.

Notably, a similar striking sex difference was observed in the human TDP-43 A315T mouse line [105]. In accordance with our data, a strongly reduced survival by

ovariectomy has been reported in this line with a reduced life span of 105 days compared to 200 days in sham operated controls [157]. Castration of TDP-43 A315T males resulted in a minor lifespan decrease with a median survival of 91 compared to 102 days in sham operated controls. A recent study further investigated the role of progesterone in this mouse model, showing a reduced rate of loss of locomotor control in progesterone treated males but no significant increase in survival of the mice [192]. Thus, these and our data indicate a beneficial effect of female gonadal hormones in TDP-43 animal models.

The presence of sex differences and the beneficial role for female sex hormones are also reported for SOD1 mouse models of ALS [189]: ovariectomy of human SOD1 G93A transgenic animals did not alter the onset age of the disease while reducing the lifespan in females by 7 days and making it comparable to that of the male transgenic mice [154]. Treatment of ovariectomized females with 17β-estradiol did not delay the onset of disease, but prevented progression of ALS motor dysfunctions for a limited time window and rescued the lifespans in ovariectomized females. A prior study observed significant acceleration of disease progression by ovariectomy and a significantly delayed disease progression by 17β-estradiol treatment in the same model, but failed to rescued the lifespans in ovariectomized females, proposing an additional effect of progesterone [193]. However, the conclusions drawn from the studies need to be treated with caution as the differences are small and other groups did not observe a detrimental effect in gonadectomised SOD1 G93A mice [194].

Female sex hormones are also positive modifiers in drug treatment experiments using the SOD1 animal models [194-197]. The involved cellular pathways are still

unknown, but recent publications revealed that deficiency in Pgc-1α, a transcriptional co-activator mediating the cellular response to metabolic demands, resulted in male-specific earlier disease onset in SOD1 G93A mouse models [198-200]. Strikingly, SNPs in the brain-specific promoter region of PGC-1α do also influence the survival of men in clinical cohorts, but not in the female population [201]. In contrast to the results in the SOD1 mouse models, SOD1 G93A transgenic rats showed no significant effect of gonadectomy on disease onset and progression [194, 202]. Further investigations are needed to dissect the specific role of individual female gonadal hormones for a delayed disease onset, slowed progression and increased survival.

17β-estradiol is widely acknowledged as the most potent form of estrogens, which exert different functions such as neurotropic factors or neuroprotective agents. Binding of estrogens to estrogen receptors can induce both a genomic effect by an altered transcription as well as a fast non-genomic response modulating different cellular pathways [203]. 17β-estradiol was used as neuroprotective supplement for *in vitro* motor neuron cultures [204-206]. It can also induce an indirect neuroprotective effects in motor neuron cultures by increasing the GDNF secretion in astrocytes. This observation is worth mentioning as marked up-regulation of estrogen receptor α was observed in spinal astrocytes of amyotrophic lateral sclerosis patients [205].

Notably, also gastrointestinal motility is considerably modified by sex hormones. The absence of estrogen inhibits the gastric emptying and delays gastrointestinal transit in ovariectomized female rodents, whereas estrogen and progesterone treatment of males delayed the gut emptying; by contrast testosterone has no influence on gastric emptying or gastrointestinal transit [178, 207-210]. Estrogen receptor α and β are

both expressed in neurons in the myenteric plexus of rat and mouse [211, 212]. There is strong evidence for a similar relationship in humans as idiopathic constipation is higher in women of reproductive age than postmenopausal women or men, suggesting that female sex hormones influence gastrointestinal motility [213, 214]. The colonic transit time also correlates with the menstrual cycle as it is significantly extended during the luteal phase, characterized by high estrogen levels [215].

Due to the diverse effects of estrogens, there are different possible explanations for the protective effect in the WT-7 mouse line: estrogen might either exert a neuroprotective effect on neurons in the myenteric plexus and therefore delaying the neurotoxic effect of TDP-43 overexpression or alter the excitability of subpopulations of neurons resembling effects in the CNS [216]. Additionally, an indirect effect unrelated to the myenteric nervous system remains possible as estrogen reduces the excitability of myocytes in the intestine muscle tissue, mediated by a rapid non-genomic mechanism activating K^+ channels or inhibiting Ca^{2+} channels [217, 218].

8.7. Final conclusions

Our mouse lines overexpressing different human TDP-43 proteins represent the most diversified population of TDP-43 models expressing quite comparable levels different TDP-43 constructs on a pure genetic background.

In contrast to transgenic expression of human TDP-43, neither overexpression of TDP-43 with ALS-associated mutations nor TDP-43 with forced cytoplasmic localization was sufficient to induce a pathological in our models, thereby arguing against a toxic gain-of-function mechanism of human pathogenic mutations and

increased levels of cytoplasmic TDP-43. Particularly NLS lines will be valuable tool to further address the role of stress factors and seeding in inclusion body formation.

While WT-7 mice with predominant affection of the ENS do not reflect characteristic pathological and biochemical features of human TDP-43 proteinopathies, they will be valuable models to further investigate the function of TDP-43 and to identify dysregulated pathways upon transgene expression in neuron e.g. by proteomics and transcriptomics analysis of isolated ENS. Furthermore, they will allow to further address the influence of sex hormones on TDP-43 mediated toxicity.

9. References

1. Geser, F., et al., *Amyotrophic lateral sclerosis, frontotemporal dementia and beyond: the TDP-43 diseases.* J Neurol, 2009. 256(8): p. 1205-14.
2. Mackenzie, I.R. and H.H. Feldman, *Ubiquitin immunohistochemistry suggests classic motor neuron disease, motor neuron disease with dementia, and frontotemporal dementia of the motor neuron disease type represent a clinicopathologic spectrum.* J Neuropathol Exp Neurol, 2005. 64(8): p. 730-9.
3. Riedl, L., et al., *Frontotemporal lobar degeneration: current perspectives.* Neuropsychiatr Dis Treat, 2014. 10: p. 297-310.
4. Pan, X.D. and X.C. Chen, *Clinic, neuropathology and molecular genetics of frontotemporal dementia: a mini-review.* Transl Neurodegener, 2013. 2(1): p. 8.
5. Hirtz, D., et al., *How common are the "common" neurologic disorders?* Neurology, 2007. 68(5): p. 326-37.
6. Mitchell, J.D. and G.D. Borasio, *Amyotrophic lateral sclerosis.* Lancet, 2007. 369(9578): p. 2031-41.
7. Charcot, J.M. and A. Joffroy, *Deux cas d'atrophie musculaire progressive avec lesions de la substance grise et des faisceaux anterolateraux de la moelle epiniere.* Archives de Physiologie, 1869. 2: p. 354.
8. Lomen-Hoerth, C., T. Anderson, and B. Miller, *The overlap of amyotrophic lateral sclerosis and frontotemporal dementia.* Neurology, 2002. 59(7): p. 1077-9.
9. Murphy, J.M., et al., *Continuum of frontal lobe impairment in amyotrophic lateral sclerosis.* Arch Neurol, 2007. 64(4): p. 530-4.
10. Ringholz, G.M., et al., *Prevalence and patterns of cognitive impairment in sporadic ALS.* Neurology, 2005. 65(4): p. 586-90.
11. Phukan, J., N.P. Pender, and O. Hardiman, *Cognitive impairment in amyotrophic lateral sclerosis.* Lancet Neurol, 2007. 6(11): p. 994-1003.
12. Renton, A.E., A. Chio, and B.J. Traynor, *State of play in amyotrophic lateral sclerosis genetics.* Nat Neurosci, 2014. 17(1): p. 17-23.
13. Rosen, D.R., *Mutations in Cu/Zn superoxide dismutase gene are associated with familial amyotrophic lateral sclerosis.* Nature, 1993. 364(6435): p. 362.
14. Neumann, M., et al., *Ubiquitinated TDP-43 in frontotemporal lobar degeneration and amyotrophic lateral sclerosis.* Science, 2006. 314(5796): p. 130-3.
15. Sreedharan, J., et al., *TDP-43 mutations in familial and sporadic amyotrophic lateral sclerosis.* Science, 2008. 319(5870): p. 1668-72.
16. Deng, H.X., et al., *Mutations in UBQLN2 cause dominant X-linked juvenile and adult-onset ALS and ALS/dementia.* Nature, 2011. 477(7363): p. 211-5.
17. Johnson, J.O., et al., *Exome sequencing reveals VCP mutations as a cause of familial ALS.* Neuron, 2010. 68(5): p. 857-64.
18. Wu, C.H., et al., *Mutations in the profilin 1 gene cause familial amyotrophic lateral sclerosis.* Nature, 2012. 488(7412): p. 499-503.
19. DeJesus-Hernandez, M., et al., *Expanded GGGGCC hexanucleotide repeat in noncoding region of C9ORF72 causes chromosome 9p-linked FTD and ALS.* Neuron, 2011. 72(2): p. 245-56.
20. Renton, A.E., et al., *A hexanucleotide repeat expansion in C9ORF72 is the cause of chromosome 9p21-linked ALS-FTD.* Neuron, 2011. 72(2): p. 257-68.
21. Maruyama, H., et al., *Mutations of optineurin in amyotrophic lateral sclerosis.* Nature, 2010. 465(7295): p. 223-6.

22. Fecto, F., et al., *SQSTM1 mutations in familial and sporadic amyotrophic lateral sclerosis.* Arch Neurol, 2011. 68(11): p. 1440-6.
23. Millecamps, S., et al., *SOD1, ANG, VAPB, TARDBP, and FUS mutations in familial amyotrophic lateral sclerosis: genotype-phenotype correlations.* J Med Genet, 2010. 47(8): p. 554-60.
24. de Belleroche, J., R. Orrell, and A. King, *Familial amyotrophic lateral sclerosis/motor neurone disease (FALS): a review of current developments.* J Med Genet, 1995. 32(11): p. 841-7.
25. Leigh, P.N., et al., *Ubiquitin-immunoreactive intraneuronal inclusions in amyotrophic lateral sclerosis. Morphology, distribution, and specificity.* Brain, 1991. 114 (Pt 2): p. 775-88.
26. Lowe, J., et al., *Inclusion bodies in motor cortex and brainstem of patients with motor neurone disease are detected by immunocytochemical localisation of ubiquitin.* Neurosci Lett, 1989. 105(1-2): p. 7-13.
27. Sampathu, D.M., et al., *Pathological heterogeneity of frontotemporal lobar degeneration with ubiquitin-positive inclusions delineated by ubiquitin immunohistochemistry and novel monoclonal antibodies.* Am J Pathol, 2006. 169(4): p. 1343-52.
28. Mackenzie, I.R., R. Rademakers, and M. Neumann, *TDP-43 and FUS in amyotrophic lateral sclerosis and frontotemporal dementia.* Lancet Neurol, 2010. 9(10): p. 995-1007.
29. Rohrer, J.D., et al., *TDP-43 subtypes are associated with distinct atrophy patterns in frontotemporal dementia.* Neurology, 2010. 75(24): p. 2204-11.
30. Mackenzie, I.R., et al., *Nomenclature for neuropathologic subtypes of frontotemporal lobar degeneration: consensus recommendations.* Acta Neuropathol, 2009. 117(1): p. 15-8.
31. Geser, F., et al., *Evidence of multisystem disorder in whole-brain map of pathological TDP-43 in amyotrophic lateral sclerosis.* Arch Neurol, 2008. 65(5): p. 636-41.
32. Lillo, P. and J.R. Hodges, *Frontotemporal dementia and motor neurone disease: overlapping clinic-pathological disorders.* J Clin Neurosci, 2009. 16(9): p. 1131-5.
33. Arai, T., et al., *TDP-43 is a component of ubiquitin-positive tau-negative inclusions in frontotemporal lobar degeneration and amyotrophic lateral sclerosis.* Biochem Biophys Res Commun, 2006. 351(3): p. 602-11.
34. Rutherford, N.J., et al., *Novel mutations in TARDBP (TDP-43) in patients with familial amyotrophic lateral sclerosis.* PLoS Genet, 2008. 4(9): p. e1000193.
35. Cruts, M., J. Theuns, and C. Van Broeckhoven, *Locus-specific mutation databases for neurodegenerative brain diseases.* Hum Mutat, 2012. 33(9): p. 1340-4.
36. Janssens, J., et al., *The role of mutant TAR DNA-binding protein 43 in amyotrophic lateral sclerosis and frontotemporal lobar degeneration.* Biochem Soc Trans, 2011. 39(4): p. 954-9.
37. Tamaoka, A., et al., *TDP-43 M337V mutation in familial amyotrophic lateral sclerosis in Japan.* Intern Med, 2010. 49(4): p. 331-4.
38. Kuhnlein, P., et al., *Two German kindreds with familial amyotrophic lateral sclerosis due to TARDBP mutations.* Arch Neurol, 2008. 65(9): p. 1185-9.
39. Del Bo, R., et al., *TARDBP (TDP-43) sequence analysis in patients with familial and sporadic ALS: identification of two novel mutations.* Eur J Neurol, 2009. 16(6): p. 727-32.
40. Lagier-Tourenne, C., M. Polymenidou, and D.W. Cleveland, *TDP-43 and FUS/TLS: emerging roles in RNA processing and neurodegeneration.* Hum Mol Genet, 2010. 19(R1): p. R46-64.
41. Sieben, A., et al., *The genetics and neuropathology of frontotemporal lobar degeneration.* Acta Neuropathol, 2012. 124(3): p. 353-72.
42. Chen-Plotkin, A.S., V.M. Lee, and J.Q. Trojanowski, *TAR DNA-binding protein 43 in neurodegenerative disease.* Nat Rev Neurol, 2010. 6(4): p. 211-20.
43. Geser, F., et al., *Pathological 43-kDa transactivation response DNA-binding protein in older adults with and without severe mental illness.* Arch Neurol, 2010. 67(10): p. 1238-50.

44. **Wilson, A.C., et al., *TDP-43 in aging and Alzheimer's disease - a review.* Int J Clin Exp Pathol, 2011. 4(2): p. 147-55.**

45. **Nakashima-Yasuda, H., et al., *Co-morbidity of TDP-43 proteinopathy in Lewy body related diseases.* Acta Neuropathol, 2007. 114(3): p. 221-9.**

46. **Ou, S.H., et al., *Cloning and characterization of a novel cellular protein, TDP-43, that binds to human immunodeficiency virus type 1 TAR DNA sequence motifs.* J Virol, 1995. 69(6): p. 3584-96.**

47. **Buratti, E. and F.E. Baralle, *Characterization and functional implications of the RNA binding properties of nuclear factor TDP-43, a novel splicing regulator of CFTR exon 9.* J Biol Chem, 2001. 276(39): p. 36337-43.**

48. **Mercado, P.A., et al., *Depletion of TDP 43 overrides the need for exonic and intronic splicing enhancers in the human apoA-II gene.* Nucleic Acids Res, 2005. 33(18): p. 6000-10.**

49. **Dreumont, N., et al., *Antagonistic factors control the unproductive splicing of SC35 terminal intron.* Nucleic Acids Res, 2010. 38(4): p. 1353-66.**

50. **Bose, J.K., et al., *TDP-43 overexpression enhances exon 7 inclusion during the survival of motor neuron pre-mRNA splicing.* J Biol Chem, 2008. 283(43): p. 28852-9.**

51. **Ayala, Y.M., et al., *Structural determinants of the cellular localization and shuttling of TDP-43.* J Cell Sci, 2008. 121(Pt 22): p. 3778-85.**

52. **Nemeth, L. and P. Puri, *The innervation of human bowel mucosa and its alterations in Hirschsprung's disease using a whole-mount preparation technique.* Pediatr Surg Int, 2000. 16(4): p. 277-81.**

53. **Buratti, E., et al., *Nuclear factor TDP-43 binds to the polymorphic TG repeats in CFTR intron 8 and causes skipping of exon 9: a functional link with disease penetrance.* Am J Hum Genet, 2004. 74(6): p. 1322-5.**

54. **Tollervey, J.R., et al., *Characterizing the RNA targets and position-dependent splicing regulation by TDP-43.* Nat Neurosci, 2011. 14(4): p. 452-8.**

55. **Polymenidou, M., et al., *Long pre-mRNA depletion and RNA missplicing contribute to neuronal vulnerability from loss of TDP-43.* Nat Neurosci, 2011. 14(4): p. 459-68.**

56. **Sephton, C.F., et al., *Identification of neuronal RNA targets of TDP-43-containing ribonucleoprotein complexes.* J Biol Chem, 2011. 286(2): p. 1204-15.**

57. **Alami, N.H., et al., *Axonal transport of TDP-43 mRNA granules is impaired by ALS-causing mutations.* Neuron, 2014. 81(3): p. 536-43.**

58. **Freibaum, B.D., et al., *Global analysis of TDP-43 interacting proteins reveals strong association with RNA splicing and translation machinery.* J Proteome Res, 2010. 9(2): p. 1104-20.**

59. **Ling, S.C., et al., *ALS-associated mutations in TDP-43 increase its stability and promote TDP-43 complexes with FUS/TLS.* Proc Natl Acad Sci U S A, 2010. 107(30): p. 13318-23.**

60. **Kim, S.H., et al., *Amyotrophic lateral sclerosis-associated proteins TDP-43 and FUS/TLS function in a common biochemical complex to co-regulate HDAC6 mRNA.* J Biol Chem, 2010. 285(44): p. 34097-105.**

61. **Buratti, E., et al., *TDP-43 binds heterogeneous nuclear ribonucleoprotein A/B through its C-terminal tail: an important region for the inhibition of cystic fibrosis transmembrane conductance regulator exon 9 splicing.* J Biol Chem, 2005. 280(45): p. 37572-84.**

62. **D'Ambrogio, A., et al., *Functional mapping of the interaction between TDP-43 and hnRNP A2 in vivo.* Nucleic Acids Res, 2009. 37(12): p. 4116-26.**

63. **Fuentealba, R.A., et al., *Interaction with polyglutamine aggregates reveals a Q/N-rich domain in TDP-43.* J Biol Chem, 2010. 285(34): p. 26304-14.**

64. **Udan, M. and R.H. Baloh, *Implications of the prion-related Q/N domains in TDP-43 and FUS.* Prion, 2011. 5(1): p. 1-5.**

65. **Furukawa, Y., et al., *A seeding reaction recapitulates intracellular formation of Sarkosyl-insoluble transactivation response element (TAR) DNA-binding protein-43 inclusions.* J Biol Chem, 2011. 286(21): p. 18664-72.**
66. **Kwong, L.K., et al., *TDP-43 proteinopathies: neurodegenerative protein misfolding diseases without amyloidosis.* Neurosignals, 2008. 16(1): p. 41-51.**
67. **Chen, A.K., et al., *Induction of amyloid fibrils by the C-terminal fragments of TDP-43 in amyotrophic lateral sclerosis.* J Am Chem Soc, 2010. 132(4): p. 1186-7.**
68. **Bigio, E.H., et al., *Inclusions in frontotemporal lobar degeneration with TDP-43 proteinopathy (FTLD-TDP) and amyotrophic lateral sclerosis (ALS), but not FTLD with FUS proteinopathy (FTLD-FUS), have properties of amyloid.* Acta Neuropathol, 2013. 125(3): p. 463-5.**
69. **Nonaka, T., et al., *Prion-like properties of pathological TDP-43 aggregates from diseased brains.* Cell Rep, 2013. 4(1): p. 124-34.**
70. **Udan-Johns, M., et al., *Prion-like nuclear aggregation of TDP-43 during heat shock is regulated by HSP40/70 chaperones.* Hum Mol Genet, 2013.**
71. **Zhang, Y.J., et al., *The dual functions of the extreme N-terminus of TDP-43 in regulating its biological activity and inclusion formation.* Hum Mol Genet, 2013. 22(15): p. 3112-22.**
72. **Wang, Y.T., et al., *The truncated C-terminal RNA recognition motif of TDP-43 protein plays a key role in forming proteinaceous aggregates.* J Biol Chem, 2013. 288(13): p. 9049-57.**
73. **Shodai, A., et al., *Aberrant assembly of RNA recognition motif 1 links to pathogenic conversion of TAR DNA-binding protein of 43 kDa (TDP-43).* J Biol Chem, 2013. 288(21): p. 14886-905.**
74. **Voigt, A., et al., *TDP-43-mediated neuron loss in vivo requires RNA-binding activity.* PLoS One, 2010. 5(8): p. e12247.**
75. **Huang, Y.C., et al., *Inhibition of TDP-43 aggregation by nucleic acid binding.* PLoS One, 2013. 8(5): p. e64002.**
76. **Kuo, P.H., et al., *Structural insights into TDP-43 in nucleic-acid binding and domain interactions.* Nucleic Acids Res, 2009. 37(6): p. 1799-808.**
77. **Ayala, Y.M., T. Misteli, and F.E. Baralle, *TDP-43 regulates retinoblastoma protein phosphorylation through the repression of cyclin-dependent kinase 6 expression.* Proc Natl Acad Sci U S A, 2008. 105(10): p. 3785-9.**
78. **Godena, V.K., et al., *TDP-43 regulates Drosophila neuromuscular junctions growth by modulating Futsch/MAP1B levels and synaptic microtubules organization.* PLoS One, 2011. 6(3): p. e17808.**
79. **Fiesel, F.C., et al., *Knockdown of transactive response DNA-binding protein (TDP-43) downregulates histone deacetylase 6.* EMBO J, 2010. 29(1): p. 209-21.**
80. **Kwon, S., Y. Zhang, and P. Matthias, *The deacetylase HDAC6 is a novel critical component of stress granules involved in the stress response.* Genes Dev, 2007. 21(24): p. 3381-94.**
81. **Buchan, J.R. and R. Parker, *Eukaryotic stress granules: the ins and outs of translation.* Mol Cell, 2009. 36(6): p. 932-41.**
82. **McDonald, K.K., et al., *TAR DNA-binding protein 43 (TDP-43) regulates stress granule dynamics via differential regulation of G3BP and TIA-1.* Hum Mol Genet, 2011. 20(7): p. 1400-10.**
83. **Gregory, R.I., et al., *The Microprocessor complex mediates the genesis of microRNAs.* Nature, 2004. 432(7014): p. 235-40.**
84. **Casafont, I., et al., *TDP-43 localizes in mRNA transcription and processing sites in mammalian neurons.* J Struct Biol, 2009. 167(3): p. 235-41.**
85. **Buratti, E., et al., *Nuclear factor TDP-43 can affect selected microRNA levels.* FEBS J, 2010. 277(10): p. 2268-81.**

86. **Fukuda, T., et al., *DEAD-box RNA helicase subunits of the Drosha complex are required for processing of rRNA and a subset of microRNAs.* Nat Cell Biol, 2007. 9(5): p. 604-11.**
87. **Ayala, Y.M., et al., *TDP-43 regulates its mRNA levels through a negative feedback loop.* EMBO J, 2011. 30(2): p. 277-88.**
88. **Wu, L.S., et al., *TDP-43, a neuro-pathosignature factor, is essential for early mouse embryogenesis.* Genesis, 2010. 48(1): p. 56-62.**
89. **Wu, L.S., W.C. Cheng, and C.K. Shen, *Targeted depletion of TDP-43 expression in the spinal cord motor neurons leads to the development of amyotrophic lateral sclerosis-like phenotypes in mice.* J Biol Chem, 2012. 287(33): p. 27335-44.**
90. **Iguchi, Y., et al., *Loss of TDP-43 causes age-dependent progressive motor neuron degeneration.* Brain, 2013. 136(Pt 5): p. 1371-82.**
91. **Chiang, P.M., et al., *Deletion of TDP-43 down-regulates Tbc1d1, a gene linked to obesity, and alters body fat metabolism.* Proc Natl Acad Sci U S A, 2010. 107(37): p. 16320-4.**
92. **Yang, C., et al., *Partial loss of TDP-43 function causes phenotypes of amyotrophic lateral sclerosis.* Proc Natl Acad Sci U S A, 2014. 111(12): p. E1121-9.**
93. **Yang, C., et al., *The C-terminal TDP-43 fragments have a high aggregation propensity and harm neurons by a dominant-negative mechanism.* PLoS One, 2010. 5(12): p. e15878.**
94. **Iguchi, Y., et al., *TDP-43 depletion induces neuronal cell damage through dysregulation of Rho family GTPases.* J Biol Chem, 2009. 284(33): p. 22059-66.**
95. **van Eersel, J., et al., *Cytoplasmic accumulation and aggregation of TDP-43 upon proteasome inhibition in cultured neurons.* PLoS One, 2011. 6(7): p. e22850.**
96. **Zhang, T., et al., *Caenorhabditis elegans RNA-processing protein TDP-1 regulates protein homeostasis and life span.* J Biol Chem, 2012. 287(11): p. 8371-82.**
97. **Lin, M.J., C.W. Cheng, and C.K. Shen, *Neuronal function and dysfunction of Drosophila dTDP.* PLoS One, 2011. 6(6): p. e20371.**
98. **Diaper, D.C., et al., *Loss and gain of Drosophila TDP-43 impair synaptic efficacy and motor control leading to age-related neurodegeneration by loss-of-function phenotypes.* Hum Mol Genet, 2013. 22(8): p. 1539-57.**
99. **Feiguin, F., et al., *Depletion of TDP-43 affects Drosophila motoneurons terminal synapsis and locomotive behavior.* FEBS Lett, 2009. 583(10): p. 1586-92.**
100. **Kabashi, E., et al., *Gain and loss of function of ALS-related mutations of TARDBP (TDP-43) cause motor deficits in vivo.* Hum Mol Genet, 2010. 19(4): p. 671-83.**
101. **Hewamadduma, C.A., et al., *Tardbpl splicing rescues motor neuron and axonal development in a mutant tardbp zebrafish.* Hum Mol Genet, 2013. 22(12): p. 2376-86.**
102. **Schmid, B., et al., *Loss of ALS-associated TDP-43 in zebrafish causes muscle degeneration, vascular dysfunction, and reduced motor neuron axon outgrowth.* Proc Natl Acad Sci U S A, 2013. 110(13): p. 4986-91.**
103. **Arnold, E.S., et al., *ALS-linked TDP-43 mutations produce aberrant RNA splicing and adult-onset motor neuron disease without aggregation or loss of nuclear TDP-43.* Proc Natl Acad Sci U S A, 2013. 110(8): p. E736-45.**
104. **Xu, Y.F., et al., *Wild-type human TDP-43 expression causes TDP-43 phosphorylation, mitochondrial aggregation, motor deficits, and early mortality in transgenic mice.* J Neurosci, 2010. 30(32): p. 10851-9.**
105. **Wegorzewska, I., et al., *TDP-43 mutant transgenic mice develop features of ALS and frontotemporal lobar degeneration.* Proc Natl Acad Sci U S A, 2009. 106(44): p. 18809-14.**
106. **Xu, Y.F., et al., *Expression of mutant TDP-43 induces neuronal dysfunction in transgenic mice.* Mol Neurodegener, 2011. 6: p. 73.**
107. **Kuo, P.H., et al., *The crystal structure of TDP-43 RRM1-DNA complex reveals the specific recognition for UG- and TG-rich nucleic acids.* Nucleic Acids Res, 2014. 42(7): p. 4712-22.**

108. **Austin, J.A., et al., *Disease causing mutants of TDP-43 nucleic acid binding domains are resistant to aggregation and have increased stability and half-life.* Proc Natl Acad Sci U S A, 2014. 111(11): p. 4309-14.**

109. **Winton, M.J., et al., *Disturbance of nuclear and cytoplasmic TAR DNA-binding protein (TDP-43) induces disease-like redistribution, sequestration, and aggregate formation.* J Biol Chem, 2008. 283(19): p. 13302-9.**

110. **Barmada, S.J. and S. Finkbeiner, *Pathogenic TARDBP mutations in amyotrophic lateral sclerosis and frontotemporal dementia: disease-associated pathways.* Rev Neurosci, 2010. 21(4): p. 251-72.**

111. **Igaz, L.M., et al., *Dysregulation of the ALS-associated gene TDP-43 leads to neuronal death and degeneration in mice.* J Clin Invest, 2011. 121(2): p. 726-38.**

112. **Dayton, R.D., et al., *Selective Forelimb Impairment in Rats Expressing a Pathological TDP-43 25 kDa C-terminal Fragment to Mimic Amyotrophic Lateral Sclerosis.* Mol Ther, 2013. 21(7): p. 1324-34.**

113. **Ritson, G.P., et al., *TDP-43 mediates degeneration in a novel Drosophila model of disease caused by mutations in VCP/p97.* J Neurosci, 2010. 30(22): p. 7729-39.**

114. **Miguel, L., et al., *Both cytoplasmic and nuclear accumulations of the protein are neurotoxic in Drosophila models of TDP-43 proteinopathies.* Neurobiol Dis, 2011. 41(2): p. 398-406.**

115. **Igaz, L.M., et al., *Expression of TDP-43 C-terminal Fragments in Vitro Recapitulates Pathological Features of TDP-43 Proteinopathies.* J Biol Chem, 2009. 284(13): p. 8516-24.**

116. **Wils, H., et al., *TDP-43 transgenic mice develop spastic paralysis and neuronal inclusions characteristic of ALS and frontotemporal lobar degeneration.* Proc Natl Acad Sci U S A, 2010. 107(8): p. 3858-63.**

117. **Tsai, K.J., et al., *Elevated expression of TDP-43 in the forebrain of mice is sufficient to cause neurological and pathological phenotypes mimicking FTLD-U.* J Exp Med, 2010. 207(8): p. 1661-73.**

118. **Cannon, A., et al., *Neuronal sensitivity to TDP-43 overexpression is dependent on timing of induction.* Acta Neuropathol, 2012. 123(6): p. 807-23.**

119. **Shan, X., et al., *Altered distributions of Gemini of coiled bodies and mitochondria in motor neurons of TDP-43 transgenic mice.* Proc Natl Acad Sci U S A, 2010. 107(37): p. 16325-30.**

120. **Liu, R., et al., *Reducing TDP-43 aggregation does not prevent its cytotoxicity.* Acta Neuropathol Commun, 2013. 1(1): p. 49.**

121. **Bentmann, E., et al., *Requirements for stress granule recruitment of fused in sarcoma (FUS) and TAR DNA-binding protein of 43 kDa (TDP-43).* J Biol Chem, 2012. 287(27): p. 23079-94.**

122. **Liu-Yesucevitz, L., et al., *Tar DNA binding protein-43 (TDP-43) associates with stress granules: analysis of cultured cells and pathological brain tissue.* PLoS One, 2010. 5(10): p. e13250.**

123. **Volkening, K., et al., *Tar DNA binding protein of 43 kDa (TDP-43), 14-3-3 proteins and copper/zinc superoxide dismutase (SOD1) interact to modulate NFL mRNA stability. Implications for altered RNA processing in amyotrophic lateral sclerosis (ALS).* Brain Res, 2009. 1305: p. 168-82.**

124. **Aulas, A., S. Stabile, and C. Vande Velde, *Endogenous TDP-43, but not FUS, contributes to stress granule assembly via G3BP.* Mol Neurodegener, 2012. 7: p. 54.**

125. **Budini, M., et al., *Role of selected mutations in the Q/N rich region of TDP-43 in EGFP-12xQ/N-induced aggregate formation.* Brain Res, 2012. 1462: p. 139-50.**

126. **Dormann, D. and C. Haass, *TDP-43 and FUS: a nuclear affair.* Trends Neurosci, 2011.**

127. **Halliday, G., et al., *Mechanisms of disease in frontotemporal lobar degeneration: gain of function versus loss of function effects.* Acta Neuropathol, 2012. 124(3): p. 373-82.**

128. **Buratti, E. and F.E. Baralle, *The multiple roles of TDP-43 in pre-mRNA processing and gene expression regulation.* RNA Biol, 2010. 7(4): p. 420-9.**

129. **Fischer, M., et al.,** ***Prion protein (PrP) with amino-proximal deletions restoring susceptibility of PrP knockout mice to scrapie.*** **EMBO J, 1996. 15(6): p. 1255-64.**

130. **Guillemin, I., et al.,** ***A subcellular prefractionation protocol for minute amounts of mammalian cell cultures and tissue.*** **Proteomics, 2005. 5(1): p. 35-45.**

131. **Rehm, H. and T. Letzel,** ***Der Experimentator: Proteinbiochemie, Proteomics*****. 6. Aufl. ed. <<Der>> Experimentator. 2010, Heidelberg: Spektrum Akad. Verl. XIV, 390 S.**

132. **Neumann, M., et al.,** ***Phosphorylation of S409/410 of TDP-43 is a consistent feature in all sporadic and familial forms of TDP-43 proteinopathies.*** **Acta Neuropathol, 2009. 117(2): p. 137-49.**

133. **Livak, K.J. and T.D. Schmittgen,** ***Analysis of relative gene expression data using real-time quantitative PCR and the 2(-Delta Delta C(T)) Method.*** **Methods, 2001. 25(4): p. 402-8.**

134. **Crawley, J.N.,** ***Mouse behavioral assays relevant to the symptoms of autism.*** **Brain Pathol, 2007. 17(4): p. 448-59.**

135. **Antunes, M. and G. Biala,** ***The novel object recognition memory: neurobiology, test procedure, and its modifications.*** **Cogn Process, 2012. 13(2): p. 93-110.**

136. **Moolenbeek, C. and E.J. Ruitenberg,** ***The "Swiss roll": a simple technique for histological studies of the rodent intestine.*** **Lab Anim, 1981. 15(1): p. 57-9.**

137. **Karnovsky, M.J. and L. Roots,** ***A "Direct-Coloring" Thiocholine Method for Cholinesterases.*** **J Histochem Cytochem, 1964. 12: p. 219-21.**

138. **Maxwell, S.E. and H.D. Delaney,** ***Designing experiments and analyzing data : a model comparison perspective*****. 2nd ed. 2004, Mahwah, N.J.: Lawrence Erlbaum Associates.**

139. **Corrado, L., et al.,** ***High frequency of TARDBP gene mutations in Italian patients with amyotrophic lateral sclerosis.*** **Hum Mutat, 2009. 30(4): p. 688-94.**

140. **Kirby, J., et al.,** ***Broad clinical phenotypes associated with TAR-DNA binding protein (TARDBP) mutations in amyotrophic lateral sclerosis.*** **Neurogenetics, 2010. 11(2): p. 217-25.**

141. **Kabashi, E., et al.,** ***TARDBP mutations in individuals with sporadic and familial amyotrophic lateral sclerosis.*** **Nat Genet, 2008. 40(5): p. 572-4.**

142. **Daoud, H., et al.,** ***Contribution of TARDBP mutations to sporadic amyotrophic lateral sclerosis.*** **J Med Genet, 2009. 46(2): p. 112-4.**

143. **Asante, E.A., et al.,** ***Expression pattern of a mini human PrP gene promoter in transgenic mice.*** **Neurobiol Dis, 2002. 10(1): p. 1-7.**

144. **Huang, C., P.Y. Xia, and H. Zhou,** ***Sustained expression of TDP-43 and FUS in motor neurons in rodent's lifetime.*** **Int J Biol Sci, 2010. 6(4): p. 396-406.**

145. **Avendano-Vazquez, S.E., et al.,** ***Autoregulation of TDP-43 mRNA levels involves interplay between transcription, splicing, and alternative polyA site selection.*** **Genes Dev, 2012. 26(15): p. 1679-84.**

146. **Bembich, S., et al.,** ***Predominance of spliceosomal complex formation over polyadenylation site selection in TDP-43 autoregulation.*** **Nucleic Acids Res, 2013.**

147. **Hanson, K.A., S.H. Kim, and R.S. Tibbetts,** ***RNA-binding proteins in neurodegenerative disease: TDP-43 and beyond.*** **Wiley Interdiscip Rev RNA, 2012. 3(2): p. 265-85.**

148. **Dale, G., et al.,** ***Diagnostic value of rectal mucosal acetylcholinesterase levels in Hirschsprung's disease.*** **Lancet, 1979. 1(8112): p. 347-9.**

149. **Wedel, T., et al.,** ***Enteric nerves and interstitial cells of Cajal are altered in patients with slow-transit constipation and megacolon.*** **Gastroenterology, 2002. 123(5): p. 1459-67.**

150. **Lee, S.Y., et al.,** ***17beta-estradiol activates ICI 182,780-sensitive estrogen receptors and cyclic GMP-dependent thioredoxin expression for neuroprotection.*** **FASEB J, 2003. 17(8): p. 947-8.**

151. **Kitamura, N., et al.,** ***Beneficial effects of estrogen in a mouse model of cerebrovascular insufficiency.*** **PLoS One, 2009. 4(4): p. e5159.**

152. **Carroll, J.C. and C.J. Pike, *Selective estrogen receptor modulators differentially regulate Alzheimer-like changes in female 3xTg-AD mice.* Endocrinology, 2008. 149(5): p. 2607-11.**

153. **Rosario, E.R., J. Carroll, and C.J. Pike, *Testosterone regulation of Alzheimer-like neuropathology in male 3xTg-AD mice involves both estrogen and androgen pathways.* Brain Res, 2010. 1359: p. 281-90.**

154. **Choi, C.I., et al., *Effects of estrogen on lifespan and motor functions in female hSOD1 G93A transgenic mice.* J Neurol Sci, 2008. 268(1-2): p. 40-7.**

155. **Esmaeili, M.A., et al., *Premature death of TDP-43 (A315T) transgenic mice due to gastrointestinal complications prior to development of full neurological symptoms of amyotrophic lateral sclerosis.* Int J Exp Pathol, 2013. 94(1): p. 56-64.**

156. **Guo, Y., et al., *HO-1 induction in motor cortex and intestinal dysfunction in TDP-43 A315T transgenic mice.* Brain Res, 2012. 1460: p. 88-95.**

157. **Hatzipetros, T., et al., *C57BL/6J congenic Prp-TDP43A315T mice develop progressive neurodegeneration in the myenteric plexus of the colon without exhibiting key features of ALS.* Brain Res, 2013.**

158. **Toepfer, M., et al., *Gastrointestinal dysfunction in amyotrophic lateral sclerosis.* Amyotroph Lateral Scler Other Motor Neuron Disord, 1999. 1(1): p. 15-9.**

159. **Mannino, M., et al., *Telephone follow-up for patients with amyotrophic lateral sclerosis.* Eur J Neurol, 2007. 14(1): p. 79-84.**

160. **Horimoto, Y., et al., *Autonomic dysfunctions in dementia with Lewy bodies.* J Neurol, 2003. 250(5): p. 530-3.**

161. **Wakabayashi, K., et al., *Involvement of the peripheral nervous system in synucleinopathies, tauopathies and other neurodegenerative proteinopathies of the brain.* Acta Neuropathol, 2010. 120(1): p. 1-12.**

162. **Natale, G., et al., *Parallel manifestations of neuropathologies in the enteric and central nervous systems.* Neurogastroenterol Motil, 2011. 23(12): p. 1056-65.**

163. **Arai, T., et al., *Phosphorylated TDP-43 in Alzheimer's disease and dementia with Lewy bodies.* Acta Neuropathol, 2009. 117(2): p. 125-36.**

164. **Rayaprolu, S., et al., *TARDBP mutations in Parkinson's disease.* Parkinsonism Relat Disord, 2013. 19(3): p. 312-5.**

165. **Quadri, M., et al., *Broadening the phenotype of TARDBP mutations: the TARDBP Ala382Thr mutation and Parkinson's disease in Sardinia.* Neurogenetics, 2011. 12(3): p. 203-9.**

166. **Tian, T., et al., *TDP-43 potentiates alpha-synuclein toxicity to dopaminergic neurons in transgenic mice.* Int J Biol Sci, 2011. 7(2): p. 234-43.**

167. **Amiel, J., et al., *Hirschsprung disease, associated syndromes and genetics: a review.* J Med Genet, 2008. 45(1): p. 1-14.**

168. **Bergeron, K.F., D.W. Silversides, and N. Pilon, *The developmental genetics of Hirschsprung's disease.* Clin Genet, 2013. 83(1): p. 15-22.**

169. **Barlow, A., E. de Graaff, and V. Pachnis, *Enteric nervous system progenitors are coordinately controlled by the G protein-coupled receptor EDNRB and the receptor tyrosine kinase RET.* Neuron, 2003. 40(5): p. 905-16.**

170. **Uesaka, T., et al., *Diminished Ret expression compromises neuronal survival in the colon and causes intestinal aganglionosis in mice.* J Clin Invest, 2008. 118(5): p. 1890-8.**

171. **Liu, Y.C., P.M. Chiang, and K.J. Tsai, *Disease animal models of TDP-43 proteinopathy and their pre-clinical applications.* Int J Mol Sci, 2013. 14(10): p. 20079-111.**

172. **Stallings, N.R., et al., *Progressive motor weakness in transgenic mice expressing human TDP-43.* Neurobiol Dis, 2010. 40(2): p. 404-14.**

173. **Swarup, V., et al., *Pathological hallmarks of amyotrophic lateral sclerosis/frontotemporal lobar degeneration in transgenic mice produced with TDP-43 genomic fragments.* Brain, 2011. 134(Pt 9): p. 2610-26.**

174. **Janssens, J., et al., *Overexpression of ALS-Associated p.M337V Human TDP-43 in Mice Worsens Disease Features Compared to Wild-type Human TDP-43 Mice.* Mol Neurobiol, 2013. 48(1): p. 22-35.**

175. **Dang, T.N., et al., *Increased metal content in the TDP-43(A315T) transgenic mouse model of frontotemporal lobar degeneration and amyotrophic lateral sclerosis.* Front Aging Neurosci, 2014. 6: p. 15.**

176. **Janssens, J. and C. Van Broeckhoven, *Pathological mechanisms underlying TDP-43 driven neurodegeneration in FTLD-ALS spectrum disorders.* Hum Mol Genet, 2013.**

177. **Manson, J., et al., *The prion protein gene: a role in mouse embryogenesis?* Development, 1992. 115(1): p. 117-22.**

178. **Shiina, Y., et al., *TDP-43 dimerizes in human cells in culture.* Cell Mol Neurobiol, 2010. 30(4): p. 641-52.**

179. **Ash, P.E., et al., *Neurotoxic effects of TDP-43 overexpression in C. elegans.* Hum Mol Genet, 2010. 19(16): p. 3206-18.**

180. **Ihara, R., et al., *RNA binding mediates neurotoxicity in the transgenic Drosophila model of TDP-43 proteinopathy.* Hum Mol Genet, 2013.**

181. **Barmada, S.J., et al., *Cytoplasmic mislocalization of TDP-43 is toxic to neurons and enhanced by a mutation associated with familial amyotrophic lateral sclerosis.* J Neurosci, 2010. 30(2): p. 639-49.**

182. **Li, Y.R., et al., *Stress granules as crucibles of ALS pathogenesis.* J Cell Biol, 2013. 201(3): p. 361-72.**

183. **Dewey, C.M., et al., *TDP-43 aggregation in neurodegeneration: are stress granules the key?* Brain Res, 2012. 1462: p. 16-25.**

184. **Bentmann, E., C. Haass, and D. Dormann, *Stress granules in neurodegeneration - lessons learnt from TAR DNA binding protein of 43 kDa and fused in sarcoma.* FEBS J, 2013. 280(18): p. 4348-70.**

185. **Parker, S.J., et al., *Endogenous TDP-43 localized to stress granules can subsequently form protein aggregates.* Neurochem Int, 2012. 60(4): p. 415-24.**

186. **Johnson, B.S., et al., *TDP-43 is intrinsically aggregation-prone, and amyotrophic lateral sclerosis-linked mutations accelerate aggregation and increase toxicity.* J Biol Chem, 2009. 284(30): p. 20329-39.**

187. **Gitler, A.D. and J. Shorter, *RNA-binding proteins with prion-like domains in ALS and FTLD-U.* Prion, 2011. 5(3): p. 179-87.**

188. **Polymenidou, M. and D.W. Cleveland, *The seeds of neurodegeneration: prion-like spreading in ALS.* Cell, 2011. 147(3): p. 498-508.**

189. **McCombe, P.A. and R.D. Henderson, *Effects of gender in amyotrophic lateral sclerosis.* Gend Med, 2010. 7(6): p. 557-70.**

190. **Mohammed, H.O., et al., *Risk factors associated with equine motor neuron disease: a possible model for human MND.* Neurology, 1993. 43(5): p. 966-71.**

191. **Haverkamp, L.J., V. Appel, and S.H. Appel, *Natural history of amyotrophic lateral sclerosis in a database population. Validation of a scoring system and a model for survival prediction.* Brain, 1995. 118 (Pt 3): p. 707-19.**

192. **Dang, T.N., et al., *Endogenous progesterone levels and frontotemporal dementia: modulation of TDP-43 and Tau levels in vitro and treatment of the A315T TARDBP mouse model.* Dis Model Mech, 2013.**

193. **Groeneveld, G.J., et al., *Ovariectomy and 17beta-estradiol modulate disease progression of a mouse model of ALS.* Brain Res, 2004. 1021(1): p. 128-31.**

194. **Bame, M., et al., *Effect of sex on lifespan, disease progression, and the response to methionine sulfoximine in the SOD1 G93A mouse model for ALS.* Gend Med, 2012. 9(6): p. 524-35.**

195. **Cervetto, C., et al., *Motor neuron dysfunction in a mouse model of ALS: Gender-dependent effect of P2X7 antagonism.* Toxicology, 2013. 311(1-2): p. 69-77.**

196. **Naumenko, N., et al., *Gender-Specific Mechanism of Synaptic Impairment and Its Prevention by GCSF in a Mouse Model of ALS.* Front Cell Neurosci, 2011. 5: p. 26.**

197. **Praline, J., et al., *Co-occurrence of progressive anarthria with an S393L TARDBP mutation and ALS within a family.* Amyotroph Lateral Scler, 2012. 13(1): p. 155-7.**

198. **Thau, N., et al., *Decreased mRNA expression of PGC-1alpha and PGC-1alpha-regulated factors in the SOD1G93A ALS mouse model and in human sporadic ALS.* J Neuropathol Exp Neurol, 2012. 71(12): p. 1064-74.**

199. **Zhao, W., et al., *Peroxisome proliferator activator receptor gamma coactivator-1alpha (PGC-1alpha) improves motor performance and survival in a mouse model of amyotrophic lateral sclerosis.* Mol Neurodegener, 2011. 6(1): p. 51.**

200. **Liang, H., et al., *PGC-1alpha protects neurons and alters disease progression in an amyotrophic lateral sclerosis mouse model.* Muscle Nerve, 2011. 44(6): p. 947-56.**

201. **Eschbach, J., et al., *PGC-1alpha is a male-specific disease modifier of human and experimental amyotrophic lateral sclerosis.* Hum Mol Genet, 2013. 22(17): p. 3477-84.**

202. **Hayes-Punzo, A., et al., *Gonadectomy and dehydroepiandrosterone (DHEA) do not modulate disease progression in the G93A mutant SOD1 rat model of amyotrophic lateral sclerosis.* Amyotroph Lateral Scler, 2012. 13(3): p. 311-4.**

203. **Lokuge, S., et al., *The rapid effects of estrogen: a mini-review.* Behav Pharmacol, 2010. 21(5-6): p. 465-72.**

204. **Luty, A.A., et al., *Sigma nonopioid intracellular receptor 1 mutations cause frontotemporal lobar degeneration-motor neuron disease.* Ann Neurol, 2010. 68(5): p. 639-49.**

205. **Platania, P., et al., *17beta-estradiol rescues spinal motoneurons from AMPA-induced toxicity: a role for glial cells.* Neurobiol Dis, 2005. 20(2): p. 461-70.**

206. **Cardona-Rossinyol, A., et al., *Neuroprotective effects of estradiol on motoneurons in a model of rat spinal cord embryonic explants.* Cell Mol Neurobiol, 2013. 33(3): p. 421-32.**

207. **Wu, C.L., et al., *Involvement of cholecystokinin receptor in the inhibition of gastrointestinal motility by estradiol in ovariectomized rats.* Scand J Gastroenterol, 2002. 37(10): p. 1133-9.**

208. **Chen, T.S., et al., *Effects of sex steroid hormones on gastric emptying and gastrointestinal transit in rats.* Am J Physiol, 1995. 268(1 Pt 1): p. G171-6.**

209. **Ryan, J.P. and A. Bhojwani, *Colonic transit in rats: effect of ovariectomy, sex steroid hormones, and pregnancy.* Am J Physiol, 1986. 251(1 Pt 1): p. G46-50.**

210. **Murayama, S., *[Neuropathology of frontotemporal dementia].* Rinsho Shinkeigaku, 2008. 48(11): p. 998.**

211. **Campbell-Thompson, M., K.K. Reyher, and L.B. Wilkinson, *Immunolocalization of estrogen receptor alpha and beta in gastric epithelium and enteric neurons.* J Endocrinol, 2001. 171(1): p. 65-73.**

212. **Kawano, N., et al., *Identification and localization of estrogen receptor alpha- and beta-positive cells in adult male and female mouse intestine at various estrogen levels.* Histochem Cell Biol, 2004. 121(5): p. 399-405.**

213. **Turnbull, G.K., et al., *Relationships between symptoms, menstrual cycle and orocaecal transit in normal and constipated women.* Gut, 1989. 30(1): p. 30-4.**

214. **Kamm, M.A., et al., *Steroid hormone abnormalities in women with severe idiopathic constipation.* Gut, 1991. 32(1): p. 80-4.**

215. **Jung, H.K., D.Y. Kim, and I.H. Moon, *Effects of gender and menstrual cycle on colonic transit time in healthy subjects.* Korean J Intern Med, 2003. 18(3): p. 181-6.**

216. **Finocchi, C. and M. Ferrari, *Female reproductive steroids and neuronal excitability.* Neurol Sci, 2011. 32 Suppl 1: p. S31-5.**

217. **Diaz, M., et al., *Acute relaxation of mouse duodenum [correction of duodenun] by estrogens. Evidence for an estrogen receptor-independent modulation of muscle excitability.* Eur J Pharmacol, 2004. 501(1-3): p. 161-78.**

218. **Beckett, E.A., et al., *Effects of female steroid hormones on A-type K+ currents in murine colon.* J Physiol, 2006. 573(Pt 2): p. 453-68.**

10. Acknowledgements

For providing lots of help & support to make this work successful I am grateful to many people:

First and foremost, I would like to thank Manuela Neumann for all her support during almost five years of my thesis, for giving me the opportunity to work on the forefront of ALS research, for clear-cut reviews of experiments and conclusions, and for her abundance of patience.

I would also like to thank Adriano Aguzzi for the opportunity to do my PhD thesis in his institute, for lively discussions at the progress reports, and for offering new perspectives and approaches.

Many thanks to Peter Sonderegger for his remarks at the PhD-Committee meetings and his positive influence on the project.

A special thanks goes to Margarete Arras for being a great supervisor at mouse surgerys, to Simone Hornemann for sharing her knowledge on protein purification with me and to Tobias Welt for his support and enthusiasm regard the behaviorial phenotyping.

Many thanks to all co-workers in the Neumann group, both in Zürich and in Tübingen. In particular I would like to thank Chiara Valori and Said Abdel Aziz for help and discussion as well Vignesh Sakthivelu, Jasvir Kaur and Lim Tiong-Ti for serious discussion about future experiments.

Furthermore I am very thankful to many people offering technical support and animal care; you make the difference: Mareike Wagner, Jay Tracy, Petra Schwarz, Rita Moos, Mirzet Delic, Katrin Trautmann, Dorothea Kreuder, Stefanie Mack, Julia Rieber and Nada Matijevic.

I would like to thank all the past and present members of the Institute of Neuropathology Zürich.I think we had a great time in the lab and much fun outside the lab. I would also like to thank the collegues at DZNE for scientific discussion as well as for collegial lab routine. Looking forward to see major breakthroughs in the future.

I would like to thank the Synapse Foundation for funding parts of this thesis and the Life Science Graduate School Zurich offering guidance and information beyond one´s own nose.

Last but not least, I would like to thank my parents, my family and fellow friends for their great support. A special thanks goes to Maren, who was backing me all the way up the hill.